REPORT DOCUMENTATION PAGE

Form Approved
OMB No. 0704-0188

1. REPORT DATE *(DD-MM-YYYY)*	2. REPORT TYPE	3. DATES COVERED *(From - To)*
05/05/01		SBIR Phase II 08/05/98 08/05/01

4. TITLE AND SUBTITLE
"An automated system for accurately tracking and measuring multiple targets in six dimensions"

5a. CONTRACT NUMBER
F04611-98-C-0020

5b. GRANT NUMBER

5c. PROGRAM ELEMENT NUMBER

6. AUTHOR(S)
Yong-Sheng Chao

5d. PROJECT NUMBER

5e. TASK NUMBER

5f. WORK UNIT NUMBER

7. PERFORMING ORGANIZATION NAME(S) AND ADDRESS(ES)
Advanced Optical Technologies, Inc.
111 Founders Plaza, Suite 603
East Hartford, CT 06108

8. PERFORMING ORGANIZATION REPORT NUMBER
AOT0102

9. SPONSORING/MONITORING AGENCY NAME(S) AND ADDRESS(ES)
Directorate of Contracting
AFFTC/PKAE
5 South Wolfe Avenue
Edwards AFB, CA 93524-1185

10. SPONSOR/MONITOR'S ACRONYM(S)

11. SPONSOR/MONITOR'S REPORT NUMBER(S)

12. DISTRIBUTION/AVAILABILITY STATEMENT
Public

DISTRIBUTION STATEMENT A
Approved for Public Release
Distribution Unlimited

20020729 227

13. SUPPLEMENTARY NOTES

14. ABSTRACT

Report developed under SBIR contract. Airplane test programs require deployment of a large number of test assets around a System Under Test. A large number of 6D placement data must be recorded. An electro-optical 6D measurement system can significantly enhance the work efficiency. As a first step towards an automated system, we identified, developed, and tested critical components for the 6D measurements. These include: (1) a systematic mathematical theory for 6D calculations; (2) a laser beam delivering system free of mechanical moving parts; (3) a retroreflective modulator; (4) a direction-resolvable 2D intelligent photo-detection system; and (5) a data communication system between the test assets and the measurement station. These critical components are the technical foundation for any optical 6D measurement approaches. Based on the successful development and the availability of these critical components, an automated 6D measurement system is feasible. Report produced for the AFFTC under SBIR Topic Number AF97-235, Contract Number F04611-98-C-0020, work performed from May 8, 1998, to May 8, 2001.

15. SUBJECT TERMS
Target Tracking, Infrared Sensor, Airplane Test, Vehicle Test. Industrial Measurement System, Six-Dimension Measurements

16. SECURITY CLASSIFICATION OF:			17. LIMITATION OF ABSTRACT	18. NUMBER OF PAGES	19a. NAME OF RESPONSIBLE PERSON
a. REPORT	b. ABSTRACT	c. THIS PAGE			Yong-Sheng Chao
Unclassified	Unclassified	Unclassified	Unlimited	119	19b. TELEPHONE NUMBER *(Include area code)* (860)610-0464

ABSTRACT

Airplane test programs performed in the anechoic chamber require placement of a large number of testing assets at various locations in the chamber around a System Under Test. The test assets can be placed anywhere with any orientation inside the Chamber. In certain test sequences, very large number of 6D data regarding all the test assets must be recorded. If an electro-optical 6D measurement system is available for doing this routine job, the efficiency of the airplane test work could be significantly enhanced. In the present contract, as a first step towards an automated 6D measurement system, critical components were identified, developed and tested. These include: (1) a systematic mathematical theory for 6D calculations; (2) a laser beam delivering system with full electronic control of light direction in a broad field of view; (3) a retroreflective modulator; (4) an intelligent 2D direction-resolvable photo-detection system; and (5) a data communication system between the test assets and the measurement station. These critical components, representing a number of essentially new technology areas, are the technical foundation for the present, as well as for any other future 6D measurement approaches. Based on the successful development and availability of these critical components, an automated 6D-measurement system is feasible.

This page intentionally left blank

Table of Contents

LIST OF FIGURES

1. The need for a 6D measurement system

In this section we will first present a brief review of the need for a 6D measurement system. Then we will summarize the most important requirements of the 6D measurement system. Finally, we will present a brief outline description of the most important parts in a 6D measurement system as identified through the present Phase II Contract work.

(1-a) The need for a 6D measurement system

Airplane test programs performed in the anechoic chamber require placement of a large number of testing assets at various locations in the Anechoic Chamber around a System Under Test (SUT). These test assets could be individual antennas, antenna arrays for RF stimulation, or light and heat sources for IR stimulation. The anechoic chamber is approximately 264 feet long x 250 feet wide and 70 feet high. The test assets can be placed anywhere with any orientation inside the chamber. Each test sequence includes a series of tests with a specific placement configuration of all the test assets involved in the chamber. Thus, routinely, a large amount of placement data must be reliably recorded and handled in the required test sequences.

Presently this job is done manually. However, when the number of test assets is very large, or when the orientation or position of the test assets changes rapidly, manual recording would be impractical and inevitably subjected to a great deal of human error. So an electro-optical instrument that can automatically acquire the 6D placement data, could make the airplane tests much more efficient.

(1-b) The most important requirements of a 6D measurement system

Specifically, a 6D measurement system requires:

(1-b-1) Six-dimension (6D) measurements.
The placement of a test object generally contains six independent parameters: three transnational parameters, as in a laboratory Cartesian coordinate system (X, Y, Z), and three orientation parameters (α, β, γ), described as pitch, yaw and roll. In each test, the position and orientation of each test asset in six dimensions must be accurately measured and recorded. Because the data amount is large, the task must be carried out automatically and must be handled by computer.

(1-b-2) Multiple test assets.
Each test asset, for example an antenna, is a 6D measurement target that contains a single, independent group of 6D data. The target number can be in the hundreds. The actual number of test assets may not always be so large, however, the number should be much larger than one.

(1-b-3) Broad rotation angle values.
During airplane tests, the three rotation angles of each test asset must be changed according to test tasks. The rotation angle values may change in a broad range, for example, $\leq \pm 90°$. This also presents a challenge to the measurement techniques.

(1-b-4) Broad field of view for the measurement.
For airplane tests in the anechoic chamber, the test assets must be deployed around the vicinity of an airplane, and the measurement instrument for controlling the measurement process and gathering all the test results must be deployed at one of few fixed locations. The personnel conducting the tests usually stays with the measurement instruments at the selected fixed location. The measurement location usually must have a computer, and thus may be represented by the computer location. Because of appreciable size of the airplane, the test assets occupy a large field of view in relation to the computer location. In an ideal case, if the computer location is fixed at one point that can look over the entire anechoic chamber, the maximum field of view must be at least $\pm 120°$. If the computer location can be moved to fit different test designs, the field of view must be at least $\pm 60°$.

(1-c) The most important components for the development of a 6D measurement system

According to the above requirements, the following five new technology components are considered necessary for any optical measurement system:

(1-c-1) Development of a light beam control system
(1-c-2) Development of a retroreflective modulator
(1-c-3) Development of a microprocessor-controlled intelligent photo-detection system
(1-c-4) Development of a free-space optical data communication method
(1-c-5) Development of a mathematical method for evaluation of 6D measurement results

These components are necessary for system operation. At the same time, each component represents a new technology not completely available at the present time. In the present Phase II Contract we came to realize that development of these new components requires substantial efforts. On the other hand, without any one of these components a 6D measurement system cannot be constructed. Because of this, it is appropriate for the present contract to first focus efforts on the development of these components.

The following is a more detailed description.

(1-c-1) Development of a light beam control system.
Development of a laser light beam control device that can point the laser beam to an arbitrarily selected target in the anechoic chamber with high speed. Because the chamber is large, the measurement field of view is broad (1-1-d), and because the number of the targets can be large (1-1-b), the speed to control the light beam direction must be fast. As was demonstrated in the Phase I results, our development approach is a laser light beam control system with full electronic control of light beam direction in a broad angle range.

(1-c-2) Development of a retroreflective modulator.
First, the retroreflective modulator be capable of sending the retroreflected laser light beam back to the measurement station. Additionally, the retroreflective modulator must impress certain information specific to the target and to the measurement. For example, because a large number of such retroreflectors must be present in the measurement (1-1-b), the retroreflective modulator must at least be able to tell the measurement station its order number (which one it is) so that the measurement station knows for sure that the light is retroreflected from this specific retroreflector. Otherwise, no meaningful data can be obtained. Thus, a simplistic retroreflector cannot do the job.

(1-c-3) Development of a microprocessor-controlled intelligent photo-detection system.
The necessity of developing a microprocessor-controlled intelligent photo-detection system is dictated by the complexity of system operation. The target detector must be placed far from the control computer. The target photo-detector must be able to perform data acquisition and data processing completely under its own control. The target photo-detector must also have the ability to communicate with the main computer. Based on the present Phase II Contract, without substantial system intelligence, it is impossible to fulfill the system requirement for 6D measurements.

(1-c-4) Development of a free-space optical data communication method.
The free-space optical communication system is for data exchange between the test assets and the measurement station. Since the target (the test assets) must be located a distance from the measurement station (the control computer), and the data exchange between the target and the measurement station is a necessary component of the system, such data exchange can only be implemented through a free-space optical communication method. Before the start of the present Phase II Contract, we did not realize the full scope of the work to be done to establish a free-space communication system. Through the work in the present contract, we came to realize that no shortcut exists for construction of such a communication system.

(1-c-5) Development of a mathematical method for calculation of 6D measurement results.
Through the work of the present Phase II Contract we realized that the mathematical method for calculation of 6D measurement results is not an established routine computational task. On the contrary, it is an unsolved scientific problem. Because of this, development of a mathematical method for evaluation of 6D measurement data is critical and a prerequisite for the development of a 6D measurement system.

Figure 1 Basic layout of the 6D measurement system

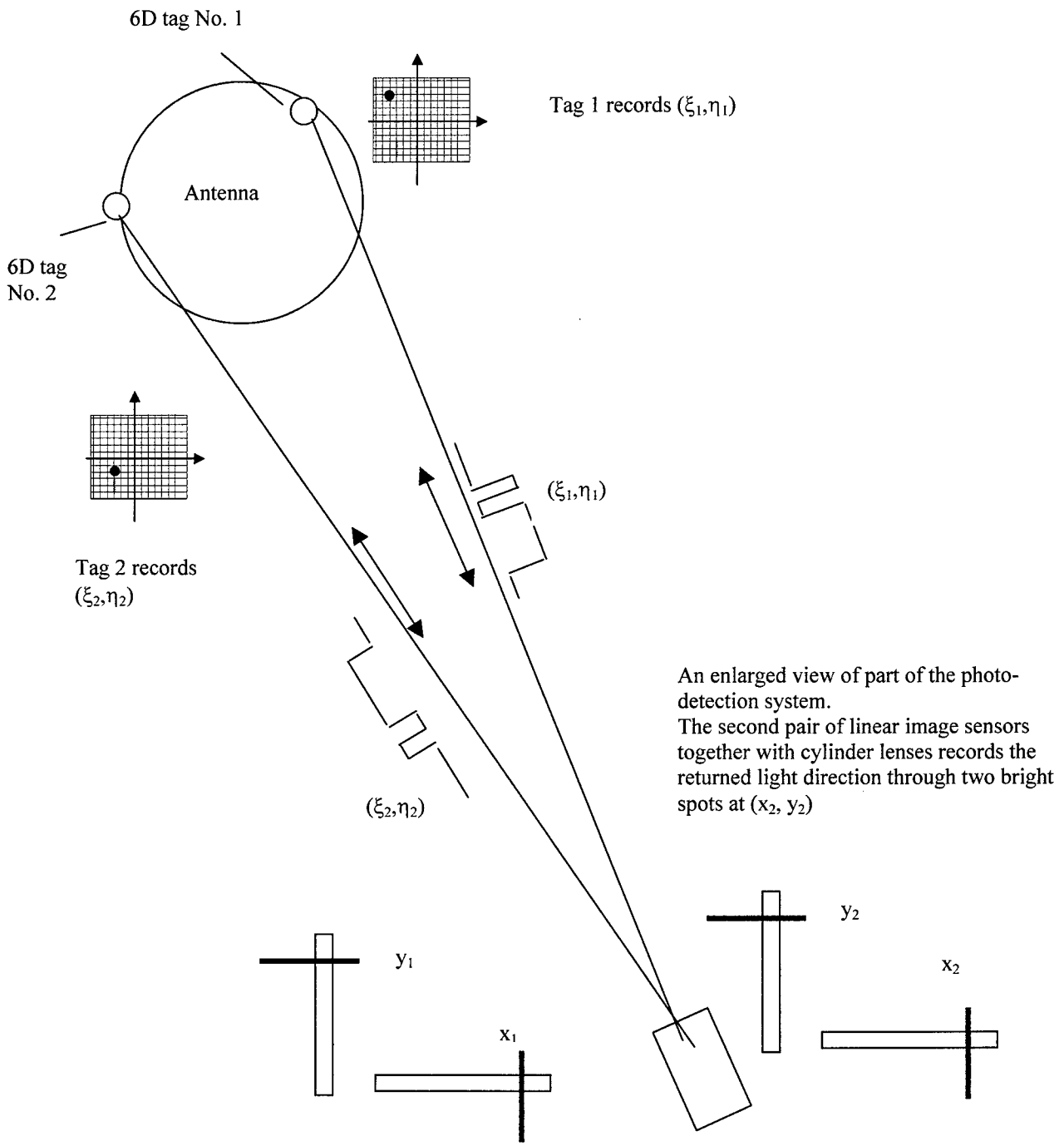

(1-d) A brief analysis of the theodolite-based method

During the Phase II Contract, we realized the complexity of the task, and consequently we reconsidered and reanalyzed an alternate approach based on the use of commercially available theodolite instruments as the basis for system development. We collected the data regarding the most recent theodolite instruments, and conducted extensive analysis. However, **our conclusion is: the above listed five basic technical elements are common to all systems for multiple target 6D measurements in the anechoic chamber, including using a theodolite-based or other laser range-finder-based instrument systems. The best help the commercially available theodolite instruments can provide is to simplify certain photo-detection, but this cannot replace the above listed five basic technical elements. That is, even with the best use of the commercially available theodolite instruments, the above listed five basic technical elements remain the most important components of a 6D measurement system.**

The following is a brief explanation:

(1-d-1) Regarding the mathematical method for evaluation of 6D measurement results.

It is obvious that the mathematical theory and computation software is common to any 6D measurement approach. As described in this report, the mathematical method for 6D calculation is essentially an unsolved scientific problem and is substantially different from any currently available land-surveying calculations. Without a systematic mathematical theory, no meaningful 6D results can be gained at all for any experimental measurements.

(1-d-2) Regarding the capability limitation of the currently available position measurement systems.

The most sophisticated, up-to-date, commercially available theodolite instrument system has the capability for mechanically rotating the entire measurement station via computer control to search and identify the target, and to measure the identified target. This may be used as a low speed substitute for the full electronic light source as listed in the item 1 of the 4 basic elements. The time for searching a single target is at least 5 seconds per target as given in the specification data, assuming that the slow speed is acceptable when the target number is very small. The currently available theodolite instruments do not have the capability for items 2, 3, and 4, so they cannot be used for the present multiple target 6D measurement tasks in the anechoic chamber. Specifically, the currently available theodolite instruments use simple retroreflectors, and does not have the capability for distinguishing each individual retroreflectors. When the number of the simple retroreflectors is much more than one, great difficulty would arise as to identify which data comes from which retroreflector.

To accurately identify each individual retroreflector, a new retroreflective modulator technology must be developed. Our experience in the present Phase II program is that the development of a retroreflective modulator with a broad angle coverage is a complicated

task requiring substantial effort.

Thus, even if one tries to develop a 6D measurement system based on modifying the currently available theodolite system, the above listed five technical elements still must be first developed and must be included in the system. These five technical elements are necessary for any 6D measurement system.

(1-e) A summary of major results of the present Phase II Contract

The most important results of the present Phase II Contract are presented in this Report in the following Sections:

2. Development of a light beam direction control system.
3. Development of a retroreflective modulator.
4. Development of an intelligent two-dimensional direction-resolvable photo-detection system
5. Development of a communication link btween the Target and the PC station.
6. Development of a systematic mathematical method for calculation of 6D measurement results.

2. Development of a light beam direction control system

In the present Phase II Contract, we developed a laser beam deflection system having the capability of full electronic control of light beam direction in a broad angle range. The light beam control system consists of a laser light source, an initial beam deflector, and an optical system for deflection angle amplification. The output light beam deflection angle can be quite large, for example, $\leq\pm45°$; when needed the technique can provide a very large output deflection angle, as large as $\leq\pm90°$. The new light beam deflection device is a basic technical element for multiple target 6D measurements in the anechoic chamber.

(2-a) A critical review of technical background for light beam direction control

In the following we will present a brief background review of the light beam direction control technology. In this brief critical review, we will emphasize the necessity for the development of full electronic control of light beam direction for 6D measurements of multiple targets in the anechoic chamber for airplane tests.

The control of light beam direction is a fundamental technique in industry and in military applications. In the 1960s-1970s, with the invention of the laser, extensive research efforts in the U.S. and throughout the world was conducted for gaining a better control of light beam direction. All the methods and potential physical processes related with light direction control were comprehensively explored. A unanimous conclusion was reached at that time: there is no better method other than the simple electromechanical method for light beam deflection.

Because of this, in the past several decades, almost all the efforts for light beam deflection have concentrated on perfecting engineering of the electromechanical devices (see *Handbook of Optics*) [1]. Today, as a result, more than 99% of the light beam control device market is dominated by electromechanical methods. A typical electromechanical light beam deflector is a galvano-metric mirror device composed of a rotating mirror driven by a coil in a magnetic field. The electric current passing through the coil determines the deflection angle of the coil-mirror assembly, hence determining the reflected light beam direction. Galvano-metric light beam deflectors are a well-established technique and are commercially available.

In the present case when trying to use electromechanical devices for control of light beam direction for 6D measurements in the Chamber for airplane tests, we found a number of serious problems. The most important problems are:

(1) The angle coverage is too small.

We reviewed the best electromechanical rotating mirror products and found that the largest deflection angle for a rotating mirror is $\leq\pm30°$ for one dimensional deflection, and $\leq\pm20°$ for two-dimensional deflection [2]. The narrow deflection angle range is due to the

geometry limitation of the mechanical rotating devices, and essentially leaves no room for further improvement. To point a laser beam at multiple targets under airplane test conditions, the angle coverage must be at least $\leq \pm 45°$; it is highly desirable for the angle coverage to be $\leq \pm 60°$, or even $\leq \pm 90°$.

(2) The speed is too slow.

For the best electromechanical light beam deflection devices, the settle time of the galvano-metric mirror is not less than 20 milliseconds (ms). The settling time is defined as the minimum time between the moment that the electrical signal is applied and the time needed for the coil-mirror assembly to reach a new stable angular position. The long settling time is largely determined by the nature of mechanical movements of the device. As shown by the vendors, for the mirror to rotate to a new stable angular position, an oscillation process, which can last a long time, is required. Even for mechanical devices working at optimized conditions, more than one oscillation cycle is needed. The cycle time generally depends on the inertia and the electromagnetic driving force, and can be as long as 100 ms or more. Modern galvano-metric rotating mirror devices tend to make device size smaller and lighter, hence the intrinsic faster frequency. However, even with all engineering perfection taken into account, currently the practical settle time cannot be less than 20 ms [2].

Another type of electromechanical devices for the control of light beam direction is to utilize a electromechanical stage for rotating the entire light source. Such a primitive electromechanical approach can ensure a large angle coverage. For example, the latest theodolite instruments with automated target-searching capability utilize this approach. The problems with this approach are:

(a) The speed is extremely slow, and the settle time is very long. Because these are truly macro-mechanical systems, the inertia of the rotor is massive. The settle time for reaching a new, stable position is usually in the range of 200 ms [3].
(b) The angle accuracy is poor. Usually, mechanical encoding methods are used to determine the angle position of such a rotating stage. The practically achievable absolute angular accuracy is typically $\pm°1$ [3], which is not sufficient for the position and angle accuracy measurements in airplane tests.
(c) Such electromechanical systems are high precision electromechanical systems, and the cost is usually very high. For example, a typical theodolite instrument with an automatically controlled mechanical stage costs approximately $200,000. Even a high-cost system such as this can provide only laser range-finder data; it cannot provide a 6D measurement capability as described above.

One important accomplishment of the present contract is that we developed a new technology for electronically delivering a light beam to an arbitrarily selected target in space. Because of the new light beam deflection technology, the requirements of the light beam direction control for 6D measurements can be met. In the following section, we will describe the new technique for light beam direction control: The first type of light beam deflection system with full electronic control, the second type of light beam deflection

system with full electronic control, and further improvements.

(2-b) The first type of light beam deflection system with full electronic control

The first type of light beam deflection system with a full electronic control system consists of three major components: a. a laser source, b. an initial light beam deflector, c. a light beam deflection angle amplifier based on the use of a fiberoptic plate.

The initial light beam deflector is an improved, commercially available acoustooptical device for laser beam direction control. We used a custom-ordered, two-dimensional (2D) acoustooptical beam deflector (AOBD). The light beam deflection amplifier is a proprietary technology of Advanced Optical Technologies, Inc. In the following, we will first describe how a standard acoustooptical deflector works, and then we will show what improvements can make the device match the requirements of the present application.

An acoustooptical laser beam deflector is composed of an ultrasonic wave transducer and an acoustooptical deflector medium (Fig. 2). The frequency and intensity of the ultrasonic wave is controlled by a radio frequency electrical signal. The high frequency, high intensity sonic wave propagated in the deflector medium can be figuratively considered as a traveling optical grating with a line gap equal to the wavelength of the sonic wave. Thus, the deflection angle of the laser beam is $\theta = \lambda /(2\Lambda)$, where λ is the wavelength of the light, and Λ is the wavelength of the ultrasonic wave. Because the wavelength of the sonic wave is always much larger than that of the light wave, so the deflection angle is always rather small [4].

By adjusting the frequency of the electrical signal, the deflection angle of the laser beam is conveniently controlled. By providing a sufficiently strong sonic wave, the laser beam can be diffracted with good efficiency. The deflection medium is a crystal material TeO_2. The power of the electrical signal is 2W. The corresponding diffraction efficiency is 20% (20% of the laser energy is turned to the desired direction). The central frequency of the RF signal f = 100 MHz. The maximum range of tuning frequency Δf = 50 MHz. Correspondingly, the maximum deflection angle of the laser beam is about 2°. The same data set is used for two-dimensional beam steering, with two such devices assembled to provide both x and y direction deflections. Because of its simple structure, the acoustooptical deflector is very compact.

Figure 2 Basic principles of an acoustooptical deflector

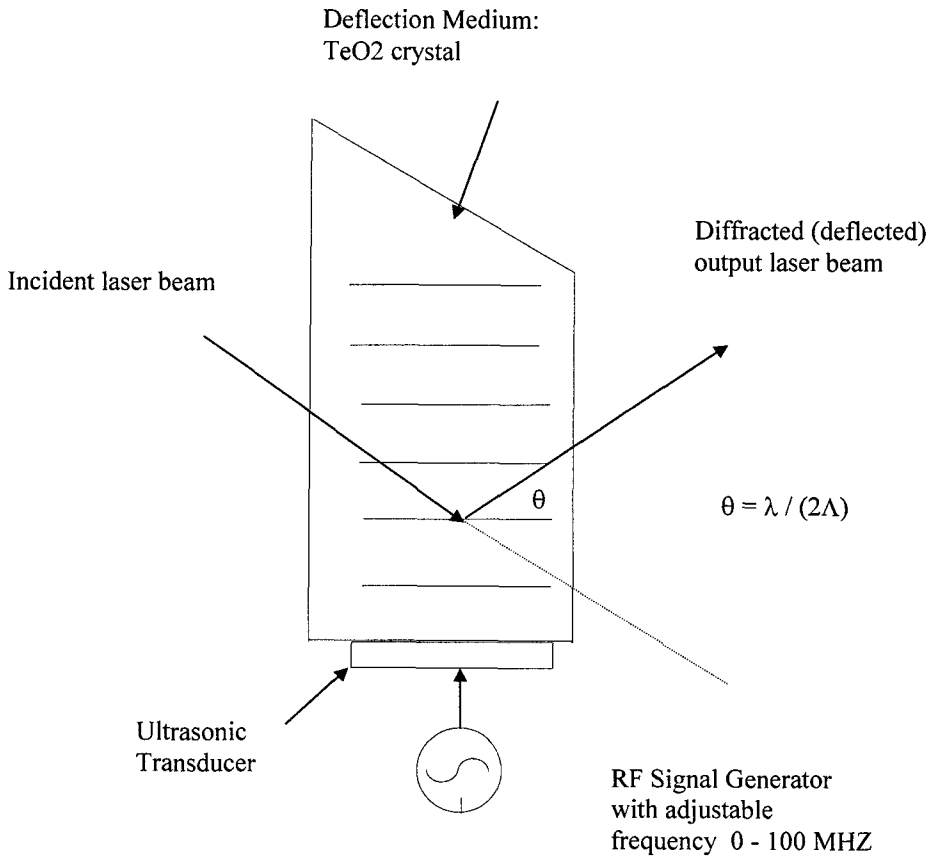

Acoustooptical deflector devices were developed largely in the 1960s and 1970s and are well established technology. The above data shows the major advantages and weakness of these devices. The most important advantage is its unique feature of electronic control. Because of this electronic control, by simply adjusting the RF signal frequency, the laser beam can be conveniently changed to different directions. Because there are no mechanical moving parts, the response is extremely fast. To change the direction of a laser beam takes only microseconds.

The problem with the acoustooptical devices is its small deflection angle(1° to 3°). Because of this, so far, practical applications of the acoustooptical deflector have been very limited.

The key element is a novel laser beam deflection angle amplification device, which is composed of a graded index sphere lens coupled to a fiberoptic plate. The incident laser beam first passes a beam size adapting device, which changes the size of the cross-section of the laser beam, while maintaining the high collimation of the laser beam. The beam size shrinking device is actually a commercially available beam size expander used in the reversed direction.

When the narrow parallel laser beam hits the fiberoptic plate, with a small portion of reflection loss, the laser energy propagates along the optic fiber, until reaching a point (or a very small area) at the junction between the fiberoptic plate and the sphere lens. The graded index sphere lens sees this point as a point light source. Because ***the point light source is always located at the focal surface of the sphere lens***, the light emitted to all directions in the sphere gives a parallel beam in a new direction (θ, φ) according to the position (x,y) of the incident point of the laser beam.

In the new direction along which the laser beam propagates to the far field, the laser beam maintains good collimation as long as the incident beam spot is small enough. Because both the fiberoptic plate and the sphere lens are highly transparent, with negligible absorption of laser energy, the size (the cross-section) of the laser beam can be reduced (for example, to 20μ to 50μ) without any danger of damaging these components.

By using the deflection angle amplifier, each point (x,y) on the input planar surface of the fiberoptic plate is mapped to a new direction (θ, φ) of the outgoing laser beam propagation. The maximum range of the x and y is the border of the fiberoptic plate or the graded index sphere lens, generally about 1 cm. The maximum angular range of the outgoing laser beam propagation is +90 and - 90 , that is, the entire half space for both θ and φ.

The planar surface of the fiberoptic plate is located at a distance *f* from the conventional lens. The distance *f* is approximately equal to the focal length of the lens. A laser beam with a moderate cross-section passes through an acoustooptical deflector. When the deflection angle is $\delta\alpha = 0$, the collimated laser beam is focused to a point $x = 0$, at the center of the fiberoptic plate surface. When the laser beam is deflected by a small angle $\delta\alpha$, the beam will be focused to a point $x = f \cdot \tan(\alpha) \cong f \cdot \alpha$. If $\alpha = 1°$, $x \leq 0.5$ cm, *f*

would be about 25 cm. Shown in Fig. 3, Fig. 4, Fig. 5, and Fig. 6 are schematic presentations of the accoustooptic light beam deflector constructed in the present contract.

Figure 3 The acoustooptical deflector constructed in the present contract

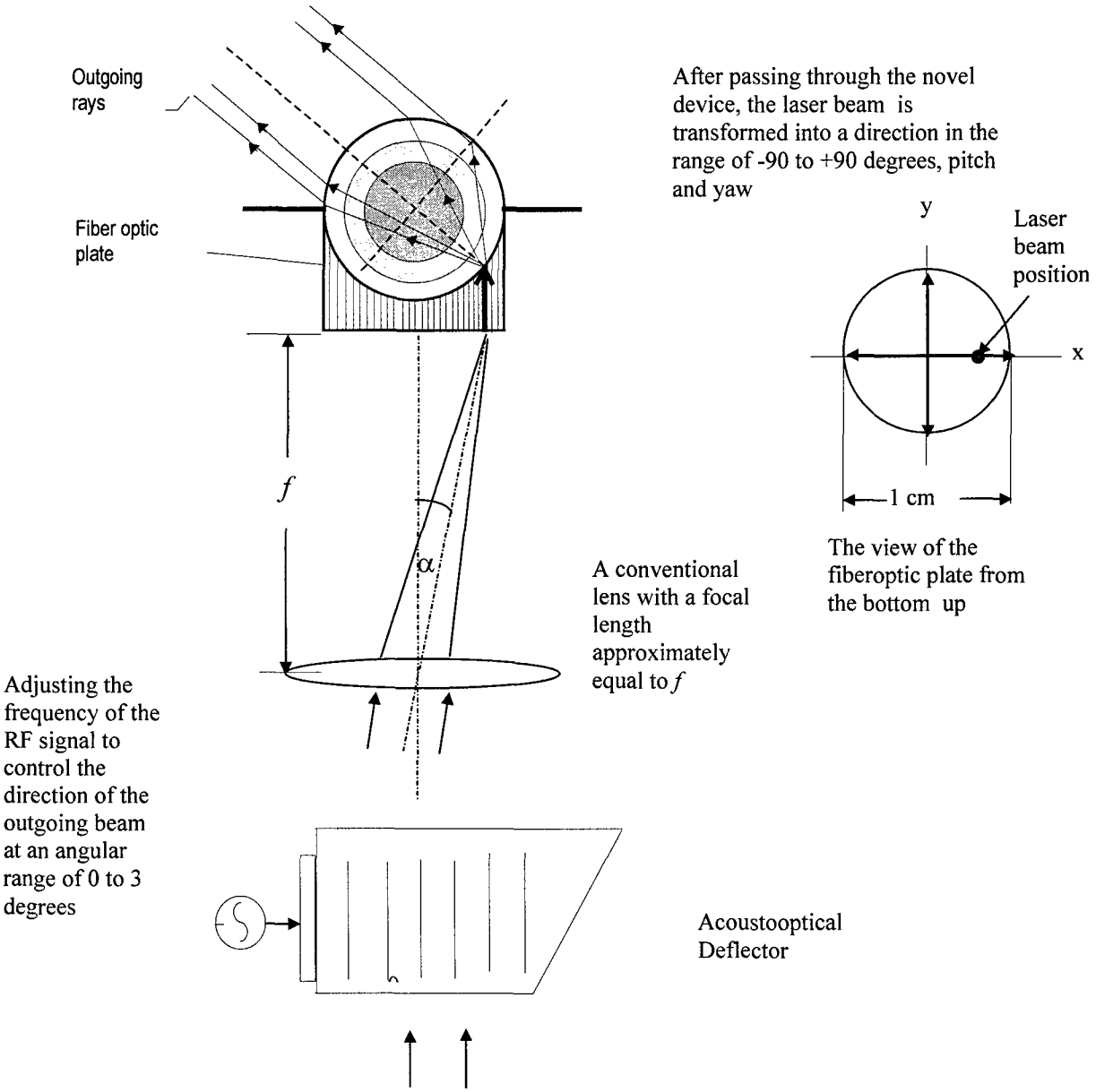

Figure 4 Structures of the sphere-lens-fiberoptic plate assembly

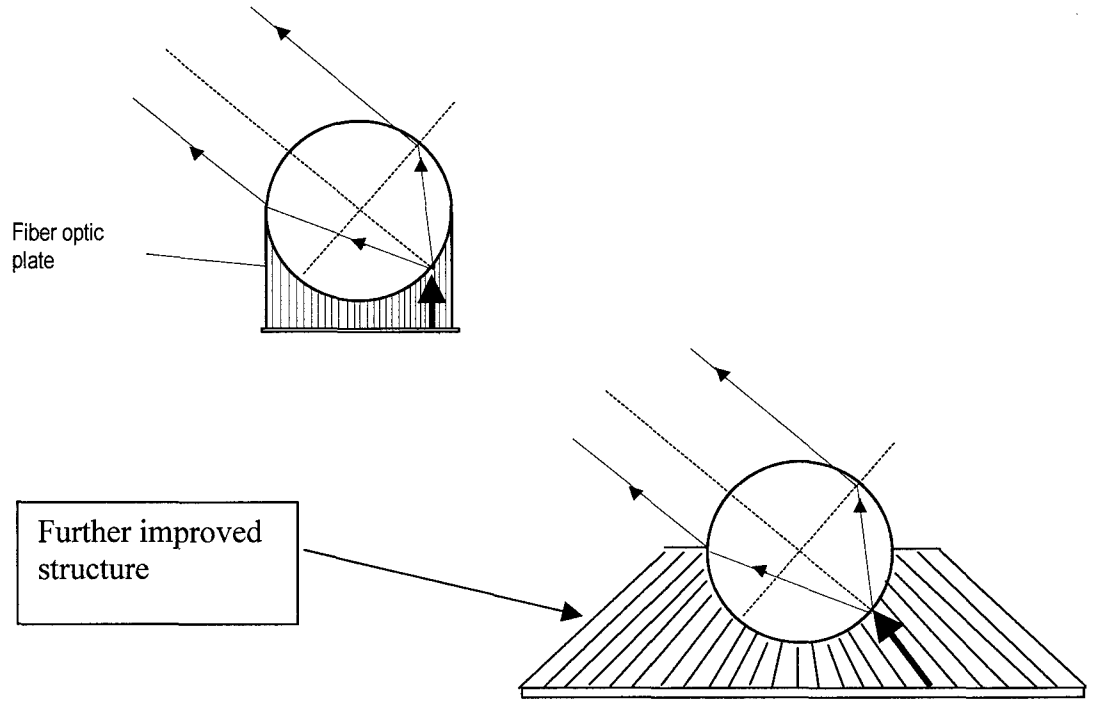

Figure 5 A picture of fiberoptic plates and sphere lenses

Fig. 5 A Picture of fiberoptic plates

Figure 6 Electronic driving circuits for the acoustooptical deflector

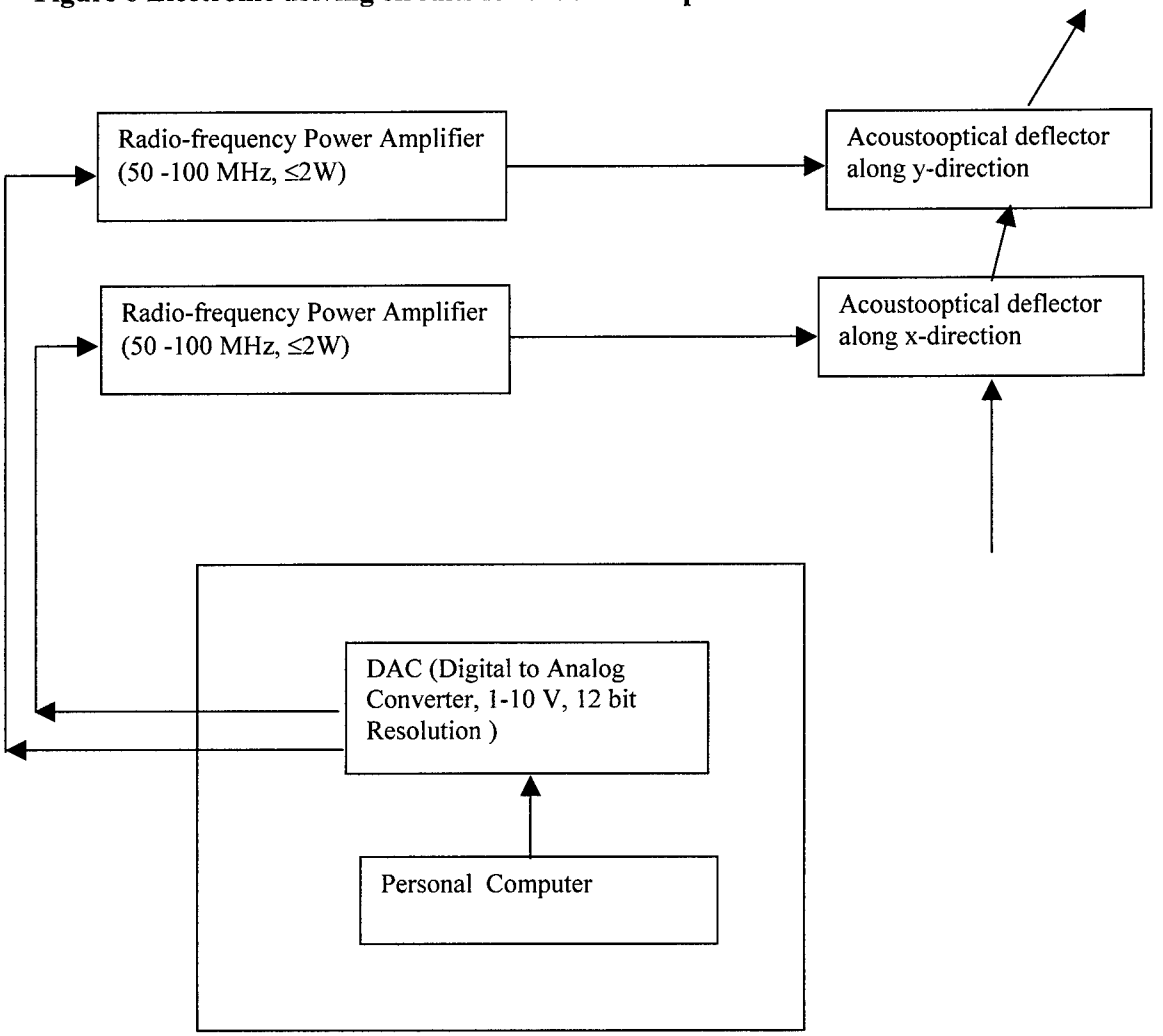

The acoustooptical deflector requires an RF power amplifier to drive the ultrasonic transducer. The power output of the RF amplifier is approximately 2W for each transducer. The x-direction deflection and the y-direction deflection each require an independent power amplifier. The RF signal is provided by the computer. There are two ways to control the signal frequency of the power amplifier. One way is to use a frequency synthesizer; another way is to use a Digital to Analog Converter (DAC). The frequency synthesizer can provide a higher accuracy in frequency control . However, for the first device, we used a DAC, purchased from CyberResearch Corp. (New Haven, CT). The DAC has 12-bit resolution and thus can provide 4,096 steps of control with an accuracy of approximately 1/4,000.

A computer program was developed in C++ in the Microsoft Windows environment to control the operation of the acoustooptical light beam deflector. The direction of the laser light beam is fully computer-controlled.

The following is a description of the technical conditions for the acoustooptical light beam deflector (AOBD).

Specifications of the acoustooptical deflector

A commercially available acoustooptical deflector was used. We chose Brimrose Corporation, one of three vendors in the U.S. Because the 2D deflector from Brimrose Corporation is compactly constructed, the deflector along the horizontal and vertical dimension are combined into a single, integrated module. The most important performance parameters are: wavelength, light transmission efficiency, maximum deflection angle, resolving power, and RF frequency range. The acoustooptical deflector is designed to work only for a single wavelength with an allowance of less than ± 10 nm. As long as the device is fabricated and the crystal is cut, the wavelength cannot be changed. System operation requires a wavelength at approximately 850 nm. The maximum deflection angle is generally within ≤ ± 1.5° for the RF frequency swing between 50 MHz and 100 MHz. The acoustooptical deflector used a birefregent TeO2 single crystal as the ultrasonic medium where the light deflection take place. The light transmission efficiency is defined as the ratio of the output laser power over the input laser power. This efficiency is important because a higher output light power is desired. The light transmission efficiency can be designed as high as 80%. However, conventional commercial products provide only 40% for one-dimensional deflection, and 20% for two-dimensional deflection. When it is needed, higher efficiency devices can be obtained through custom order. The major performance data of the acoustooptical deflector is listed below:

Figure 7 Performance parameters of the acoustooptical deflector

Item	Value	Unit
Laser Wavelength	850	Nm
Optical Aperture	9.3 x 9.3	mm x mm
Optical Transmission	>95%	
Diffraction efficiency	>25%	
Center RF Frequency	75	MHz
Bandwidth(RF Frequency Swing)	50	MHz
Resolving Power	750 x 750	Points
Maximum Deflection Angle	±1.5	°
Access Time (Scan Settle Time)	<15	μs
Optical Polarization	Linear	
Maximum RF Driving Power	4	W

The commercially available acoustooptical deflector is composed of two modules: an acoustooptical light beam deflection module and an RF driving module. The beam deflection module has an input window and an output window with the crystal contained inside. The ultrasonic wave is generated in the crystal medium by an ultrasonic transducer. The ultrasonic wave is generated by a RF signal with a power of about 2W

for each dimension. Another module is an RF power signal generator. To control beam deflection, the RF signal frequency is changed. To change the RF frequency, an adapter board can be used and plugged into the computer. There are two types of boards for changing the RF signal frequency through a computer: a frequency synthesizer and a digital to analog converter. Either of these boards can be purchased. The frequency synthesizer can provide an RF output with very high frequency stability (as high as 10^{-5}). However, in the present application, the stability is limited by the maximum resolvable points Nm, which is only about 750. Thus, an DAC with about a 12-bit amplitude resolution can meet the stability requirements. A DAC board was purchased and installed in the computer.

(a) Focusing lens L_1.

The focusing lens L_1 is to focuses the collimated laser beam into a point on the receiving surface of the fiberoptic plate. The focal length of the lens L_1 is determined by the deflection distance of the light spot in relation to the center of the fiberoptic plate.

$S = L_1 \cdot \tan(\alpha_0)$. When $\alpha_0 = 1.5°$, s = 1 cm, giving $f \cong 38$ cm. The deflection distance is determined by a reasonable value of the size of the fiberoptic plate. Usually a fiberoptic plate disk diameter of approximately 1 inch is appropriate. Thus the S = 1 cm is chosen. Because the L_1 lens focal length is rather large (38 cm), and the incident laser beam size is small (1 cm x 1 cm) the optical aperture of the lens L_1 is small, thus a commercial singlet lens or a doublet achromat lens is sufficient.

(b) Sphere lens and the fiberoptic plate assembly.

The sphere lens and the fiberoptic plate must be specially designed for the light beam deflection system. No commercially available component can be directly used.

Two types of sphere lenses were designed and fabricated: a single sphere and a sphere lens with a multiple layer structure. The multiple-layer lens is to improve focusing capability. In addition to using the standard lens design software "Optical System Layout and Optimization" (OSLO) software package by Sinclair Optics (Rochester, NY), we also used our own light tracing programs specially developed for designing the sphere lens. The sphere lens was fabricated by Triptar (Rochester, NY), a company whose services AOT has frequently used.

(c) Design of the fiberoptic plate.

Two types of fiberoptic plate were designed and fabricated: a conventional fiberoptic plate and a tapered fiberoptic plate. The tapered fiberoptic plate is to improve light transmission at larger angles.

Typical fiberoptic plate performance is: Fiber size 10 μ. Plate diameter 18 mm. Absorbent material EMA (dark absorption). Plate height 3 cm. Light transmission > 60%. The fiberoptic plate will be custom-made by Schott (MA) or INCOM (MA). AOT frequently uses the services of these companies. The external optics were assembled and tested at AOT.

All the optical components of the light beam deflector are packed in a plastic box. The mechanical structure of the box is shown in Fig. 8.

Figure 8 Layout of the acoustooptical deflector

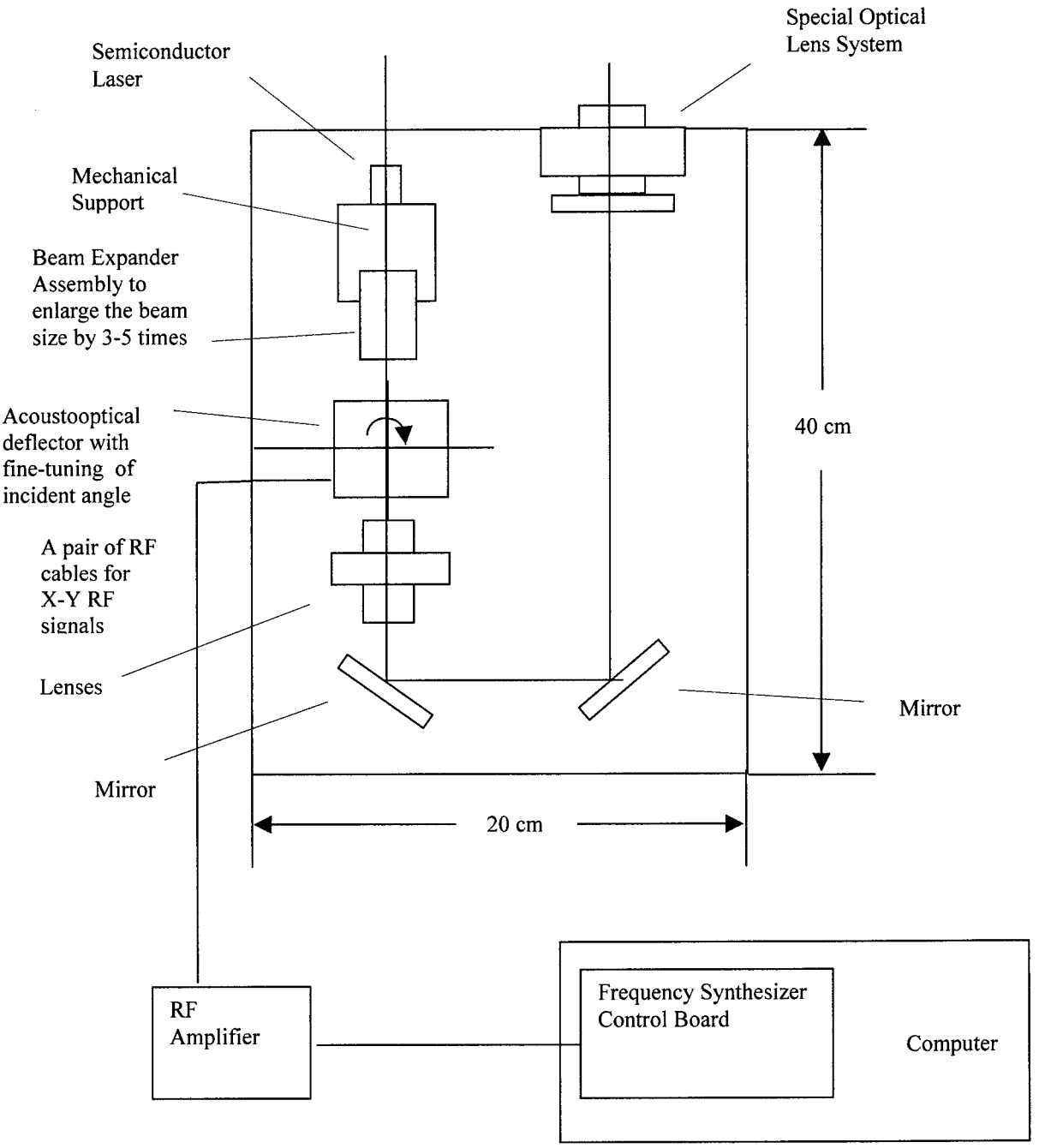

Figure 9 A picture of AOBD

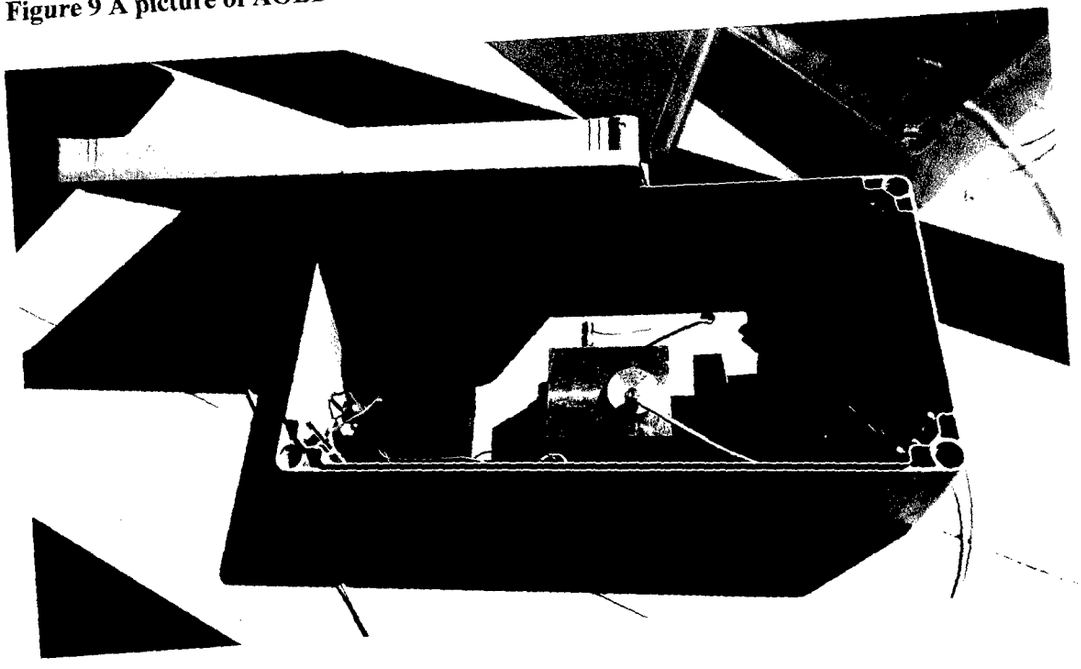

Figure 10 A light spot pattern on a screen of the AOBD

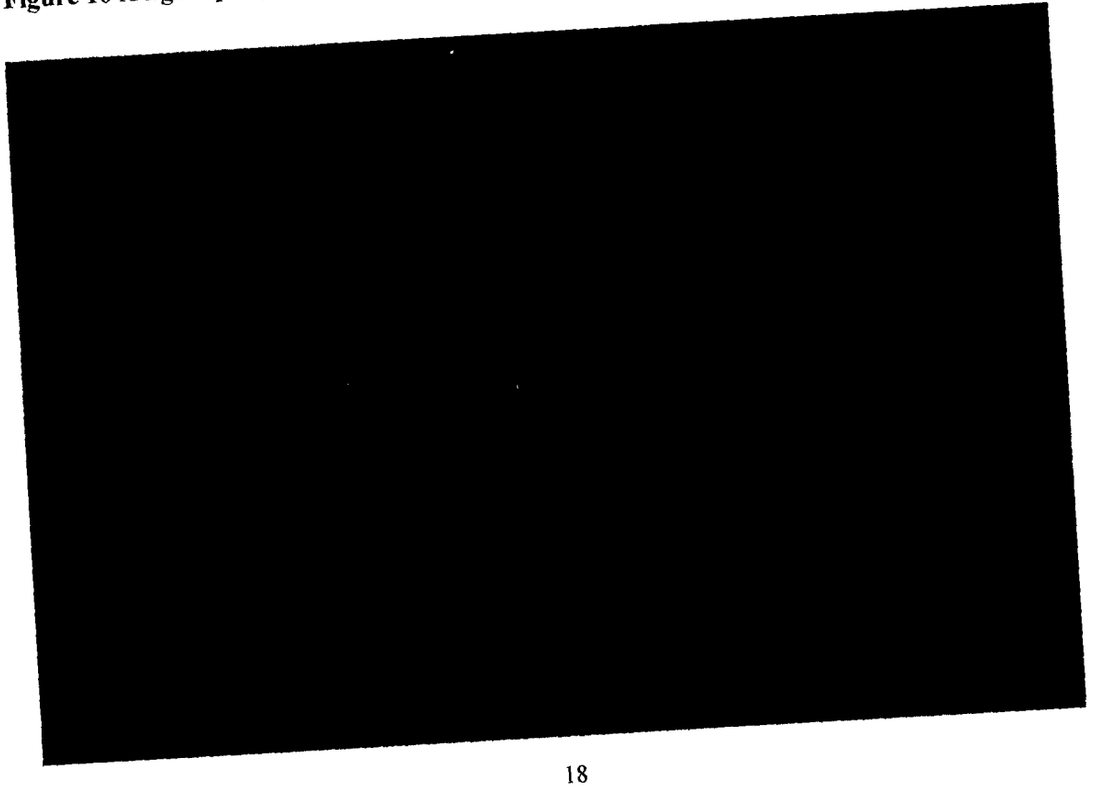

(2-c) The second type of light beam deflection system with full electronic control

The second approach for constructing a dynamic controlled light beam deflection system is based on the use of a lens system for the deflection angle amplifier.

In the first approach, a fiberoptic plate with a hemispherical configuration is used. Such a device is difficult to make, and is expensive because it is not a commercially available standard product.

For commercialization of the technology, we developed another approach: using commercially available lenses to construct a light beam deflection amplification system. Note that currently there does not exist any lens system that can provide a deflection amplification as large as required by the present application for delivering laser light beam to a broad field of view. The technology of dynamic control of a laser beam in a broad field of view is also very important for a number of commercial applications. The following is a brief review of background knowledge about light beam deflection amplification.

When we open any optics textbook and look for a lens system with the capability of amplifying the deflection angle of a light beam, we will find that only two such types of lens systems exist: Galilean and Keplerian. These two lens systems were invented in the 1600s for construction of telescopes and have been successfully used for more than 300 years without any important change [5][6]. The lens system for amplification of deflection angle is called an afocal lens system because it has a collimated light beam as input and a collimated light beam as output with the output beam deflection angle larger than that for the incident light beam.

When we try to use classic telescope lens systems for amplification of the deflection angle we found that the most severe problem is that the maximum output deflection angle that these lens systems can provide is too small. Typical maximum deflection angle is less than $\pm 10°$. Can the deflection angle be larger? We did a systematic survey, from the data of all the technical publications, the most recent commercial products, and through direct discussions with the vendors of state-of-the-art systems. All the data uniformly show that current afocal lens systems cannot provide a larger output deflection angle.

For the present application for 6D measurements in airplane tests, the maximum output deflection value of $10°$ is too small. For many commercial and military applications, the maximum output deflection value of $10°$ is also too small. Is it possible that the deflection angle of the classic telescope lens system can be improved? This seems to be a formidable task because, for 300 years, there have been many efforts to improve the telescope lens system, but improvement has been very limited [7].

However, when we look at other area of optics, we see some important hints on how to solve the problem. In the 1860s cameras were invented. Cameras use a lens system called an imaging lens. Early cameras had a very small field of view. After incremental

development for nearly 100 years, wide-angle imaging lens systems were developed. Since the 1970s and 1980s, very wide-angle imaging lens systems have been developed. In modern cameras, a standard imaging lens system usually can cover approximately ±20°. A good commercial wide-angle imaging lens can cover ±45°. Special wide-angle imaging lens, such as "fish eye" imaging lens, can cover as much as ±90°. An imaging lens system is quite different from the light beam deflection lens system. One notable difference is that the imaging lens system collects the light beam from "outside" (the far field) and gives a image inside (a near field). The light beam propagation direction for the light beam deflection lens system is just the opposite: the light beam is emitted from "inside" (the near field) to "outside" (the far field). But there are some connections, between the two systems and the history of wide-angle imaging system development provides important hints for us to develop a new type of lens system for deflection angle amplification with an extraordinarily wide output field of view.

(2-d) A new type of deflection angle amplification lens system

We realized that to develop a deflection angle amplification lens system with a large output angle, we cannot merely rely on the telescope lens systems with only incremental improvements. With all their excellent features for human eye interface, telescope lens systems have an intrinsic limitation in the maximum output deflection angle. We carefully analyzed the telescope lens structure and identified why it is impossible for a telescope lens system to provide a large output deflection angle [7]. This intrinsic limitation is analyzed in a U.S. Patent that we filed for the new type of lens system [8] and may be the real underlying reason why for several hundred years there were very limited improvements in telescope lens systems in terms of increasing the output deflection angle.

To develop an essentially new lens system with the capability of providing a large output deflection angle, we realized we must build a deflection amplifier with two-stage amplification. The first stage of amplification is essentially a telescope lens system, because this system can provide a satisfactorily large amplification factor (not a large output deflection angle).

The second stage of deflection angle amplification must be a lens system having certain salient features of a recently developed wide-angle imaging lens structure. The most important function of the second stage is to provide a large output deflection angle. The new type of deflection angle amplification lens system has a structure of two-stage amplification, and is substantially different than those of neither Galilean nor Keplerian lens systems. Thus, it is a new type of afocal lens system. The basic structure of the two-stage deflection angle amplifier is shown schematically in Fig. 11.

Figure 11 Basic structure of the new type of afocal lens system

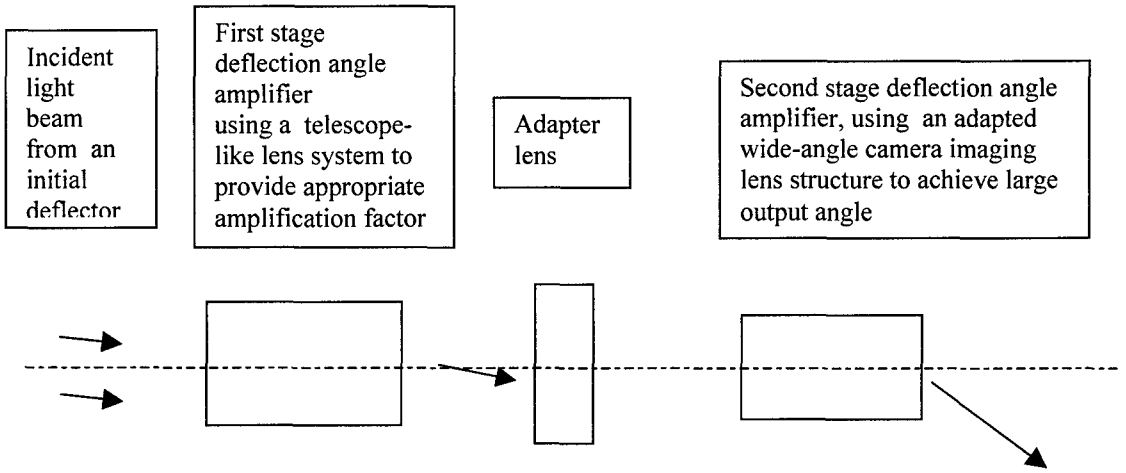

Figure 12 An illustrative lens structure of the new type of afocal lens system

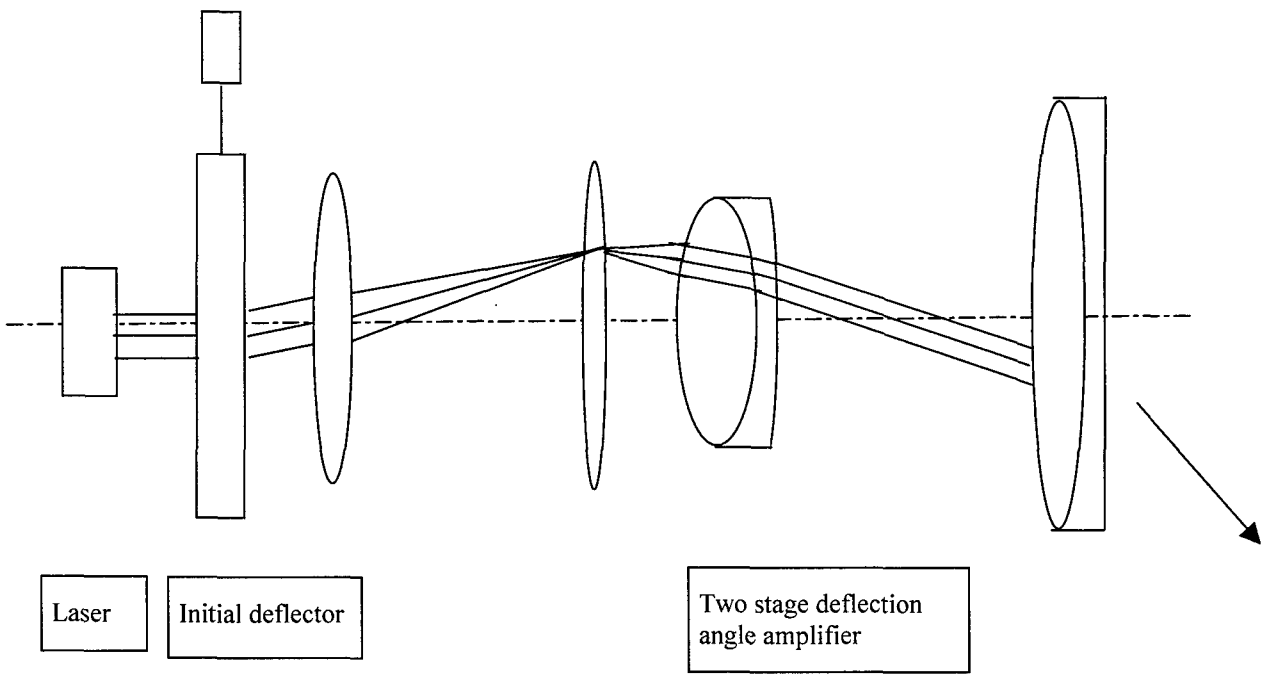

For the design of the second stage deflection amplifier, the development and design experiences for the wide-angle imaging lens system accumulated in the past 100 years provided a valuable reference. Although not all of these experiences of wide angle imaging lens systems are applicable to the present system, many concepts can be a good starting point, after certain adaptation, and extraordinarily large output deflection angles can be achieved.

We preliminarily tested the approach, which was successful. The experimental results will be reported elsewhere. The new type of lens system has been filed as a U.S. Patent [8]. The following is a summary description of the significance of the new deflection amplifiers.

With the successful development of the two-stage deflection angle amplifier with a large output deflection angle, a new type of deflection angle amplifier should become available in modern optics. The Galilean and Keplerian lens systems both have served their purposes for several hundred years. However, telescope lens systems are essentially for interfacing with human eyes, which do not require a large deflection angle [7]. This may explain why these lens systems survived several hundred years without important modifications. So the two classic types of afocal lens systems are "for eyes only" systems. They cannot meet the emerging new demand for laser light beam deflection. In modern optical engineering, the laser beam often must be delivered in free space to a large field of view. For meeting the new requirements of modern optical engineering we developed the third type of afocal lens system to provide a large output deflection angle, as large as to cover the entire half space ($\pm 90°$). We proved that such a lens system must have a two-stage amplification structure, and we successfully constructed such a lens system.

We believe this is going to be a fundamental breakthrough in optical engineering. This technology breakthrough provides a foundation for the 6D measurement system capable of measuring the 6D placement data with a large number of test assets and at an exceedingly high speed.

3. Development of a retroreflective modulator

(3-a) The need for development of a retroreflective modulator for 6D measurements

In the following we will first describe the necessity for development of a retroreflective modulator for 6D measurements. In this line, we will show that the need for development of a retroreflector with modulation capability is dictated not only by a single specific approach, such as by the present program, but also by any 6D measurement technique.

For performing 3D measurements, it has been established that at least one retroreflector must be mounted on the target. For example, in laser range-finder techniques, such as theodolite-based 3D measurement systems, it is necessary to use retroreflectors mounted on the target at a single point as a tag, so the 3D position parameters of a single point can be measured. For 6D measurements, multiple tags must be mounted on a single target, for determining the 6D parameters of a single target. To unambiguously differentiate multiple tags mounted on the same target, each tag must at least provide minimum information regarding its identification (ID) number. The retroreflector must have the capability of modulating light beam intensity. Hence the device must be a retroreflective modulator. The modulation capability becomes especially important when the number of the targets is more than one.

(3-b) Basic requirements of the retroreflective modulator for 6D measurements

The basic requirements of the retroreflective modulator for 6D measurements are:

(3-b-1) The retroreflector must have a sufficiently broad field of view.
Ideally, the retroreflector should be able to cover the entire outer hemisphere space, that is $\leq \pm 90°$, because the tag could be deployed in any orientation, and the target could be rotated at any angle position. If it is too difficult to achieve this projection, for the first devices, a field of view of $\leq \pm 45°$ may be appropriate for some preliminary experimental tests.

(3-b-2) The retroreflective modulator must be compact, lightweight, self-sustained in power supply, and draw little electric power.

This is because the tag must be mounted on the target without an external power supply.

(3-b-3) The retroreflective modulator must have sufficiently high modulation speed.

(3-b-4) The device must be controlled by an intelligent microprocessor.
This is because the device must execute rather complicated instructions. Only an intelligent microprocessor can do the job.

(3-c) Retroreflectors developed in the Phase II

In the present Phase II Contract, we designed, constructed, and tested two types of retroreflective modulators.

(3-c-1) Sphere-lens-based retroreflective modulator.

A sphere-lens-based retroreflective modulator was an ideal solution because of its largest field of view. We built a retroreflective modulator using sphere lens and a fiberoptic plate.
This configuration consists of a sphere lens and a fiberoptic plate with a hemispherical surface for exactly matching the sphere lens. The other side of the fiberoptic plate is flat, so the output surface can be conveniently interfaced to a broad range of light modulators. A typical modulator is a liquid crystal light valve. One surface of the liquid crystal modulator is in close contact with the input surface of the fiberoptic plate. The other surface has a mirror so the light energy, after passing through the liquid crystal modulator, undergoes a modulation. The modulation is controlled by an electric signal applied to the electrode pair sandwiching the liquid crystal material.

We fabricated the sphere lens, the fiberoptic plate and the liquid crystal modulator. However, we found problems with the device. The commercially available standard liquid crystal modulator must have a pair of glass substrates with sufficient thickness ($\geq$ 1 mm). The thick glass plate reduces the spatial resolution of the fiberoptic plate. To reduce the thickness of the glass plate, the standard fabrication process must be changed and an expensive special fabrication fee must be paid. So we must turn to a solution that can be constructed within our budget.

(3-c-2) Retroreflective modulator based on a wide-angle camera imaging lens, a fiberoptic plate and a liquid crystal modulator.

The structure principle is basically the same as that of a sphere lens. The liquid crystal modulator is placed between the fiberoptic plate and the wide-angle imaging lens. A mirror surface is deposited at the back of the fiberoptic plate. We prepared two types of liquid crystal valve: a conventional liquid crystal valve and a high speed liquid crystal valve. The conventional liquid crystal material is a nematic liquid crystal, which can only provide a switching time no faster than 20 ms. Using a conventional liquid crystal modulator the switching speed is too slow for the present 6D measurements. We designed and custom-made a ferroelectric liquid crystal material that can provide a switching time as fast as 35 μs. The following are some preliminary test results.

Fig. 13 is a picture of the retroreflective modulator structure. Fig. 14 shows the transmitted waveform of the liquid crystal modulator.

4. Development of an intelligent two-dimensional direction-resolvable photo-detection system

A direction-resolvable photo-detection system is different from a conventional image system in that the former records only the data for determining the direction of the incident light beam, which usually involves only few pixels, while the latter requires a complete set of image data that may involve millions of pixels. For measurements of position and orientation of an object, only a few pixel data can provide a complete set of information. Thus, the photo-detection system is direction-resolvable, but there is no need to contain a complete set of imaging data. Appropriate design of the photo-detection system can simplify the detector system enormously.

The 2D direction-resolvable photo-detection system has a pair of linear image sensors configured to be essentially perpendicular to each other. When a collimated light beam is incident on the surface of the lens, the light beam is focused to be a line on the focal plane. The linear sensor is essentially perpendicular to the focal line and always crosses the focal line at a point. The crossing point recorded by the linear sensor has the greatest signal intensity and can be evaluated through finding the position of the maximum signal intensity. So, a collimated light beam gives a pair of coordinate data as recorded by the linear sensor pair; the data pair gives the direction of the incident light beam.

In this section, we will present:

(4-a) A brief description of the photo-detector.
(4-b) The problem of low detection sensitivity in 6D measurements and the way we solved the low sensitivity problem.
(4-c) A brief review of the embedded microprocessor controlled photo-detection system.
(4-d) An outline of the major steps for using the microcontroller in the photo-detection system.
(4-e) A brief description of the target photo-detection system.
(4-f) A brief description of the photo-detector jointly controlled by the PC-MPIC.

(4-a) A brief description of the photo-detector

The photo-detector system is built in a light-tight plastic box. A spectral line filter is placed in front of the lenses so only the laser light beam can be recorded, and the background light is effectively removed.

A Fresnel lens was chosen as the cylinder lens because Fresnel lenses have a thickness suitable for combining a number of lenses into a lens with short focal length value. The Fresnel lens used in the photo-detection system is 20 mm x 20 mm, with approximately 20 mm focal length. Two such lenses combine to give a lens system with approximately a 10 mm focal length. Since the linear sensor has a length of approximately 10 mm, the field of view of the photo-detector is approximately ±45°. The lens system can have more Fresnel lenses to provide a larger field of view.

Figure 15 Layout of the direction-resolvable photo-detector

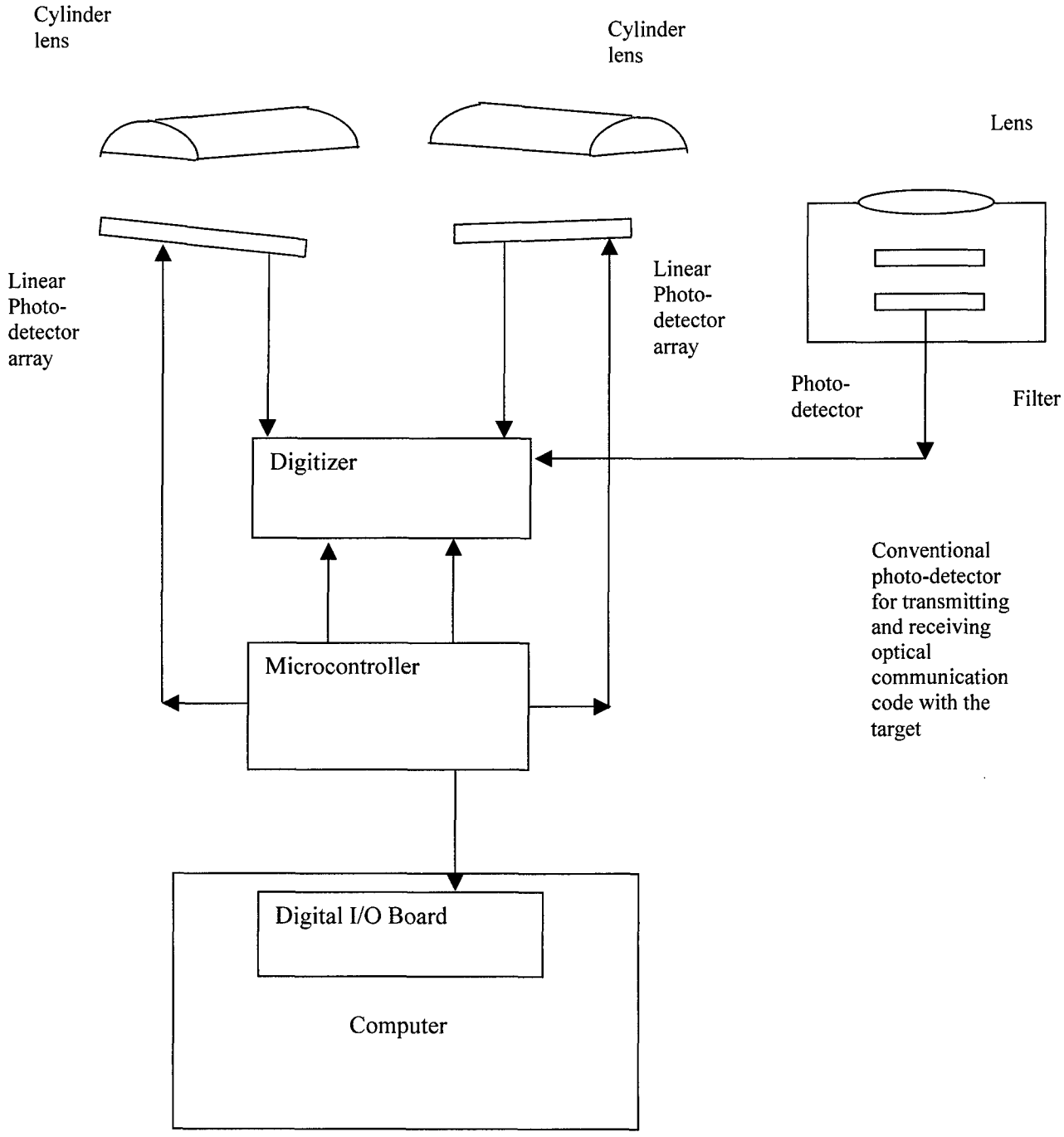

(4-b) The problem of low detection sensitivity in 6D measurements

The linear sensor used in the photo-detection system was a linear CMOS image sensor. In principle, any linear image sensor can detect the maximum intensity of the array. However, in Phase II we found that conventional linear image sensors have a problem of low sensitivity. The sensitivity problem and the way we solved the problem are described below.

When using conventional linear image sensors for 6D measurements, there is a problem with the photo-detection sensitivity: it is very low. The problem is caused by insufficient collection of incident light. For the linear image sensor to work, normally a cylinder lens is used. The cylinder lens focuses the collected light energy into a bright line crossing the axis of the linear image sensor. As shown in Fig. 16, the light energy received by the photo-diode cells in the photo-detector array is only a small portion of the light energy collected by the lens. As shown in Fig. 16, if the length of the focal line is L_f, and the pixel size dimension is L_a, the portion of the collected incident light is only (L_a / L_f). The ratio (L_a / L_f) is very small. For example, if L_a = 1 μ, L_f = 1 cm, then (L_a / L_f) = 0.0001.

Figure 16 Illustration of the low efficiency problem for a simple linear photo-detector

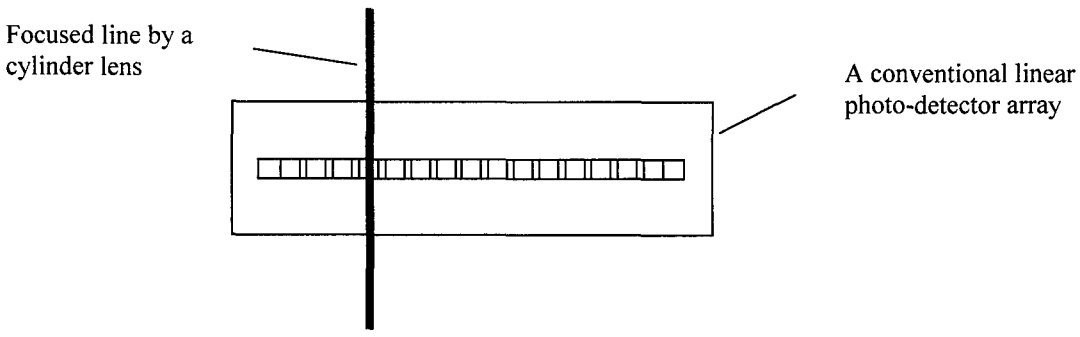

The way we solved the low sensitivity problem is by using a special photo-detector design called a spectroscopy line photo-detector array. This array has a photo-diode cell shape at one dimension that is substantially larger than the other dimension. Photo-detector arrays with such a structure were constructed for recording spectroscopic lines with high efficiency. Currently there are three vendors for the photo-detector arrays with the elongated pixel shape: EG&G, Hamamatzu, and Photon Vision. The commercial linear photo-detector arrays have a pixel number between 128 and 1,024. The size of a single pixel is approximately 10 μ x 125 μ, 10 μ x 500 μ, and 10 μ x 2,500 μ. A linear photo-detector array with a pixel number 1,024 and a pixel size 10 μ x 2.5 mm can substantially improve the light collection efficiency.

Note that the elongated pixel shape linear detector has a larger capacitance for the detector cells, hence the data transfer speed is not as fast. Even so, the speed is still reasonably high and suitable for the present application. The maximum data transfer speed is ≤ 5 MHz, or 0.2 μs per pixel.

Figure 17 Enhancement of the detection efficiency

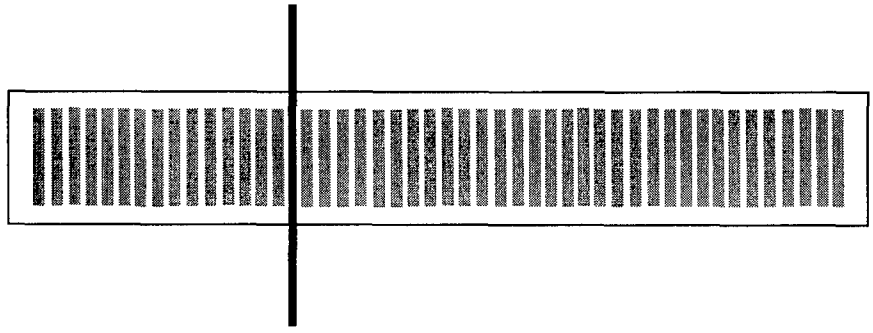

We chose the linear detector array from Photon Vision Systems, Inc. The detector has 1,024 pixels; each pixel is 10 μ x 128 μ. To transfer the recorded data from the detector, the detector has a number of mode settings. For the detector to work at the selected mode, appropriate signals must be applied to certain pins of the IC chip.

The linear sensor's driving circuit is shown in Fig. 18. The timing diagram is shown in Fig. 19.

Figure 18 Time diagram of the linear photo-detector array

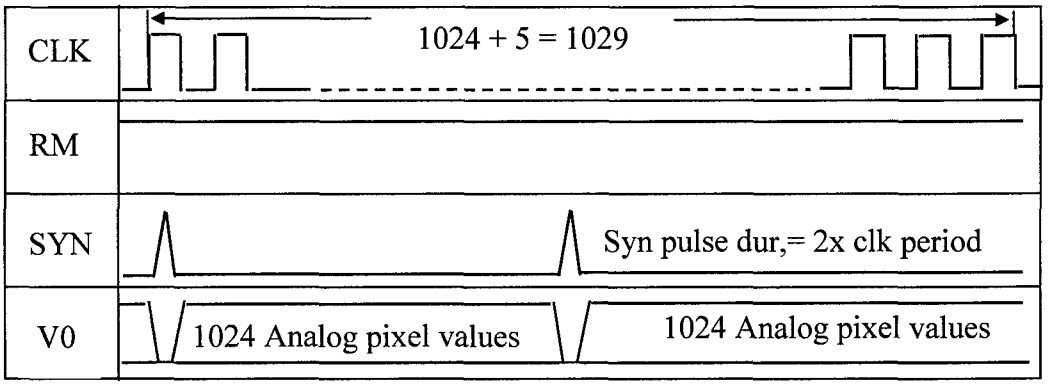

Figure 19 The operation mode setting of the LS-1024

Mode	RST	RMS	PRE	Pixel Reset /Integrating	Counter Reset /Normal	Read Mode
0	0	0	0	Integrating	Normal	Syn. Read, Cont. Integ.
1	0	0	1	Pixel Reset	Normal	Syn. Read, Async. Reset
2	1	1	0	DPR Reset	Normal	Syn. Read, Prev. Reset
3	1	1	1	DPR Reset	Normal	Syn. Read, Prev. Reset
4	0	0	0	Integrating	Reset	Asyn. Read, Cont. Integ.
5	0	0	1	Pixel Reset	Reset	Asyn. Read, Pixel Reset
6	1	1	0	DPR Reset	Reset	Asyn. Read, Prev. reset
7	1	1	1	DPR Reset	Reset	Asyn. Read, Prev. Reset

Figure 20 Control and driving circuits of the photo-detector array

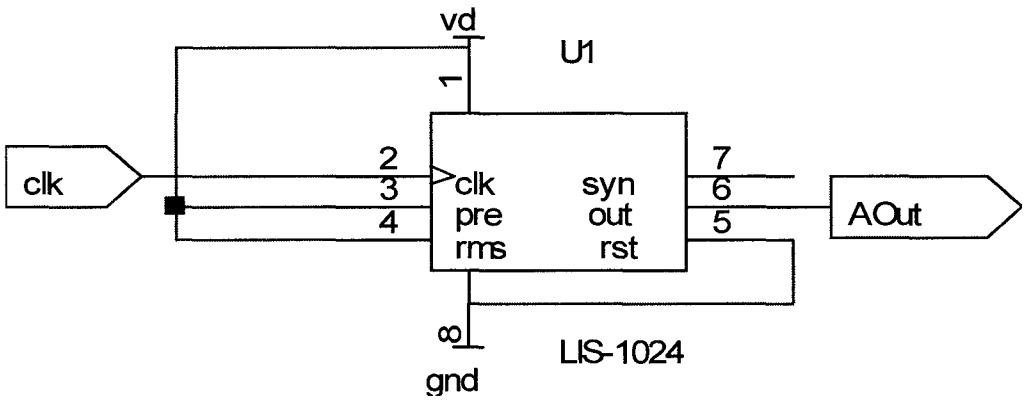

(4-c) A brief review of the embedded microprocessor-controlled photo-detection system

The most important feature of the photo-detection system is using a programmable microcontroller integrated circuit chip to control the operation of the photo-detection system. This intelligent system is not the same as conventional photo-detectors, which are usually controlled by a conventional electronic circuit without intelligence. The operation of the photo-detection system is a rather complicated process. As will be shown, it involves data acquisition, data processing, and data transmission. Generally, an electronic circuit is used to control the photo-detector. In the present case, it is impractical to use an electronic circuit to control the operation of the photo-detector, even though rather complicated electronic circuits are used. The photo-detector system must have a rather complicated intelligent operation, and the entire photo-detection system must be constructed in an extremely compact form. A very unique feature of the photo-detection system is the use of microprocessor control.

We developed two types of photo-detectors. The first is photo-detection for the station; the second type is the target photo-detector. Although they have certain similarities, their structures are quite different. A common feature is that they both use microprocessor control. The major difference is that the target photo-detector is completely controlled by its own microprocessor, while the photo-detector at the station is controlled jointly by its own microprocessor and by the computer.

We chose an embedded microprocessor PIC16C73A (microcontroller) as the basic component. The microcontroller PIC16C73A is an 8-bit microprocessor with a complete set of programmable capability, and a complete set of peripheral functionality.
The peripheral functionality includes I/O functions, built-in ROM for programming the

microprocessor in advance, built-in RAM for programming execution, communication capabilities, and various utility functions such as auto-shutoff, etc.

A schematic of the process block diagram is shown in Fig. 21.

Figure 21 A simplified block diagram of embedded microprocessor PIC67C73A

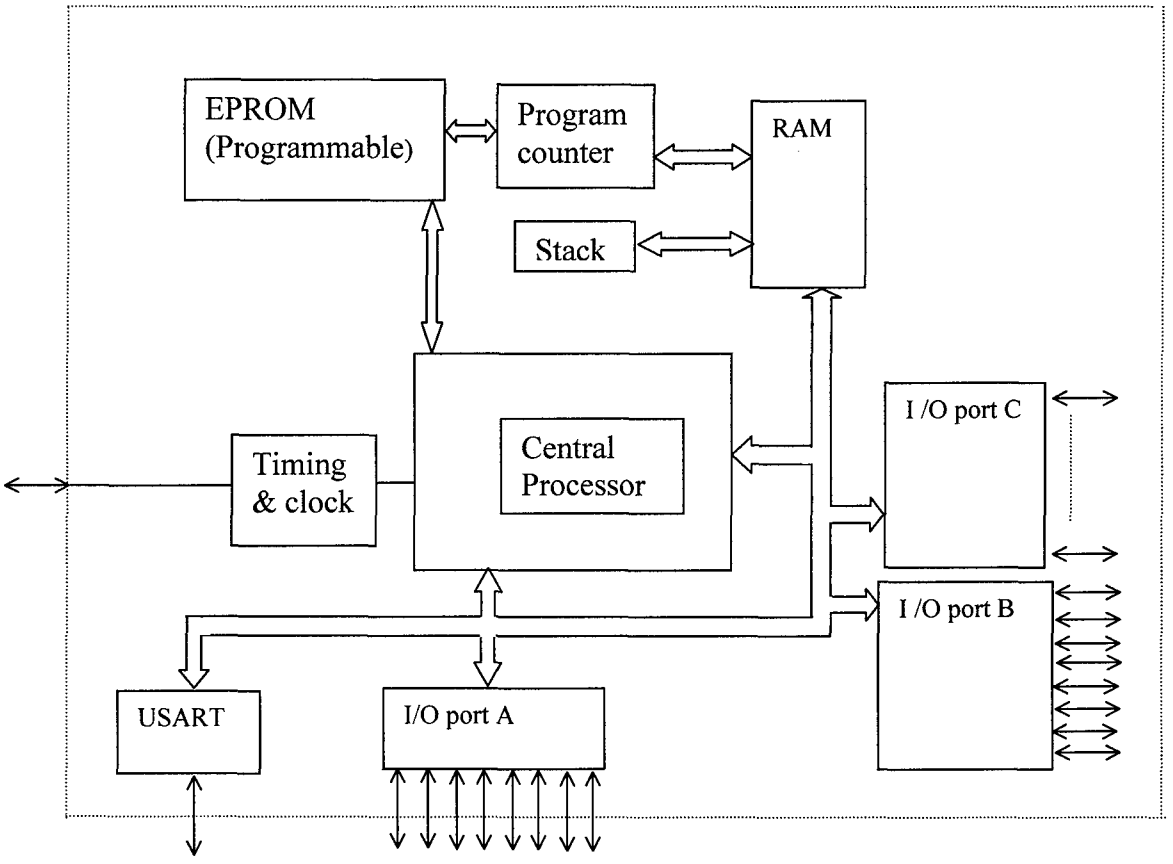

The microcontroller contains the following components:

a. A central processor with an 8-bit word length and working at a clock frequency up to 20 MHz.
b. A built-in Erasable Programmable Read-Only Memory (EPROM) with an 8 Kbyte capacity for storing the user-written program to be executed
c. An 8 Kbyte RAM for storing data and for a register file (for program execution).
d. A built-in clock pulse generator. For the operation of the clock pulses, only a standard crystal together with a minimum number of external capacitors are needed.
e. Three groups of I/O ports that can be programmed to provide any desired input and output signals for control of external objects. Each group (RA, RB, and RC) has either 8 pin or 6 pin input/output to connect to external electrical objects.
f. A number of built-in communication capabilities, including parallel and serial communication capability. Serial communication capability includes synchronous and asynchronous communication.
g. A built-in analog-to-digital converter with 8-bit resolution (256 levels of digitized data accuracy), and speed of 100 Ksamples per second.
h. Automatic power on-off mode to ensure that when the processor does not work for certain time, the power is lowered to be nearly zero at sleep mode, and returned to normal operation when a trigger signal is given.

Such a single processor has almost every functionality of a full-fledged modern microcomputer but is small, easy to use, and with a powerful functionality equivalent to a whole rack of electronic instruments. As a result, when the photo-detection system uses such an embedded microprocessor for control, the photo-detection system can execute complicated data acquisition, data processing, data transmission, and data receiving.

(4-d) An outline of the major steps for using the microcontroller in the photo-detection system

The first step is to be familiar with the microcontroller documents. It is extremely important to be familiar in great detail with the chip, including hardware and software. Because the programming is at the assembly language level, the user must plan, design, and give instructions to the chip before any reliable control of the chip can be performed.

The second step is to design the circuit.

The third step is to provide a flow diagram and a timing diagram to specify each operation of the microcontroller.

The fourth step is to write a program in the specific assembly language and to compile and to debug the program in advance. Such a program is developed using a standard PC in the Windows environment. The software for developing such programs can be purchased from manufacturers of the microcontroller chip.

The fifth step is to inject the program into the microcontroller. The steps for injecting the

program into the microcontroller are:

(1) Using a special UV lamp to illuminate the microcontroller at the UV- sensitive window for about 5 minutes, so the read-only memory inside the microcontroller is cleared;

(2) Using a special device programmer provided by the microprocessor vendor, to inject the program (originally developed and stored in the PC) to the chip. In the present case, the device programmer is "PIC Start Plus" programmer by Microchip Incorporated. The Programmer has a socket for the microcontroller to be plugged in, and has a connection to the PC through the serial port. The operation of the programmer is through a special software, MPLAB, provided by the manufacturer. The software checks all items to make sure that the conditions are correct, compiles the assembly language program into a hexadecimal format, and injects the user-developed object program into the device.

(3) After the program injection, the software also double-checks and verifies that the injected program does not have any bugs.

(4) After the microcontroller chip has received the program, the chip will be ready for use in the designed circuit.

The programmed operation of the control can be tested by using oscilloscopes or logic analyzers for monitoring the selected representative signals. In developing the photo-detection systems, we used a digitizing oscilloscope Tektronics TDS 200, and Hewlet-Packard Logic Analyzer HP 1630G for monitoring the signals.

The following is a typical example of how to control the photo-detector through programming the microcontroller. Under the programmed control, the photo-detector can perform data acquisition, data transfer, and data processing on its own and is an intelligent photo-detector. Because the programmed control is directly through the microprocessor, the program is written in an assembly language provided by the microprocessor vendor.

Figure 22 A simple circuit diagram of MPIC-driven photo-detector array

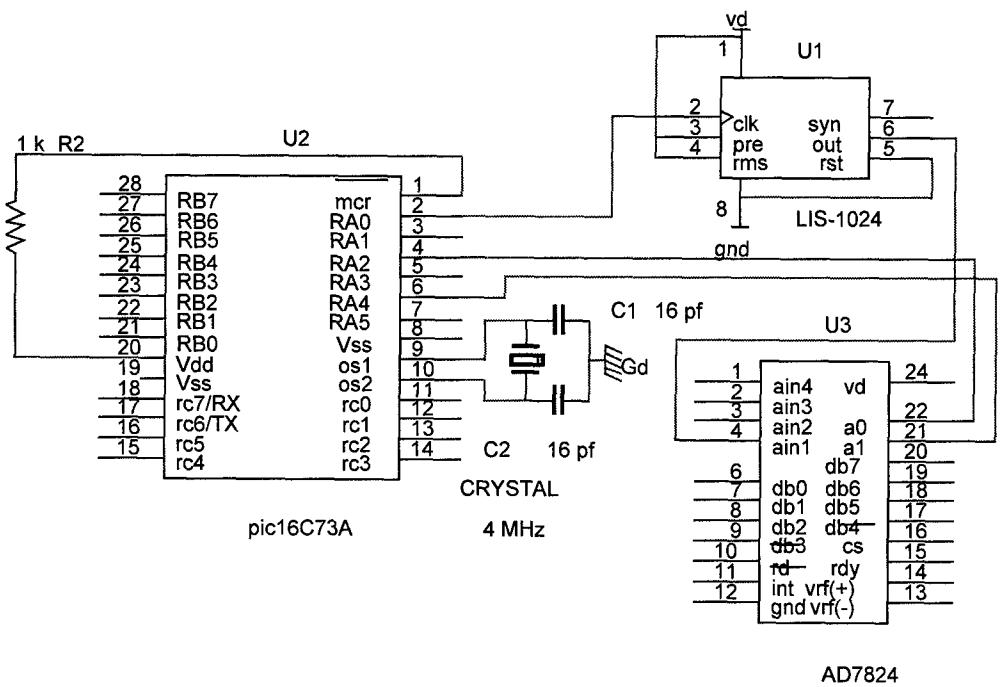

Figure 23 A simple program for MPIC to provide driving signals to the photo-detector array

```
;*****************************************
;    Filename:       acqid.asm
;    Date: 12-07-99
;*****************************************
          list      p=16c63a     ;
     #include <p16c63a.inc> ;
          __CONFIG   _HS_OSC&_WDT_OFF
; VARIABLE DEFINITIONS
pixeltemp  EQU     0x20        ;
;*****************************************

          ORG       0x000      ; prcsr reset vctr
          goto           main             ;
          ORG       0x010
main      bcf       STATUS,RP0            ;Bank0
          clrf      PORTA
          clrf      PORTB
          clrf      PORTC      ;Must for TRISC
          bsf       STATUS,RP0             ;Bank1
          movlw     B'11111111'
          movwf     TRISC ;<7:6>     ; Must be set!
          movlw     B'00000000'
          movwf     TRISA
          movlw     B'11111111'
          movwf     TRISB
          bcf       STATUS,RP0  ;Bank0
pccmd
          movlw     B'00000000'       ;ADC chnl0
          movwf     PORTA

          movlw     B'00000000'      ;Clk for lis1

          movlw     B'00000000'      ;RA2=RA4=0:address
          movwf     PORTA
          movlw     B'00001000'      ;RA3=1:latch addrs
          movwf     PORTA

          movlw     B'00000000'      ;RA3=0,start digitz
          movwf     PORTA
          goto      pccmd
          END
```

Figure 24 Illustrative output signals from MPIC

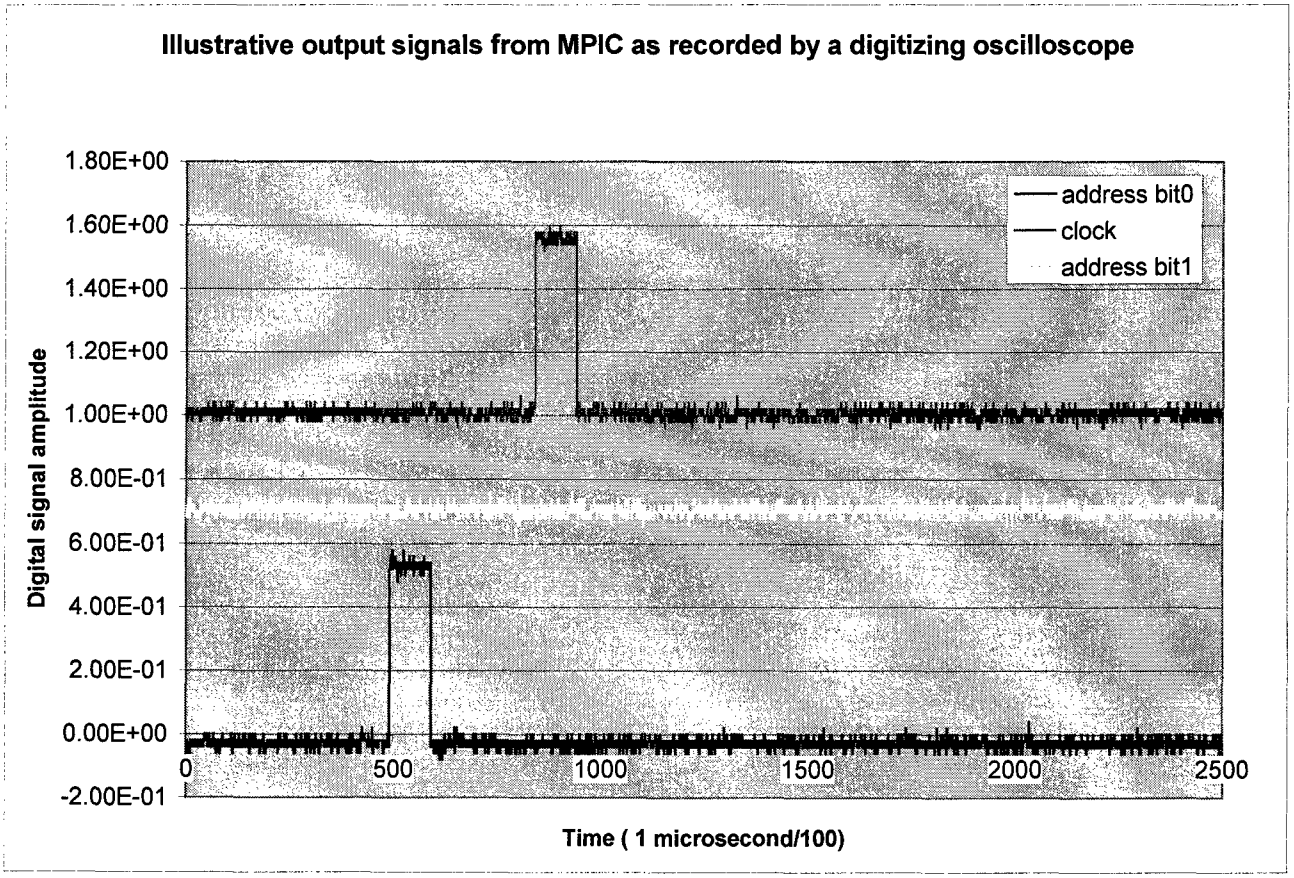

(4-e) A brief description of the target photo-detection system

The target photo-detection system consists of:

a. A pair of linear image sensors each having 1,024 pixels
b. An external analog-to-digital converter. Although the microcontroller has its own built-in analog-to-digital converter that can be conveniently used for digitizing the signal from the image sensors, the speed required by the present system is higher than that can be achieved by the built-in ADC. The built-in ADC has approximately 100 K samples per second, while the present case requires more than 1 Mega samples per second. Thus, an external ADC was used in the photo-detection system for enhanced speed. The ADC was from Analog Devices AD7824. The chip has an 8 bit resolution, and a digitizing speed as high as 1 Mega samples per second. The external ADC has 4 channels that can be connected in parallel for the present case of two sensors.
c. A microcontroller PIC16C63A for control of data acquisition, data processing, data transmission, and data communication with the measurement station.

A block diagram of the photo-detection circuit is shown in Fig. 25.

Figure 25 A block diagram of the target photo-detector

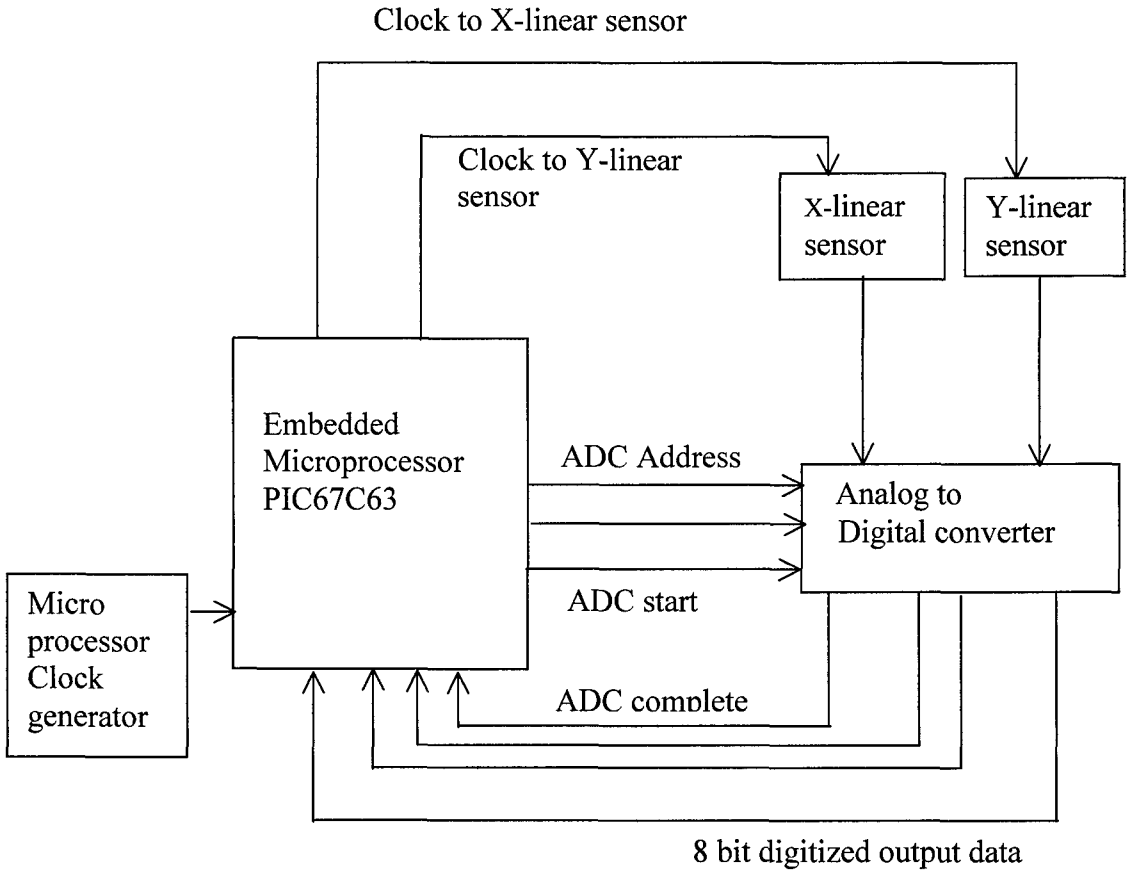

The flow chart diagram of the operation is shown in Fig. 26

Figure 26 The most basic flow chart diagram for an intelligent photo-detector array

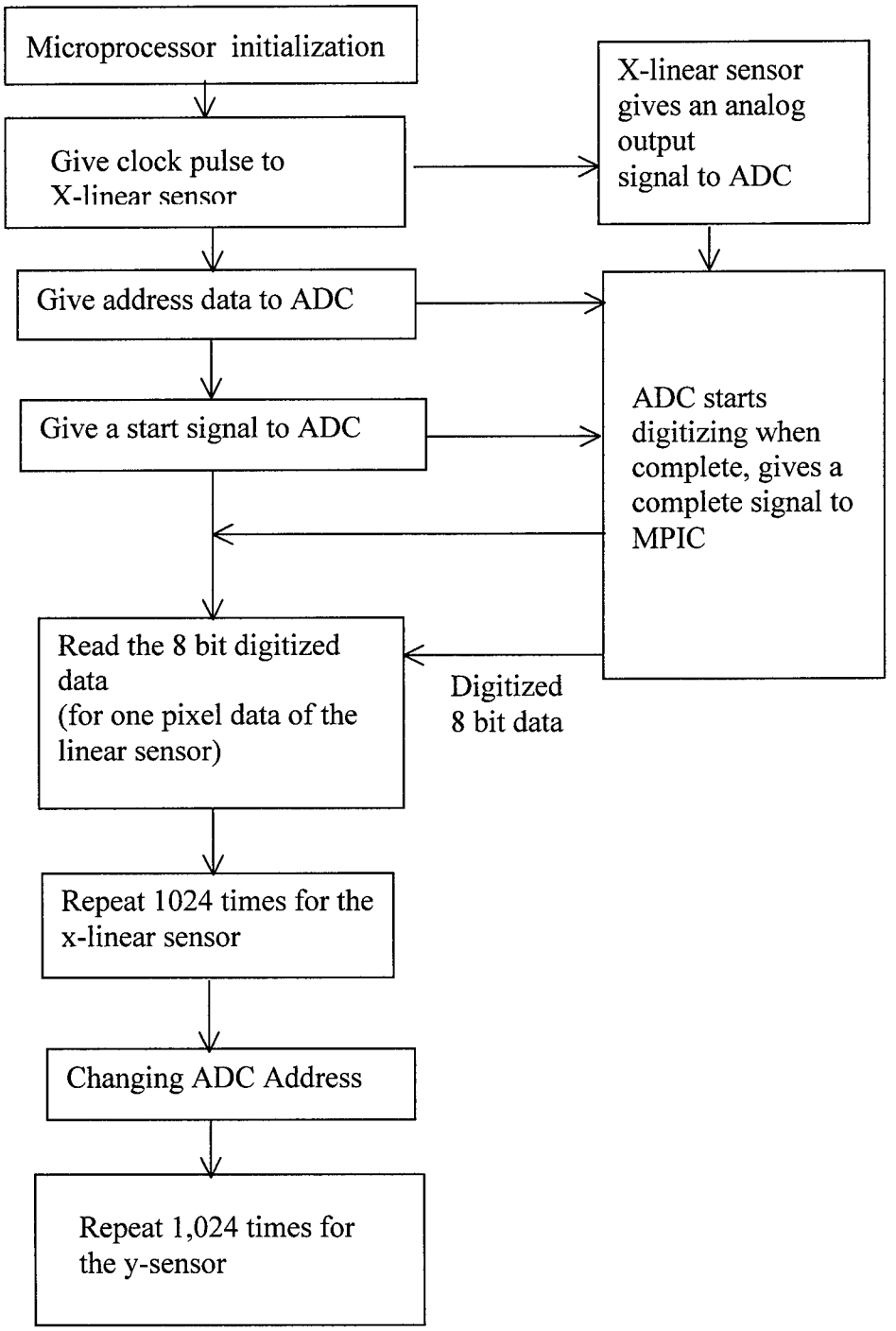

The circuit diagram is shown in Fig. 27.

Figure 27 A schematic circuit diagram of the target photo-detector array controlled by an embedded microprocessor

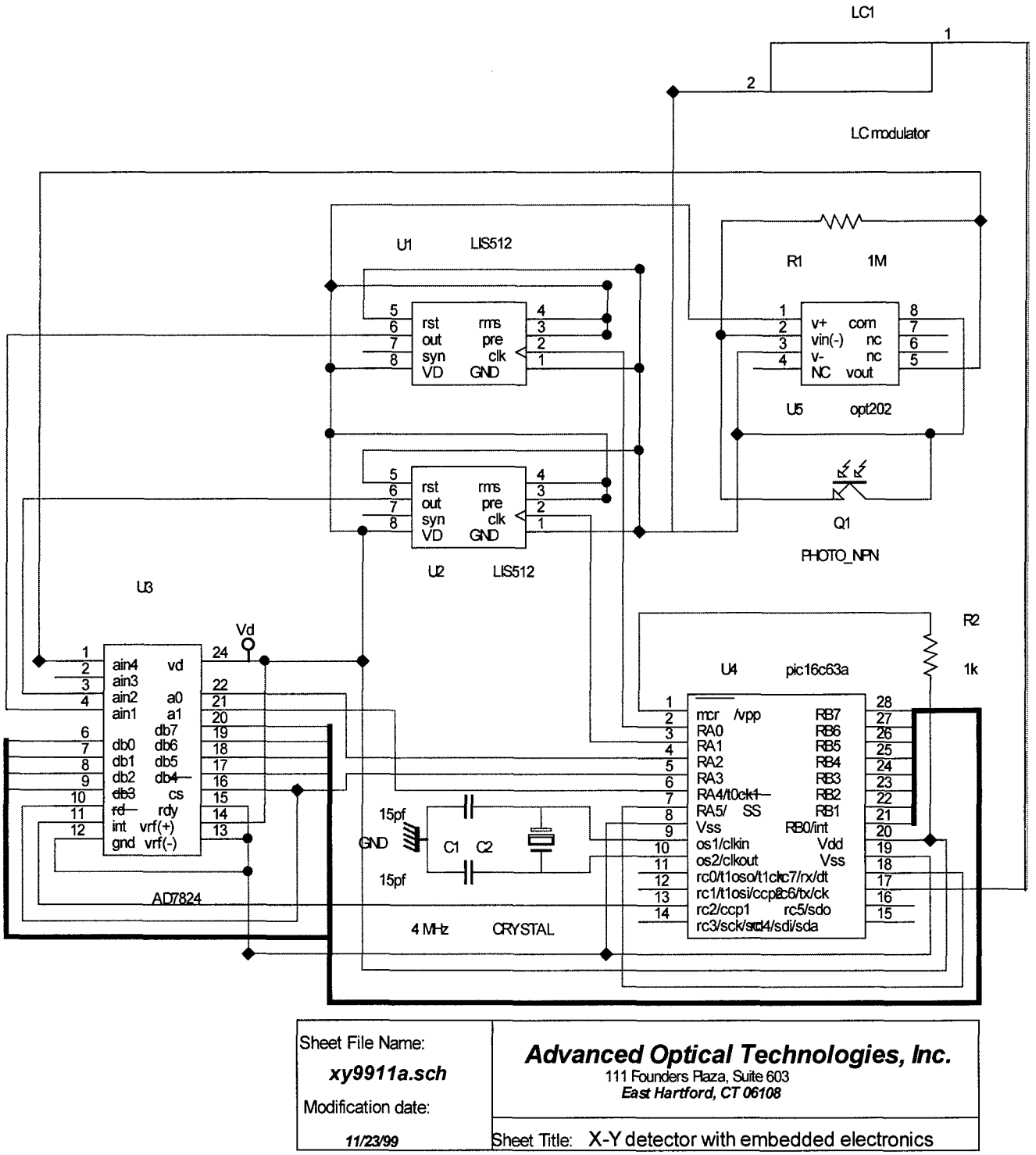

The acquired data from the linear detector array is shown in Fig. 28.

Figure 28 An illustration of the recorded analog signal from the output of the photo-detector array

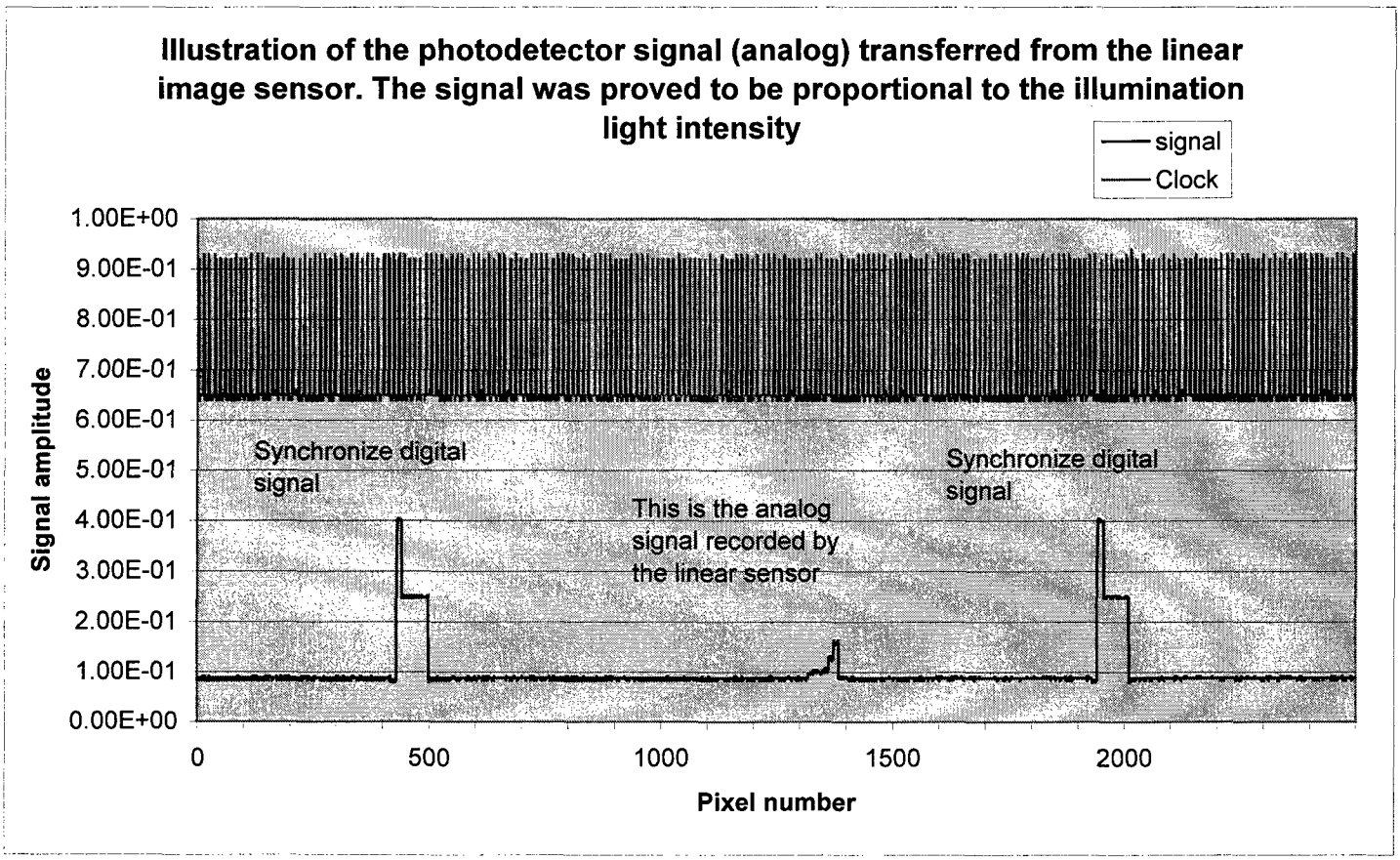

The program is shown in Fig. 29.

Figure 29 A program for control of basic data acquisition, data transfer and data processing of photo-detector array

```
;*********************************************
;     Filename:       acq00.asm
;     Date: 12-07-99
;*********************************************
      list      p=16c63a     ;
      #include <p16c63a.inc> ;
       __CONFIG    _HS_OSC&_WDT_OFF
;*********************************************
cnt1        equ   H'21'       ;at GPR location
cnt2        equ   H'23'       ;at GPR location
cntx        equ   H'25'       ;at GPR location
            ORG   H'01FF'     ;blindly copied
            goto  main

            ORG   H'0000'
main
            bcf   STATUS,RP0        ;Bank0
            clrf  PORTA
            clrf  PORTB
            clrf  PORTC             ;Must for TRISC
            bsf   STATUS,RP0        ;Bank1
            movlw B'11111111'
            movwf TRISC       ;<7:6> must be set!
            movlw B'00000000'
            movwf TRISA       ;RA: out
            movlw B'11111111'
            movwf TRISB       ;RB:in

            bcf         STATUS,RP0 ;Bank0
strt1a:     movlw       H'5'       ;32 cycles
            movwf       cnt2
loop1a:     movlw       H'5'       ;32 cycles
            movwf       cnt1
                                   ;following:acquire a pixel data
acq1a:      bcf         STATUS,RP0       ;Bank0
            movlw       B'00001000'      ;ADC chn1(RA2=RA4=0)
            movwf       PORTA            ;RA3=1 as initial value
            movlw       B'00001001'      ;ADC chn1;clk for D1
            movwf       PORTA
            movlw       B'00001000'      ;ADC chn1
            movwf       PORTA
            movlw       B'00000000'      ;ADC chn1
            movwf       PORTA      ;start digitizing
```

```
            decfsz      cnt1,1
            goto        acq1a       ;repeat 32 times for ls1
            decfsz      cnt2,1
            goto        loop1a      ;totl 32*32=1024 cycles
add1ax:     movlw       H'05'       ;additnl 5 cycles for 1029
            movwf       cntx
acq1ax:     bcf         STATUS,RP0 ;Bank0
            movlw       B'00001000';ADC chn1(RA2=RA4=0)
            movwf       PORTA       ;RA3=1 as initial value
            movlw       B'00001001';ADC chn1;clk for D1
            movwf       PORTA
            movlw       B'00001000';ADC chn1
            movwf       PORTA
            movlw       B'00000000';ADC chn1
            movwf       PORTA       ;start digitizing
            decfsz      cntx,1      ;after 1024+5=1029
            goto        acq1ax      ;next starts ls1 dummy cycle
            goto        strt1a      ; start from very begining
            END
```

The basic operation sequence of the target photo-detection system is as follows:

1. The microcontroller provides all the driving signals for the operation of the linear image sensor pair. For operating the linear image sensor, it is required that 1,024+ 5=1,029 clock pulse is provided as a cycle for acquiring a frame of image data. The clock pulse is applied at pin 2 of the linear sensor. The output analog signal from the linear image sensor is sent through the pin 6. The other pins are connected either to a constant positive level or constant ground voltage level.
2. The microcontroller provides signals for the ADC to complete the data acquisition and data digitizing and data transfer to the microcontroller.

a. First of all, the microcontroller shall provide the address signal to the ADC for the ADC to select the right channel for data acquisition and data digitizing. There are 4 pins in the ADC for selection of channels 1, 2, 3, 4. The control of the channel selection is through the PIC RA0 pin and RA1 pin of the microcontroller.
b. The microcontroller then provides the clock signal to the linear sensor for data acquisition, so the signal from the sensor goes to the ADC, either channel 1 or channel 2.
c. The microcontroller further provides a command for the ADC to start digitizing. This is implemented through pin RA3, the positive signal causes the ADC to start digitizing.
d. The microcontroller waits for completion of the digitizing. The flag signal for completion is the rise of the voltage level at the ADC pin "/int". With the application of the start digitizing signal, the voltage level of the pin /int is automatically lowered to 0, and with the completion of the digitizing, the level of the /int is automatically raised to positive.
e. With the flag signal /int raised to positive, pin rc2 receives the flag signal acknowledging the completion and becomes ready to send the digitized data from the ADC to the microcontroller.
f. The ADC's 8-bit output digital data is connected to the RB port of the microcontroller (MPIC), and the MPIC receives the 8-bit digitized data. Then MPIC transfers the data into a file register inside the microcontroller.
g. The microcontroller then can further process the data from the linear sensor.

One procedure for processing the data is to go through all the 1,024 pixel data and select the pixel number where the signal intensity has the minimum value, so the direction of the incident light beam is determined by the microcontroller. Then the MPIC transmits the pixel number to the PC measurement station.

Another optional procedure is to directly transmit each pixel data to the PC measurement station and let the PC station do the further data processing. We chose the second approach so each pixel data from the linear sensor is transmitted to the PC through the MPIC's communication function.

(4-f) A brief description of the photo-detector controlled jointly by PC and MPIC

For the photo-detector placed near the PC at the measurement station, the hardware and software are quite different from those for the target detector. The PC photo-detector must be under direct control of the PC, and the acquired data must be eventually transferred to PC. On the other hand, the photo-detector must rely on the microcontroller (MPIC) to perform data acquisition, data transfer and conduct communication with the target photo-detector. Thus, this must be a dual-microprocessor-controlled system, which is far more complex than a single microprocessor control. So, the PC-MPIC jointly controlled photo-detector needs special attention.

The basic operations are: (1) Under the PC command, start data acquisition; (2) Because the photo-detector also has its own built-in embedded microprocessor, the embedded microprocessor must work together with the PC in all operations. Each time the PC completes an operation, the PC must give a flag/signal to notify the MPIC. Each time the MPIC completes an operation, it must also notify the PC; (3) The acquired data must be transferred to the PC memory for the PC to process.

The PC control over the photo-detectors is through a digital Input/Output (I/O) board installed inside the PC. The driver functions in C++ language for the I/O board under the Microsoft Windows environment and is provided by the vendor. Specifically, the I/O board used in the present system is the PCI 48 digital I/O board made by CyberResearch (New Haven, CT). The driver functions are collected in a Universal Driver Library provided by CyberResearch.

A typical circuit diagram is shown in Fig. 30, A schematic circuit diagram of a PC-MPIC dual processor controlled photo-detector array.

Figure 30 A schematic circuit diagram of a PC-MPIC dual processor controlled photo-

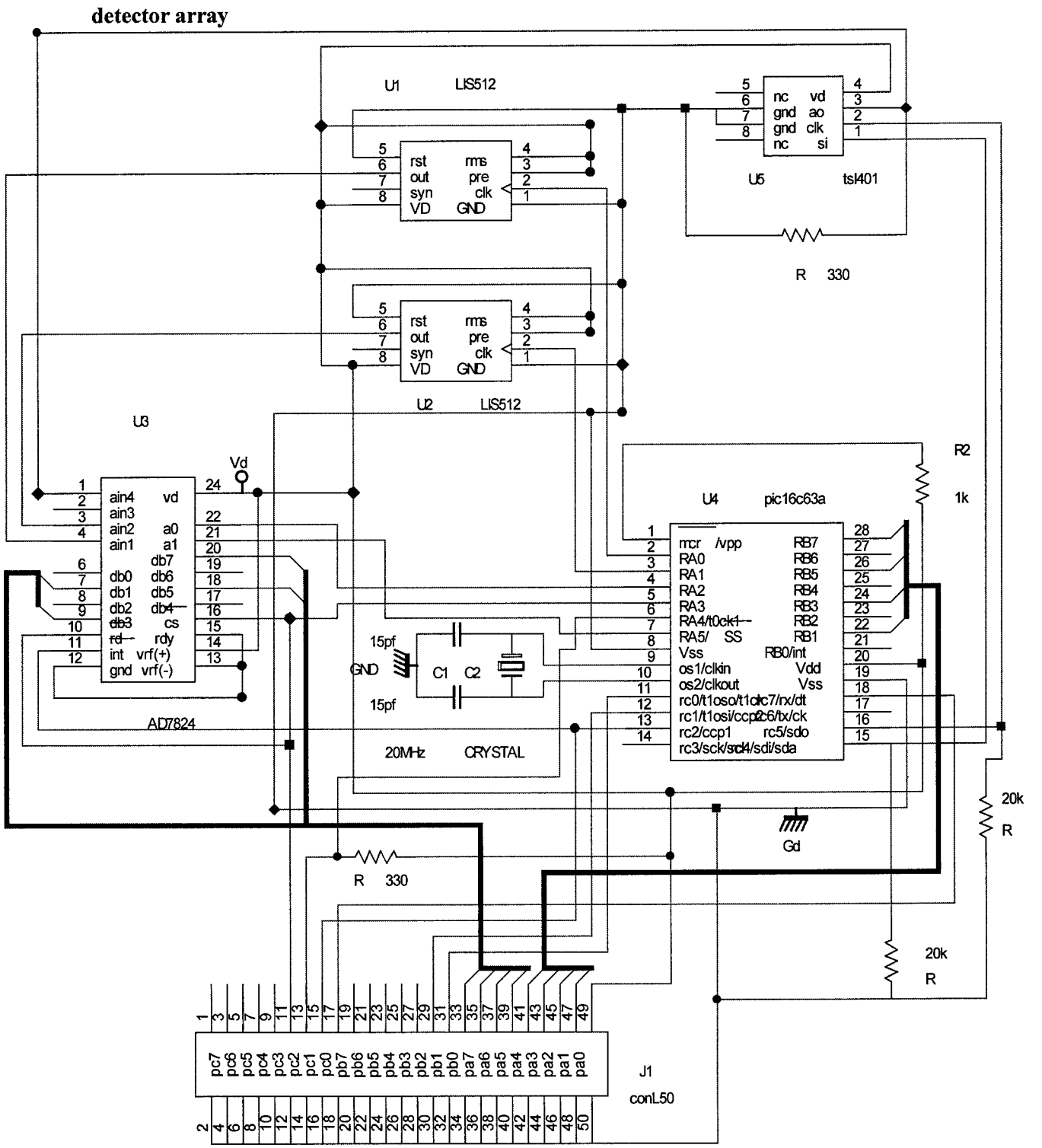

Sheet File Name: *xy008.sch*	***Advanced Optical Technologies, Inc.***
Modification date: *8/7/00*	111 Founders Plaza, Suite 603 *East Hartford, CT 06108*
	Sheet Title: X-Y detector with embedded electronics

The following is a flow chart diagram, where the PC and the embedded MPIC interactively control the data acquisition of the photo-detector arrays.

Figure 31 A flow chart diagram of the procedures for the PC-MPIC interactive control of the data acquisition of the photo-detector array

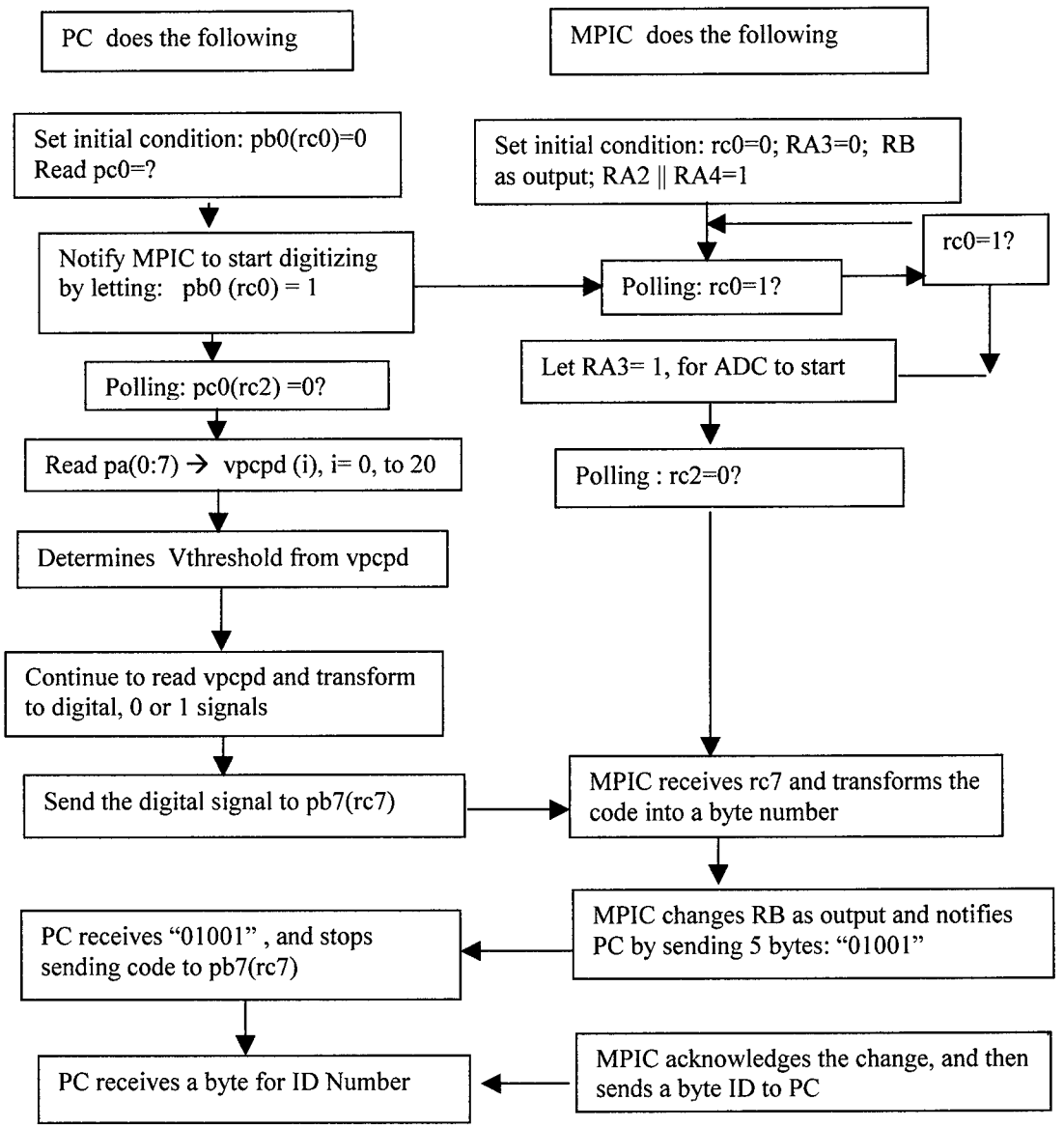

The following is a brief description of the block diagram for PC-MPIC joint control of the photo-detectors.

1. PC set default: pb0 (rc0)= 0; MPIC set default: Set initial condition: RB as input, rc: input; RA: output;RA3=0 RA2 || RA4=1
2. The photo-detector continuously sends signals to ADC analog input channel ain4
3. PC notifies MPIC to start digitizing by letting: pb0 (rc0) = 1
3. MPIC polling whether rc0=1?
4. If rc0=1, MPIC prepares for digitizing by setting ADC address: RA2=1 and RA4=1
5. MPIC starts ADC by letting RA3 =1 (Initial condition: RA3=0 control of /cs/rd of ADC).
6. PC polls if pc2(RA3)=1; after RA3=1 is confirmed, let pb0(rc0)=0;
7. MPIC then waits for PC status by polling: whether pb0 (rc0) = 0
8. PC polls if pc2(RA3)=0; when pc0(rc2)=0, PC reads pa(0:7)
9. PC goes to the beginning to start another round of data acquisition

Two programs are working cooperatively. The first program is executed by the microcontroller, and the program is written in an assembly language to control the operations of the microcontroller. The second program is executed by the PC and written in Microsoft C++ (version 6.0). The programs are rather long and will not be listed here but will be attached to the present report on disk.

Because of the dual microprocessor joint control of the photo-detection system, the control is a complicated process that requires careful programming and testing. Each step of the operation must be individually tested before any further steps can be taken. At each step, multiple signals are monitored by a logic analyzer to make sure that all the monitored signals are exactly as designed. The following is an example of the monitor signal taken from different critical points to show that the program operation is correct. (Fig. 32, Fig. 33).

Figure 32 Recorded timing diagram of PC-MIPC joint control of the photo-detector array

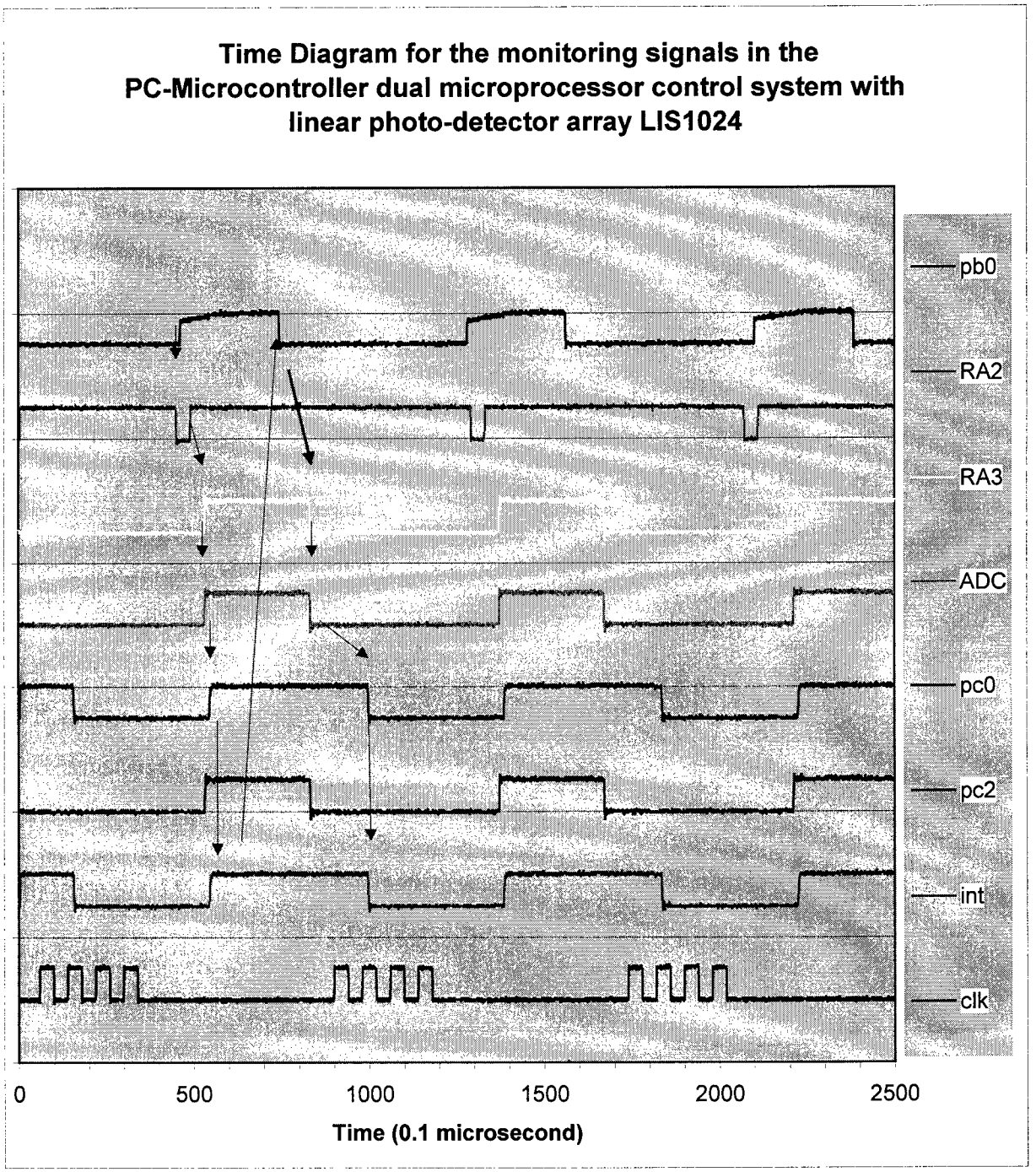

Figure 33 Recorded signal intensity in a digitized form for the photo-detector array

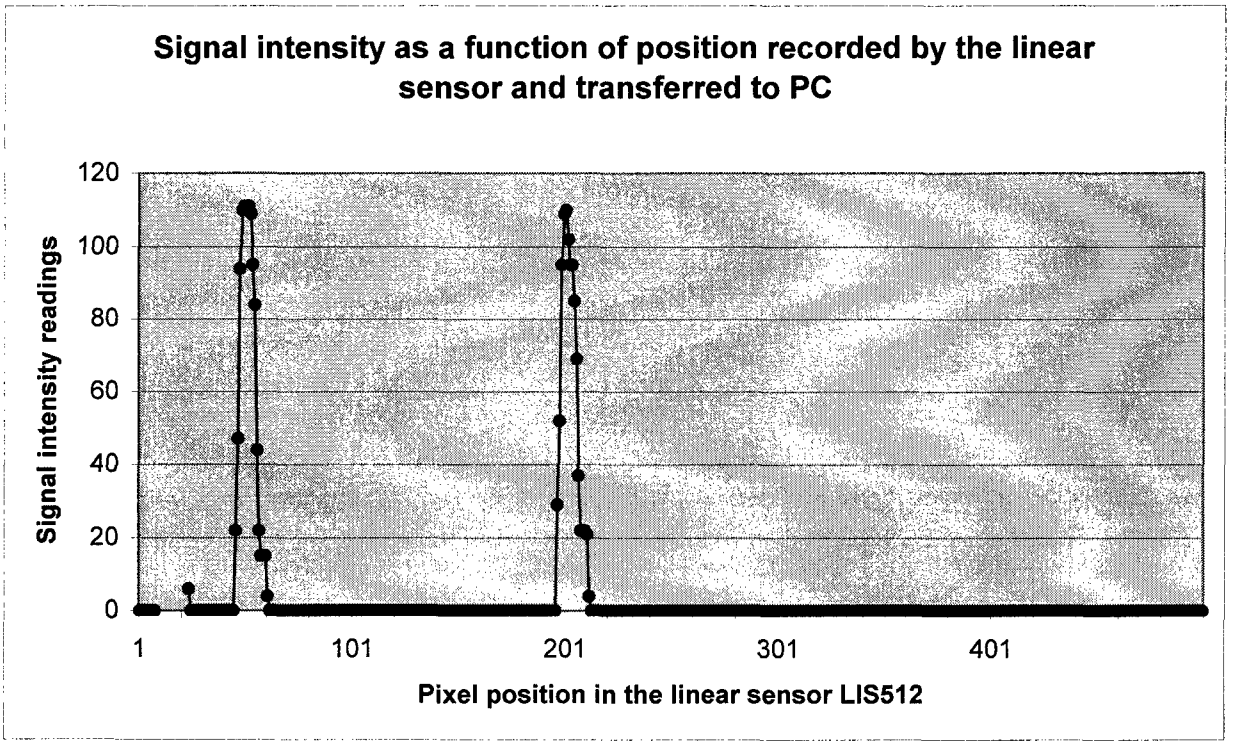

(5) Development of a communication link between the target and the PC station

(5-a) The need for the development of a communication link between the target and the PC station

For performing 6D measurements, a communication link must be established between the target and the PC station. The signals recorded by the target photo-detectors must be transmitted back to the PC station. Thus, between the target photo-detector and the PC there must be some kind of communication. There are only two types of communication connections: wired or wireless. Wireless is preferable because it does not require any cables. However, for wireless communication, radio-frequency communication may not be allowed in the chamber. So, under anechoic chamber conditions, a free-space optical communication link is the most desirable form. Such a free-space optical communication link is not only specifically required for the present 6D measurement approach, it should also be required for any 6D measurement approach. The present program is intended to establish such communication link according to program needs.

(5-b) Basic technical components for a communication link

As for any other communication link, there must be at least three basic technical components for communicating between the target and the PC station.

a. A hardware communication interface at each side. The function of the interface hardware is to transmit or receive the digital code from the standard byte data format used by the computer.
b. A low level communication software interface segment for translating the transmitted or received digital code into the data in a recognizable format. The software interface together with the hardware interface determines a communication protocol.
c. A high level communication software program to control the communication.

These components are necessary to perform the simplest communication; otherwise, the data would not be recognizable, and errors will be produced.

In the present system, we chose to use the microcontroller's built-in communication port as the interface hardware. Because of this, we do not need any additional hardware. There are several built-in communication ports in the microcontroller; we chose the serial port because it is the simplest. The communication protocol chosen is Universal Asynchronous and Synchronous Receiving and Transmission (UASRT).

The microcontroller has a unique built-in capacity to communicate through the UASRT protocol, a general protocol for communication used both in electrical and in optical communication. A brief outline of the UASRT communication protocol is as follows.

When the microcontroller starts to transmit data, the data output is given at a transmission signal pin "TX" (pin 18), and a ground pin. The data transmission is through serial data transmission. For the data to be accurately received, a strict communication protocol must

be established and strictly observed by the transmitter and by the receiver. There is a general definition of the rules for the UASRT communication protocol. The major points are: First, the data transmission side and the receiving side must have a common frequency. Both ends must have the same bit rate. For the synchronous mode, the two sides have a common clock. We chose the asynchronous mode, which requires that each side has its own clock, but the two clock frequency must be approximately the same (within a few percent). Second, the data is divided into segments. Each segment contains ten bits for transmitting a single byte. Each segment has a start bit which is always positive, and a stop bit which is always 0. Between the start bit and the stop bit, there are 8 bits for a single byte of data. There is no parity bit, and no error check bit.

Note that such a protocol is different from the standard RS-232 protocol used in PCs, and the two systems cannot be directly connected. The differences are: (a) the signal levels are different, and (b) the polarity of the start bit and stop bit are reversed.

Note that the clocks used by the transmitter and receiver are not the same. Thus, there could be slight difference (a few percent) in the clock frequency, and the slight difference in the clock frequency might cause severe error. However, the processor built-in hardware and software maintain a strict synchronization between the transmitter and the receiver even though a slight frequency difference exists, due to a built-in function.

Because the data transmitted and received are a continuous stream, it is generally impossible for an outsider to directly read the data without error. However, the transmitter and the receiver have built-in hardware and software with strict rules to provide accurate decoding procedures to ensure the data read are correct. The communication is controlled by a high level communication program. In the present case, the communication software is written in an assembly language.

(5-c) Tests of a simple communication system

We constructed a simple communication system to test the basic communication components. Only after the above described basic components have been experimentally tested can these components be proved to have no problem for further construction of complex communication systems.

The simple communication system hardware is shown in Fig. 34. This communication system uses a pair of microcontrollers directly connected with a pair of wires. One microcontroller is used as a transmitter; the other is used as a receiver. The communication programs for data transmission and receiving are shown in Fig. 35 and Fig. 36. Test results are shown in Fig. 37, and Fig. 38.

Figure 34 A circuit diagram for a simple communication system

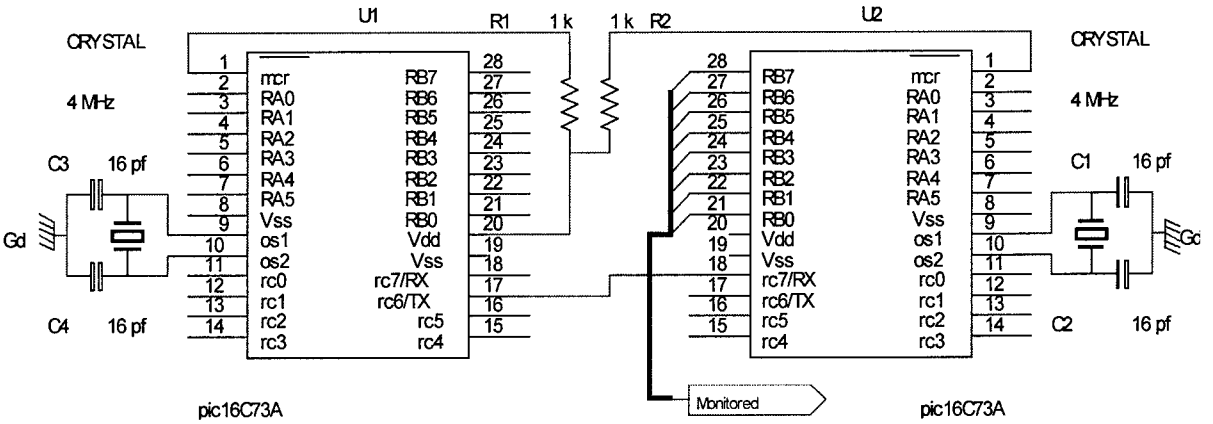

Figure 35 A simple program for performing data transmission

```
;;*****************************************************************
;uat00.asm named to be paired with uar00.asm as a pair
;of basic tx and rx program 00-18/00
;*****************************************************************
;    Filename:       uatx03.asm
;    Date: 03-08-00
;*****************************************************************
      list      p=16c63a     ; list directive for processor
      #include <p16c63a.inc> ; processor specific definitions

      __CONFIG    _HS_OSC&_WDT_OFF

; VARIABLE DEFINITIONS
count     EQU     0x20        ;
;*****************************************************************
      ORG     0x000    ; processor reset vector
      goto    main     ; go to beginning of program
      ORG     0x010
main  bcf   STATUS,RP0 ;Bank0
      clrf  PORTA
      clrf  PORTB
      clrf  PORTC ;Must for TRISC

      bsf   STATUS,RP0  ;Bank1
```

```
      movlw B'11000000'
      movwf TRISC ;<7:6> must be set for uasrt!
      movlw B'00000000'
      movwf TRISA
      movlw B'00000000'
      movwf TRISB
      bsf   STATUS,RP0  ;Bank1
      movlw D'25' ;2400 baud rate @4MHz
      movwf SPBRG ;Baud rate generator

      bsf   STATUS,RP0  ;Bank1
      movlw B'00100010' ;Sync=0,BRGH=0

      movwf TXSTA ;For preparation
      movlw B'10000000' ;For enable SPEN
      bcf   STATUS,RP0  ;Bank0
      movwf RCSTA ;S port enbled after TRISC<7:6>


transt
      bcf   STATUS,RP0 ;Bank0
      movlw B'00000000'
      movwf PORTA
      movlw B'00000001'
      movwf PORTA
      movlw B'00000000'
      movwf PORTA
      movlw B'00000001'
      movwf PORTA
      movlw B'00000000'
      movwf PORTA
      movlw B'00111110'
      movwf PORTA
      movlw B'00000000'
      movwf PORTA
      movlw B'00111110'
      movwf PORTA
      movlw B'00000000';last one must be 0
      movwf PORTA

      bcf   STATUS,RP0 ;Bank0
      movlw B'00000000' ;number to be transmitted
      movwf TXREG ;Start to send a byte now!
      bsf   STATUS,RP0 ;Bank1
PTX1: btfss TXSTA,1 ;wait for TSR empty
      goto  PTX1
      bcf   STATUS,RP0 ;Bank0
      movlw B'00000000'
      movwf TXREG ;Start to send a byte now!
      bsf   STATUS,RP0 ;Bank1
PTX2: btfss TXSTA,1 ;wait for TSR empty
      goto  PTX2
```

```
      bcf   STATUS,RP0 ;Bank0
      movlw B'00000010'
      movwf TXREG ;Start to send a byte now!
      bsf   STATUS,RP0 ;Bank1
PTX3: btfss TXSTA,1 ;wait for TSR empty
      goto  PTX3

      bcf   STATUS,RP0 ;Bank0
      movlw B'00001000'
      movwf TXREG ;Start to send a byte now!
      bsf   STATUS,RP0 ;Bank1
PTX4: btfss TXSTA,1 ;wait for TSR empty
      goto  PTX4

      bcf   STATUS,RP0 ;Bank0
      movlw B'00100000'
      movwf TXREG ;Start to send a byte now!
      bsf   STATUS,RP0 ;Bank1
PTX5: btfss TXSTA,1 ;wait for TSR empty
      goto  PTX5

      goto  transt

            END
```

Figure 36 A simple program for performing data receiving

```
;uar00.asm the most basic rx asm 03-07-00
;
;    Filename:       uar00.asm
;    Date: 3-07-00
;
;*****************************************************
      list      p=16c63a;list dirctv for processor
      #include <p16c63a.inc>;prcssr spcfic definitn

      __CONFIG    _HS_OSC&_WDT_OFF

;***** VARIABLE DEFINITIONS
pixeltemp     EQU     0x20        ;
;*****************************************************
      ORG     0x000    ; processor reset vector
      goto    main     ; go to beging of prgram
      ORG     0x010
main  bcf   STATUS,RP0 ;Bank0
      clrf  PORTA
      clrf  PORTB
      clrf  PORTC ;Must for TRISC
```

```
      bsf   STATUS,RP0  ;Bank1

      movlw B'11000000'
      movwf TRISC ;<7:6> must be set!
      movlw B'00000000'
      movwf TRISA
      movlw B'00000000'
      movwf TRISB
      movlw D'25' ;2400 baud rate @4MHz
      bsf   STATUS,RP0  ;Bank1
      movwf SPBRG ;Baud rate generator
      movlw B'0000000' ;Sync=0,BRGH=0,txen=0
      bsf   STATUS,RP0 ;Bank1
      movwf TXSTA ;
      bcf   STATUS,RP0  ;Bank0
      movlw B'10010000';1:SPEN(7),CREN(4)
      movwf RCSTA ;
      bcf   STATUS,RP0 ;Bank0
      clrf  RCREG
rceiv:
POLLR1:    btfss PIR1,5 ;wait for recvg complt
      goto  POLLR1
      movfw RCREG
      movwf PORTB
      movlw B'00000000'
      movwf PORTA
      movlw B'00011111'
      movwf PORTA
      movlw B'00000000'
      movwf PORTA
      goto  rceiv
            END
```

Figure 37 Experimentally recorded serial transmission signals for 3 consecutive bytes

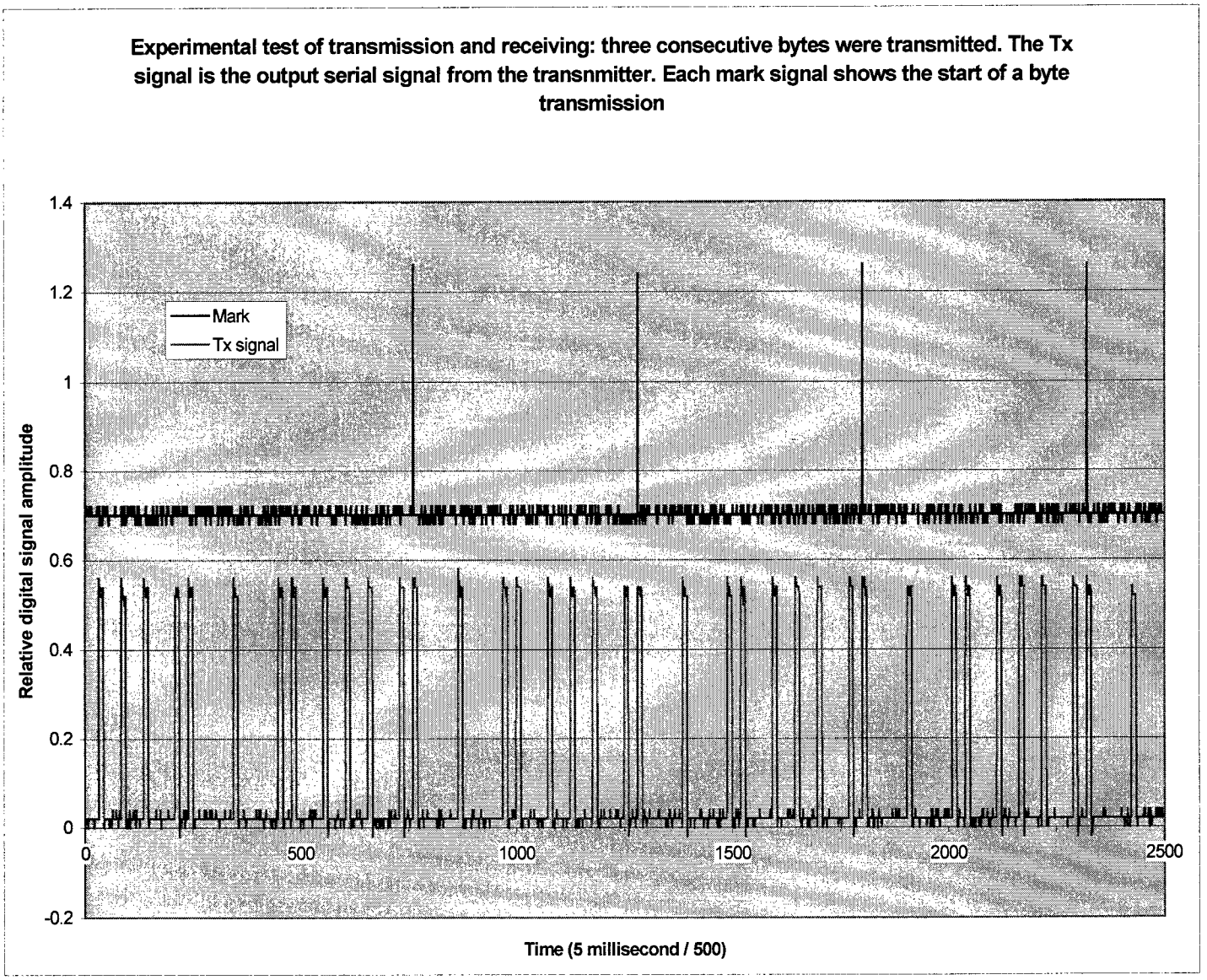

Figure 38 Experimentally recorded receiving signals for 3 consecutively transmitted bytes

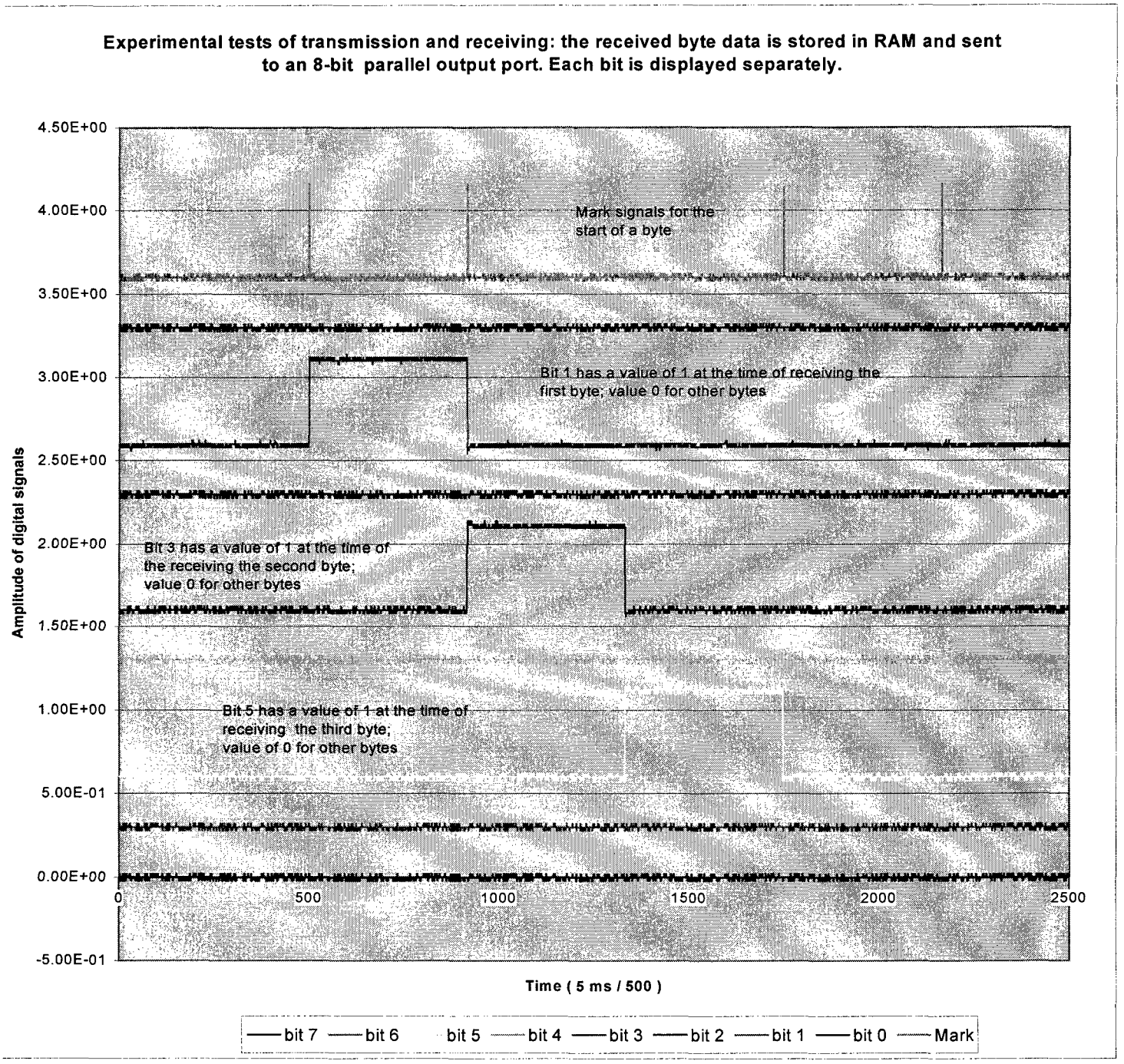

(5-d) A receiving system for free-space optical data communication

In the Phase II, we developed necessary hardware and software systems with the capability of receiving and decoding the modulated optical communication code at the computer side. This is important for establishing the optical communication link. However, this still does not contain all the necessary parts to establish a complete optical communication link. Establishing a complete free-space optical communication link requires:

(1) The PC side must be able to receive the modulated optical communication code and decoding the code into a data format (byte format) recognizable by the PC. This part has been done and will be described below.
(2) The PC side must have the capability of transmitting digital code according to a given byte data.
(3) The target side must have the capability of receiving the modulated optical communication code and decoding the code into a data format (byte format).
(4) The target side must have the capability of transmitting the digital code according to a given byte data.
(5) The system must have the capability of performing any combination of the four operations.

So far, in the present Phase II, we only did some work for item (1). The results of that work show that, according to our approach, a full-fledged optical communication system for 6D measurements is feasible. However, the amount of work needed to develop a complete optical communication system is beyond the projected schedule and budget of the present Phase II Contract. Development of such a system requires another independent contract specially allocated for optical communications. The following is the description of the work we did for the development of a receiving system.

The data acquired by the microcontroller is transmitted either through a wired connection or through free-space optical communication. In the present program, it is designed and tested so that the data from the sensor must be transmitted through free-space optical communication.

(5-e) A receiving system for optical communication

The photo-detector located near the PC measurement station is different from that in the target location. At the PC measurement station, the detector is controlled through a cooperative operation between the PC and the microcontroller, while in the target location the operation of the photo-detection system is solely controlled by the microcontroller. The following is a description of the photo-detector operation of the PC measurement station detection system

Block diagrams of the photo-detector near the PC measurement station are shown in Fig. 39 and Fig. 40.

The data receiving process performed by the photo-detection system near the PC

station includes three major parts: (1) Joint control of the photo-detectors by the PC and MPIC for data acquisition, data transfer and data processing for each pixel data from the photo-detectors. This part is close to the process as described in the previous section, (4-f) for PC measurement station photo-detection system. Most of the process described in that section can be included with certain modification as part of the operation; (2) However, there are substantial differences. For the present task of receiving the communication code, the receiving system must be able to transform the received analog signal from the photo-detector to a correct digital data: 0 or 1. This is by no means a simple task, because the signal amplitude received by the photo-detector can vary broadly. To transform the analog signal into a correct digital signal, an appropriate threshold must be set to determine whether the signal should be treated as 0 or as 1. The threshold value must be a correct value; otherwise the data would be ruined. However, a correct threshold value is determined by a number of factors, such as the average signal amplitude of all the pixels, the noise level of the photo-detectors, and the background signal value, etc. So, to determine the correct threshold value, the system must possess the capability for making judgments and decisions. That is, the system must have intelligence. (3) The receiving system must have the capability of decoding the detected digital signals into the right data according to the communication protocol.

The major steps for the PC to detect an ID number from the target is as follows:

1. PC sets Default: pb0 = 0, read pc0 =? MPIC sets default: rc0=0; RA3=0; RB: input.
2. PCLD continuously sends signals to ADC ain1.
3. PC notifies MPIC to start data acquisition and digitizing by letting: pb0 (rc0) = 1.
4. MPIC polling whether rc0=1? If rc0=1, MPIC starts data acquisition by sending a clock pulse to LIS1: RA0=0, RA0=1,RA0=0, and prepares for digitizing by: set ADC address: RA2=0||RA4=0 (ADC chnl 1).
5. MPIC67 starts ADC by letting RA3 =1, Initial condition: RA3=0 control of /cs/rd of ADC).
6. MPIC then waits for ADC completion by polling: whether pc0 (rc2) = 0.
7. PC polls if pc0(rc2)=0.
8. When pc0(rc2)=0, PC reads pa(0:7).
9. PC determines how large the PCPD signals is by: reading a whole cycle (including 0, and 1)
10. PC set the threshold voltage value for 0 and 1
11. PC sends to MPIC for decoding: PC continuously send 0 or 1 signals to rc7 (through pb7)
12. MPIC receives rc7(rx) digital bits and obtains byte data
13. MPIC sends the received byte data (UASRT protocol) to PC through RB(0:7) for doing this, MPIC must first change the PORT RB to output
14. PC reads RB(0:7) and receives a byte of data.

The flow charts of the above described process are shown in Fig. 39 and Fig. 40. The program and test results are shown in Fig. 41, and Fig. 42.

Figure 39 A decoding procedure for a PC receiving data from the target detector

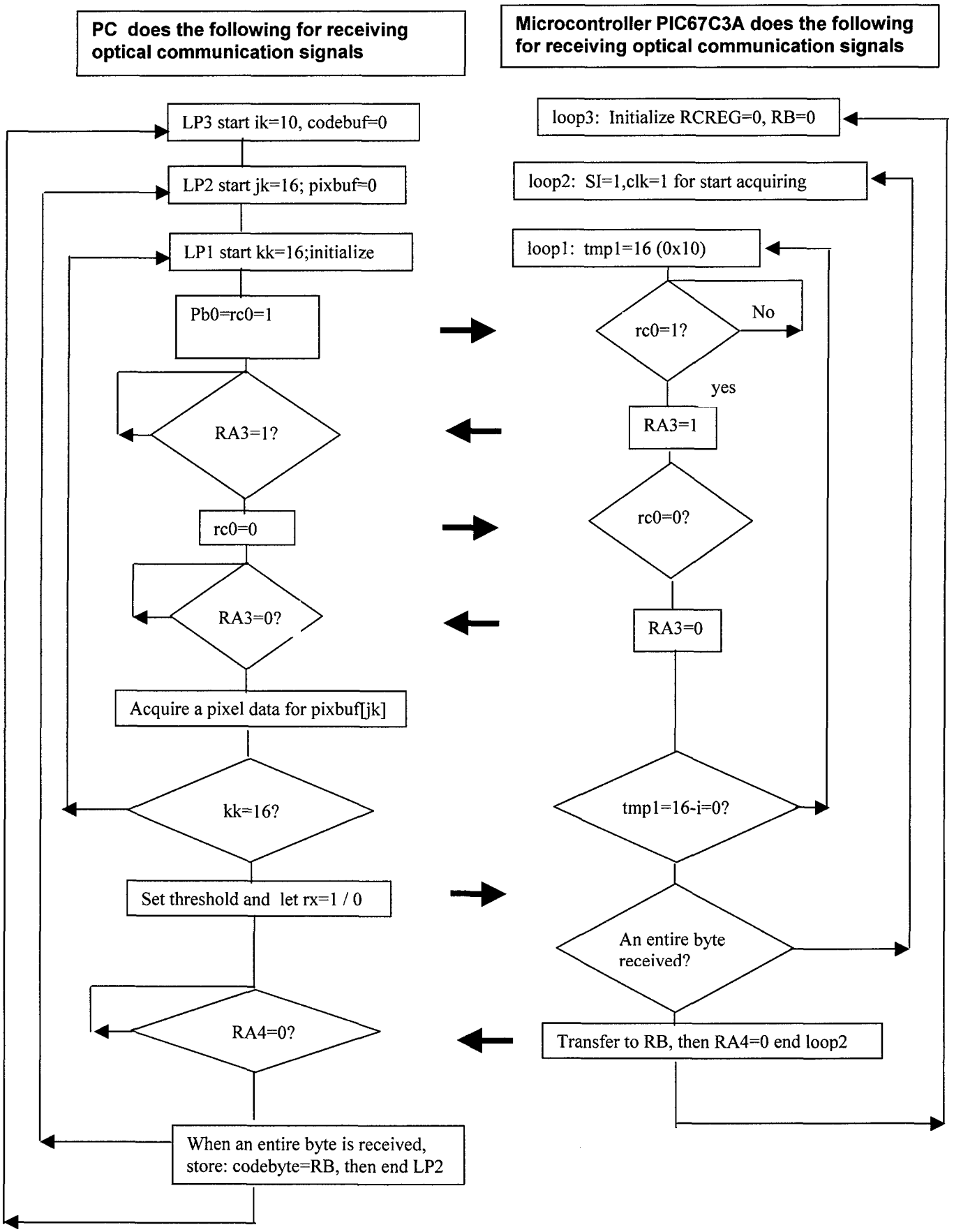

Figure 40 Software structure for a PC receiving and decoding a byte of data through optical communication

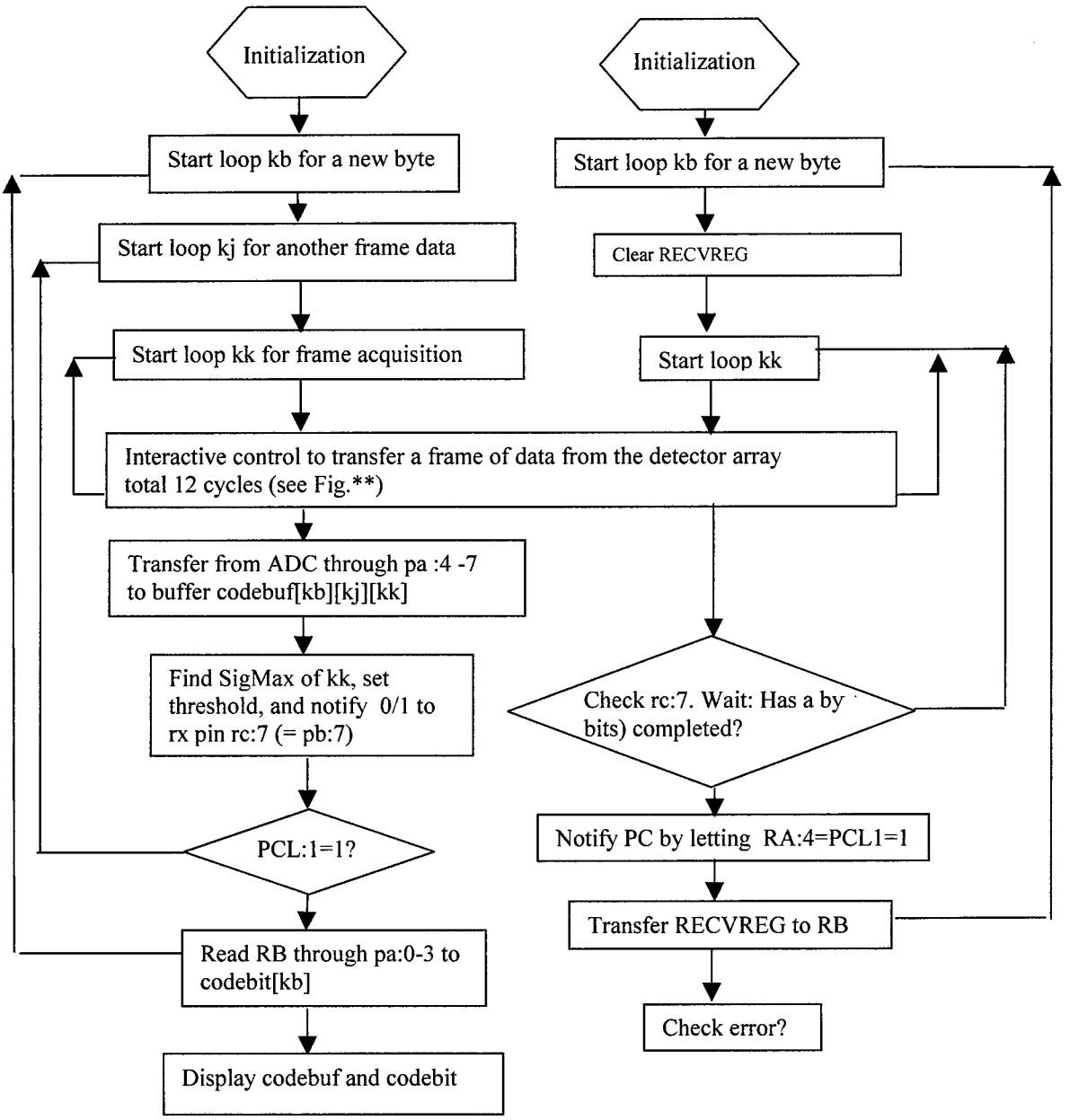

Figure 41 A computer program in C++ for PC receiving data

```
/*****************************************************************
  pcpic9.CPP
*****************************************************************/
#include <afxwin.h>
#include "Resource.h"
#include "DlgDemo1.h"
#include <math.h>
#include <windows.h>       /* Compiler's include files's */
#include <string.h>
#include <stdio.h>
#include "Cyr_pciw.h" // Board suppliers library

U16 bn;
PCI_INFO info; // PIC bus sctructure data

CMyApp myApp;
//////////////////////////////////////////////////////////////////
// CMyApp member functions

BOOL CMyApp::InitInstance ()
{
    m_pMainWnd = new CMainWindow;
    m_pMainWnd->ShowWindow (m_nCmdShow);
    m_pMainWnd->UpdateWindow ();
    return TRUE;
}
//////////////////////////////////////////////////////////////////
// CMainWindow message map and member functions

BEGIN_MESSAGE_MAP (CMainWindow, CFrameWnd)

    ON_WM_PAINT ()
    ON_COMMAND (IDM_OPTIONS_EXIT, OnOptionsExit)
    ON_COMMAND (IDM_OPTIONS_ABOUT, OnOptionsAbout)
END_MESSAGE_MAP ()

CMainWindow::CMainWindow ()
{
    Create (NULL, "Pointer Demo", WS_OVERLAPPEDWINDOW,
      rectDefault, NULL, MAKEINTRESOURCE (IDR_MAINFRAME));
}

void CMainWindow::OnPaint ()
{
      CPaintDC dc (this);
      COLORREF crbk=RGB(240,240,240);
```

```
      CRect rect;
      GetClientRect (&rect);
      dc.FillSolidRect(rect,crbk);

#define PBLOW    0x00
#define PBHIGH   0xFF
#define PB1ON    0x02
#define PB7ON    0x80
#define    PB1OFF     0xFD
#define    PB7OFF     0x7F

unsigned char PBOUT;
unsigned short pixbuf[20][300][16],ad1,ad2,ad4;
unsigned short codebuf[20],ad1x,ad2x,ad4x;
unsigned short codebit[20][10],qixbuf[20][300][16];
unsigned short sigmax,sigmin;
unsigned short i,j,k,kk,kb,kj,mkk,jb,jj;

FILE *fwp;
if((fwp=fopen("decod1.txt","w"))== NULL) {
printf("cannot open file \n");
exit(0); }

for(i=0;i<20;i++)
for(j=0;j<300;j++)
for(k=0;k<16;k++)
{
          pixbuf[i][j][k]=0;

}

for(i=0;i<20;i++) codebuf[i]=0;
// Operations:
//1. Initial value: pb0(rc0)=0;pb1(rc1)=0
//2. Give command to PIC67 to
//start acquistn by letting rc0=1&rc1=1
//(PC port:pb0(rc0)=1, pb1(rc1)=1);
//3. Watch for ADC completion:rc2=1?
//(PC port:pc0(rc2)=0?);
//4. After rc2=1, transfer RB0:RB7 of
//PIC67 to PC(pa4:pa7)
//

//initialize buffer and config ports

W_DIO48H_Initial(&bn, &info);
W_DIO48H_Config_Port(0,PCI_CH0_PA,INPUT_PORT);
W_DIO48H_Config_Port(0,PCI_CH0_PB,OUTPUT_PORT);
W_DIO48H_Config_Port(0,PCI_CH0_PCL,INPUT_PORT);
W_DIO48H_Config_Port(0,PCI_CH0_PCU,INPUT_PORT);

kb=0;kj=0;mkk=0;
```

```
PBOUT=PBLOW;
W_DIO48H_DO(0,PCI_CH0_PB,PBOUT);//uasrt"stop"
//Let pb0(rc0)=0;pb1(rc1)=0 as initl condtn
while(kb<5)
{
kj=0;
while(kj<100)
{
for(kk=0;kk<12;kk++)
{
ad1=0;ad1x=0; //Because ad1=1 will be a criterium
ad2=1;ad2x=1; //Because ad2=0 will be a criterium
ad4=1;ad4x=1; //ad3=0x2 will be a criterium
//Initial condition: pb0(rc0)=0

W_DIO48H_DO(0,PCI_CH0_PB,PBOUT);

//Let  pb1(rc1)=1 to start comnctn

PBOUT=PBOUT|PB1ON;//PB1 turned on
W_DIO48H_DO(0,PCI_CH0_PB,PBOUT);

//Wait for RA3=1 from PIC63, which causes
//pc2=1(PCL bit 2 =1)

waita:W_DIO48H_DI(0,PCI_CH0_PCL,&ad1);
      ad1x=ad1&0x4;
      if(ad1x!=4) goto waita;
// When RA3=1 is confirmed, tell PIC16 to
// start digitizing by ltting pb1(rc1)=0
PBOUT=PBOUT&PB1OFF;//pb1 turned off
W_DIO48H_DO(0,PCI_CH0_PB,PBOUT);

//PIC16 lets RA3=0, which directly causes pc2=0
//when ADC is completed, giving rc0=pc0=0
//wait for ADC completion: pc0=0 & pc2=0
waitb:W_DIO48H_DI(0,PCI_CH0_PCL,&ad2);
ad2x=ad2&0x5;
if(ad2x!=0) goto waitb;

//When ADC completion is confirmed
// acquire a pixel data from ADC

W_DIO48H_DI(0,PCI_CH0_PA,&pixbuf[kb][kj][kk]);
mkk=mkk+1;
} //kk loop ended after kk=0,..11
sigmax=0;sigmin=255;
for(i=0;i<12;i++)
{
qixbuf[kb][kj][i]=(pixbuf[kb][kj][i]&128)
+(pixbuf[kb][kj][i]&64)/2+(pixbuf[kb][kj][i]&32)/4
+(pixbuf[kb][kj][i]&16)/8;
```

```
}

for(i=0;i<12;i++)
{
if(qixbuf[kb][kj][i]>sigmax)
sigmax=qixbuf[kb][kj][i];
if(qixbuf[kb][kj][i]<=sigmin)
sigmin=qixbuf[kb][kj][i];
}

//Note that PBLOW must not affect others!
if(sigmax>30)
//if(kb>0)
//if(kj>0)
{
PBOUT=PBOUT|PB7ON;
//The first grp data cannot be used
W_DIO48H_DO(0,PCI_CH0_PB,PBOUT);
}
else
{
PBOUT=PBOUT&PB7OFF;
W_DIO48H_DO(0,PCI_CH0_PB,PBOUT);
}
kj=kj+1;
//delay for pic's action time
for(j=0;j<3;j++)

W_DIO48H_DI(0,PCI_CH0_PCL,&ad4);
ad4x=ad4&0x2; //RA:4 (PC:1)=1?
if(ad4x==2) break;
//if RA4=0, try another 12 cycles
}//end of kj loop

W_DIO48H_DI(0,PCI_CH0_PA,&codebuf[kb]);
kb=kb+1;
}//end of kb loop,5 bytes recorded


//Display recorded results
static int  CharWidth, CharHeight;
int  x,y,xc,yc;
char OutString[40], *str;
TEXTMETRIC tm;

      dc.GetTextMetrics (&tm);
      CharWidth= tm.tmAveCharWidth;
      CharHeight=tm.tmHeight;
      xc=(rect.left+rect.right)/2;
      yc=(rect.top+rect.bottom)/2;
      x = rect.left+CharWidth*2;
    y =rect.top+CharHeight*2;
```

```
    str = "Signal Intensity Distibution";
    dc.TextOut(x, y, str);

//Diplay array signal intensity (12/frame)
//First number conversion from p to q
/*
for(jb=0;jb<16;jb++)
for(jj=0;jj<200;jj++)
for(kk=0;kk<12;kk++)
{
qixbuf[jb][jj][kk]=(pixbuf[jb][jj][kk]&128)
+(pixbuf[jb][jj][kk]&64)/2+(pixbuf[jb][jj][kk]&32)/4
+(pixbuf[jb][jj][kk]&16)/8;
} */

//Display slected data
for(jj=0;jj<5;jj++)
{
y += CharHeight*1.3;
for(kk=0;kk<12;kk++)
{
x= CharWidth*(2+kk*10);
sprintf(OutString,"S[%u,%u]=%u",jj,kk,qixbuf[0][jj][kk]);
dc.TextOut(x, y, OutString);
}
}
for(jj=0;jj<6;jj++)
{
y += CharHeight*1.3;
for(kk=0;kk<12;kk++)
{
x= CharWidth*(2+kk*10);
sprintf(OutString,"S[%u,%u]=%u",jj,kk,qixbuf[4][jj][kk]);
dc.TextOut(x, y, OutString);
}
}
//Display the  bytes bitwise

for(i=0;i<5;i++)
{
codebit[i][0]=0;
codebit[i][1]=(codebuf[i]&1)/1;
codebit[i][2]=0;
codebit[i][3]=(codebuf[i]&2)/2;
codebit[i][4]=0;
codebit[i][5]=(codebuf[i]&4)/4;
codebit[i][6]=0;
codebit[i][7]=(codebuf[i]&8)/8;
}

for(jj=0;jj<5;jj++)
{
```

```
y += CharHeight*1.3;
for(kk=0;kk<8;kk++)
{
x= CharWidth*(2+kk*4);
sprintf(OutString,"%u",codebit[jj][kk]);
dc.TextOut(x, y, OutString);
}
}
x= CharWidth*(2+2);
y += CharHeight*1.3;
sprintf(OutString,"kb=%u  kj=%u  mkk=%u",
          kb,kj,mkk);
dc.TextOut(x, y, OutString);
/*
for(i=0;i<10;i++)
      {
      for(j=0;j<12;j++)
      {
      fprintf(fwp,"S[%u][%u]=%u ",i,j,qixbuf[i][j]);
      }
      fprintf(fwp,"/n");
      }*/
::Sleep(500);
CWnd::Invalidate();
}

void CMainWindow::OnOptionsExit ()
{
    SendMessage (WM_CLOSE, 0, 0);
}

void CMainWindow::OnOptionsAbout ()
{

}

;sync1a.asm peiord adjusted to be appx.
;139 microsecs 8-3-00
;*********************************************
;    Filename:       sync1.asm
;    Date: 7-29-00
;*********************************************
      list      p=16c63a     ;
      #include <p16c63a.inc> ;
       __CONFIG    _HS_OSC&_WDT_OFF
;***** VARIABLE DEFINITIONS
tmp1  EQU   0x3F
tmp2  EQU   0x4F            ;
;*********************************************
;*********************************************
```

```
      ORG     0x000    ; prcsr reset vctr
      goto    main     ;
      ORG     0x010
main  bcf   STATUS,RP0 ;Bank0
      clrf  PORTA ;Must for TRISA
      clrf  PORTB ;Must for TRISB
      clrf  PORTC ;Must for TRISC
      bsf   STATUS,RP0  ;Bank1
      movlw B'11001111'
      movwf TRISC ;<4:5> output for tx/rx
      movlw B'00000000' ;RA:ouput
      movwf TRISA
      movlw B'00000000';!RB:output
      movwf TRISB
      bcf   STATUS,RP0 ;Bank0
      movlw B'00010100' ;ADC chnl4
      movwf PORTA
                ;preparatn for rx
      movlw D'129' ;2.4k baud rate @20MHz
      bsf   STATUS,RP0  ;Bank1
      movwf SPBRG ;Baud rate generator
      movlw B'0000000' ;Sync=0,BRGH=0,txen=0
      bsf   STATUS,RP0 ;Bank1
      movwf TXSTA ;
      bcf   STATUS,RP0  ;Bank0
      movlw B'10010000';1:SPEN(7),CREN(4)
      movwf RCSTA ;
      movlw B'00100100';addrs:RA2||RA5
      movwf PORTA

loop2:                ;loop2 for recving bit code
      clrf  PORTB
      bsf   PORTB,0
      bsf   PORTB,0
      clrf  PORTB
            ;send si and 1/2 first clk
      bsf   PORTC,4;si starts
      bsf   PORTC,5;stupid trick of TI
      bcf   PORTC,4;stupid trick of TI
      bcf   PORTC,5

      movlw B'00001100';cnt#=12
      movwf tmp1
loop1:                ;PC lets rc1=0,1
           ;loop1 for 12 transfer cycls
           ;each 6 transfer, one data
pccmd:     btfss PORTC,1;if1,go for prepratn
      goto  pccmd
      bsf   PORTC,5;first dummy
      bcf   PORTC,5
      bsf   PORTC,5;second dummy
      bcf   PORTC,5
```

```
        bsf   PORTC,5;third dummy
        bcf   PORTC,5
        bsf   PORTC,5;4-th dummy
        bcf   PORTC,5
        bsf   PORTC,5;5-th dummy
        bcf   PORTC,5
        bsf   PORTC,5;one pixel data
        bsf   PORTC,5
        bsf   PORTC,5
        bcf   PORTC,5
        movlw B'00101100';RA3=1:latch addrs
        movwf PORTA
                    ;PC tests RA3=1
                    ;PC lets rc1=0
pccmda:     btfsc PORTC,1 ;if rc1=1, wait
        goto  pccmda
        movlw B'00100100' ;RA3=0,start digitz
        movwf PORTA
                    ;PC tests RA3=0&int=0
                    ;PC acquire data
        DECFSZ      tmp1,1
        goto  loop1 ;to ttlly acq 13 pxls
                    ;contrled by pc
                    ;the above loop is for
                    ;going through 64 pixels
        goto  loop2
        END
```

Figure 42 A comparison between the transmitted and received signal to show that the receiving operation is correct

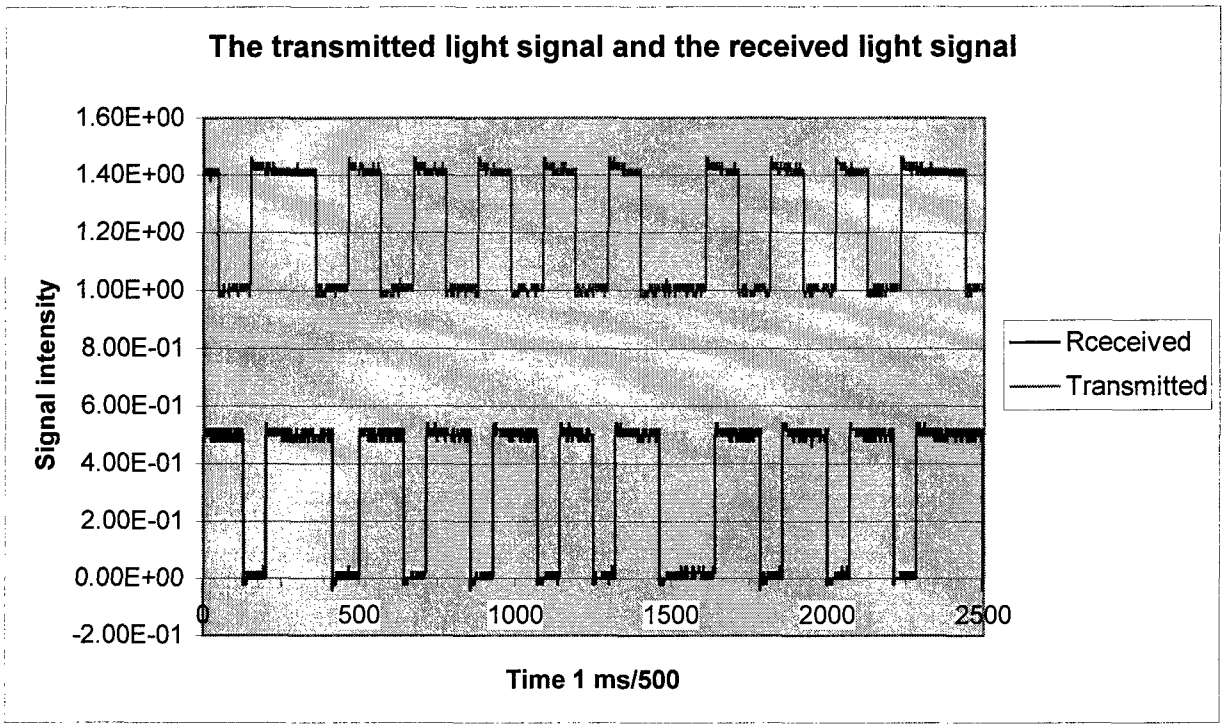

(5-f) Construction of a wired data communication system between the target and the PC station

We constructed a wired data communication system between the target photo-detector and the PC photo-detector. We planned to use this as a temporary communication system to meet the immediate needs for system construction and tests. However, in the present Phase II Contract we realized that the amount of work for the development of a free-space communication system is too much and cannot be completed in the present contract. On the other hand, to test system operation for 6D measurements, it is necessary that there be some kind of communication link between the target and the PC station. If the data acquired by the target cannot be transmitted to the PC, 6D measurements would be meaningless. For solving this problem we tried to construct a preliminary and temporary communication system to provide minimum communication capability so that the data acquired by the target can be transmitted and received by the PC.

Construction of a wired temporary communication system can avoid a substantial amount of work in connection with the specific features for an optical communications system. At the same time, the most important features of the 6D measurement system can be

maintained. After preliminary system construction and preliminary system tests have been completed, the full features of the optical communication system can be added without changing other parts.

Even a wired system with minimum communication capability requires a great deal of work because both the target photo-detectors and the PC station are controlled by independent embedded microprocessors, not simple electronic circuits. On the other hand, for transmitting and receiving data, a number of necessary operations must be done according to the communication protocol. Each step requires a certain programmed operation of the embedded microprocessor and must be independently tested before any further steps can be taken. Such link has been established. The following is a report of how to transmit and receive data from the target through a wired communication link.
The system hardware, software and test results are shown in Fig. 43 through Fig. 49.

Figure 43 Mechanical structure of the target detector for testing 6D measurements

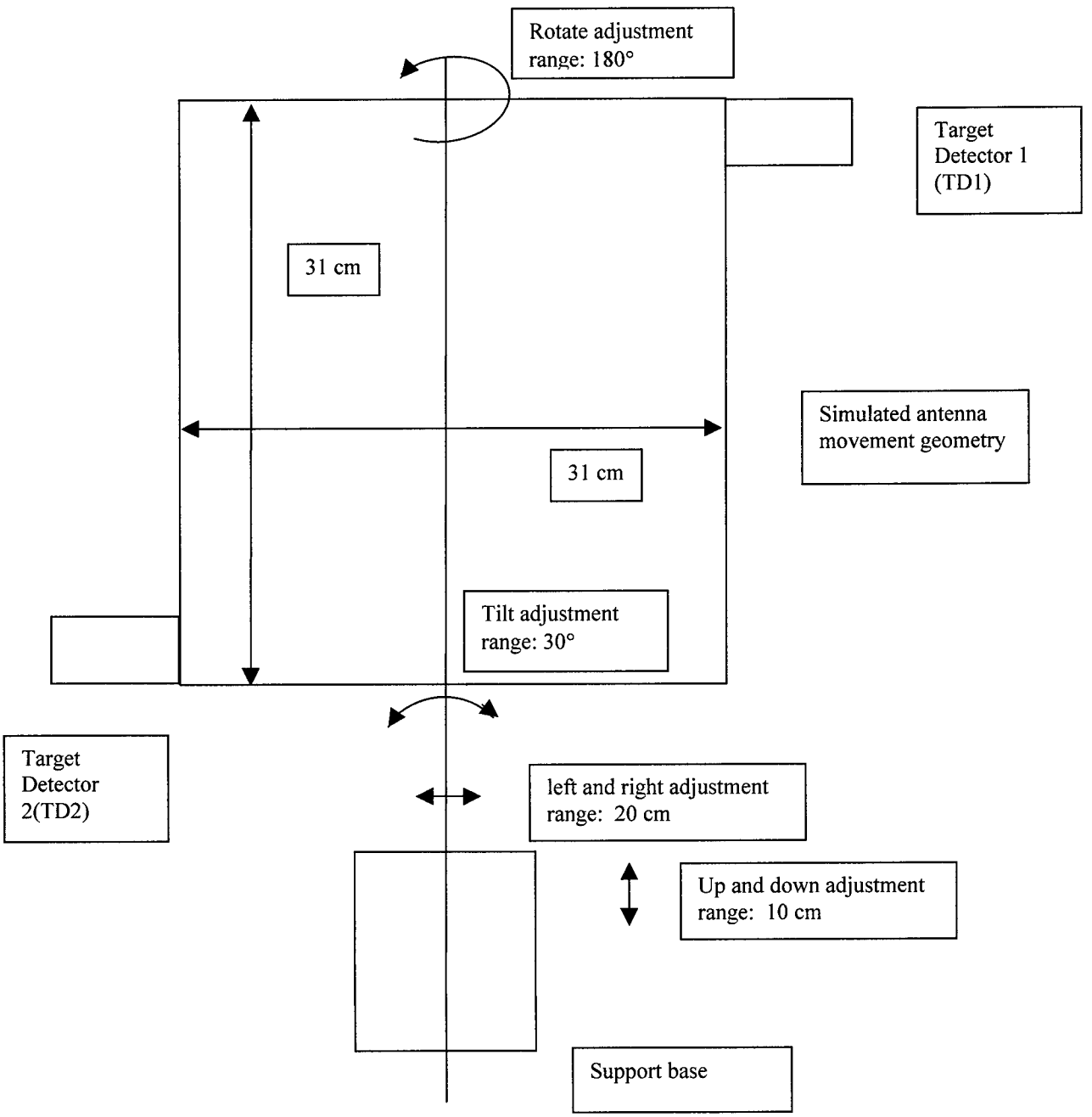

Figure 44 A schematic diagram for the two target detectors to transmit data to the PC for system tests

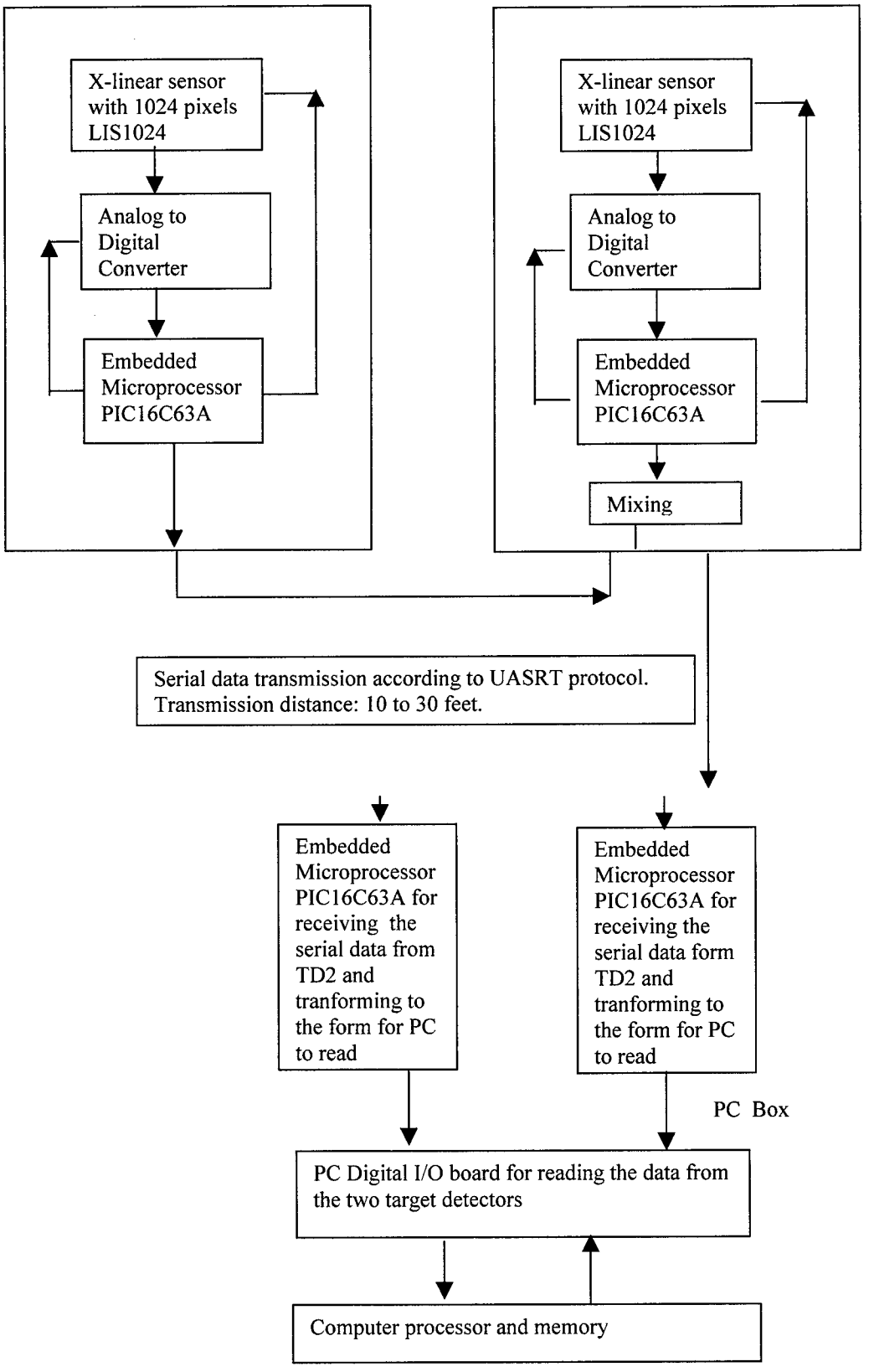

Figure 45 A picture of the two target detectors mounted on a simulated test asset

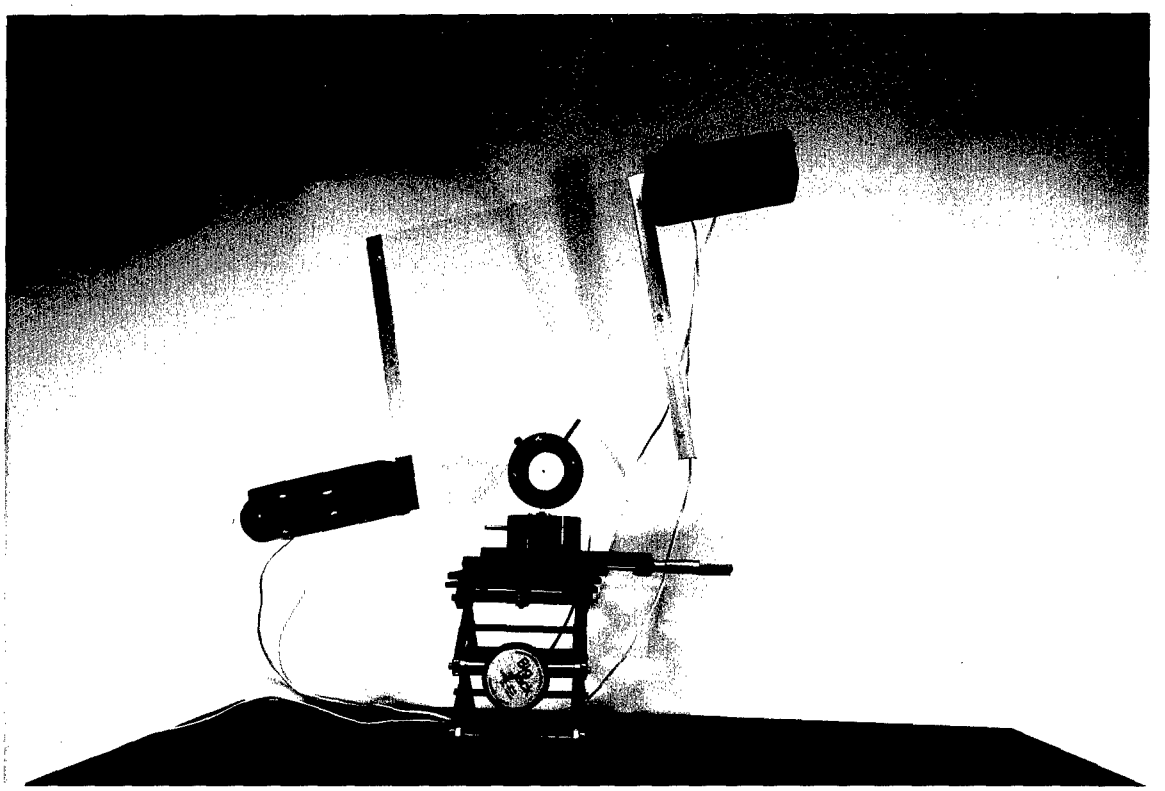

Figure 46 A picture of the photo-detector for receiving near the PC measurement station

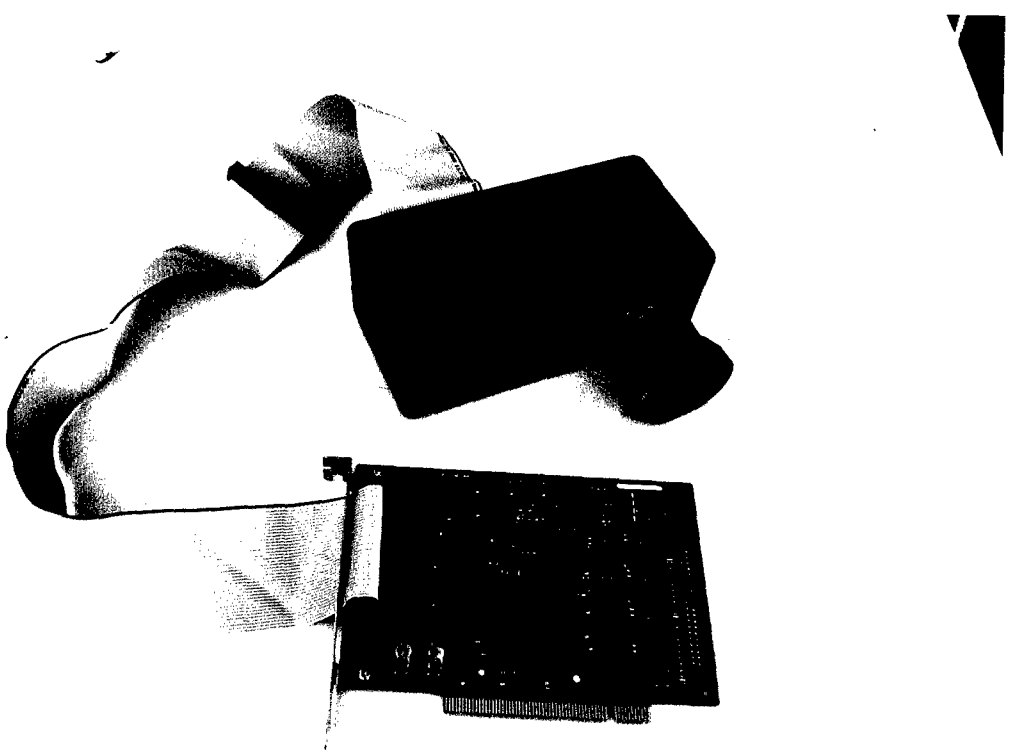

Figure 47 A flow chart diagram for the target transmission

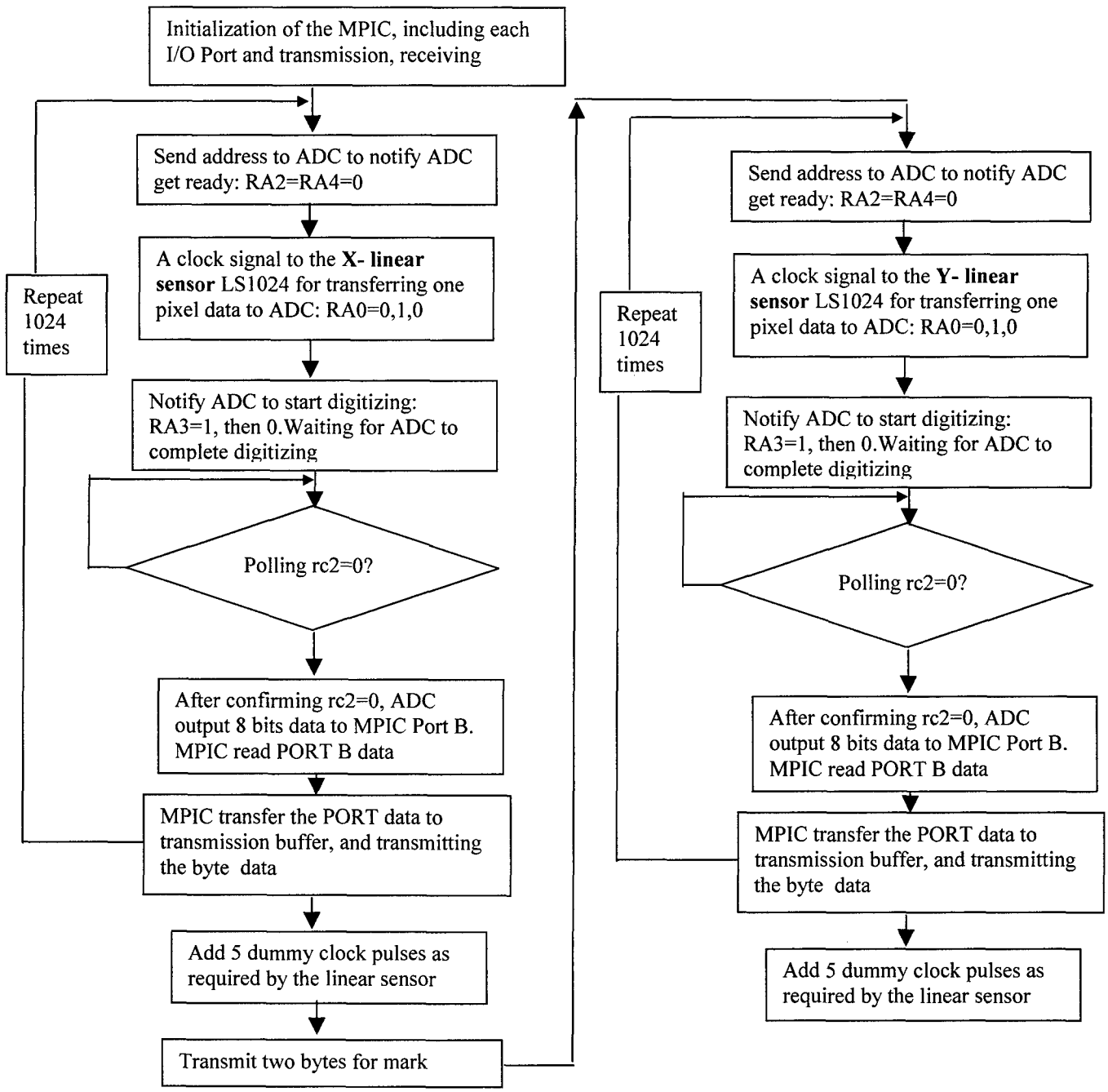

Figure 48 A flow chart diagram for receiving near PC station

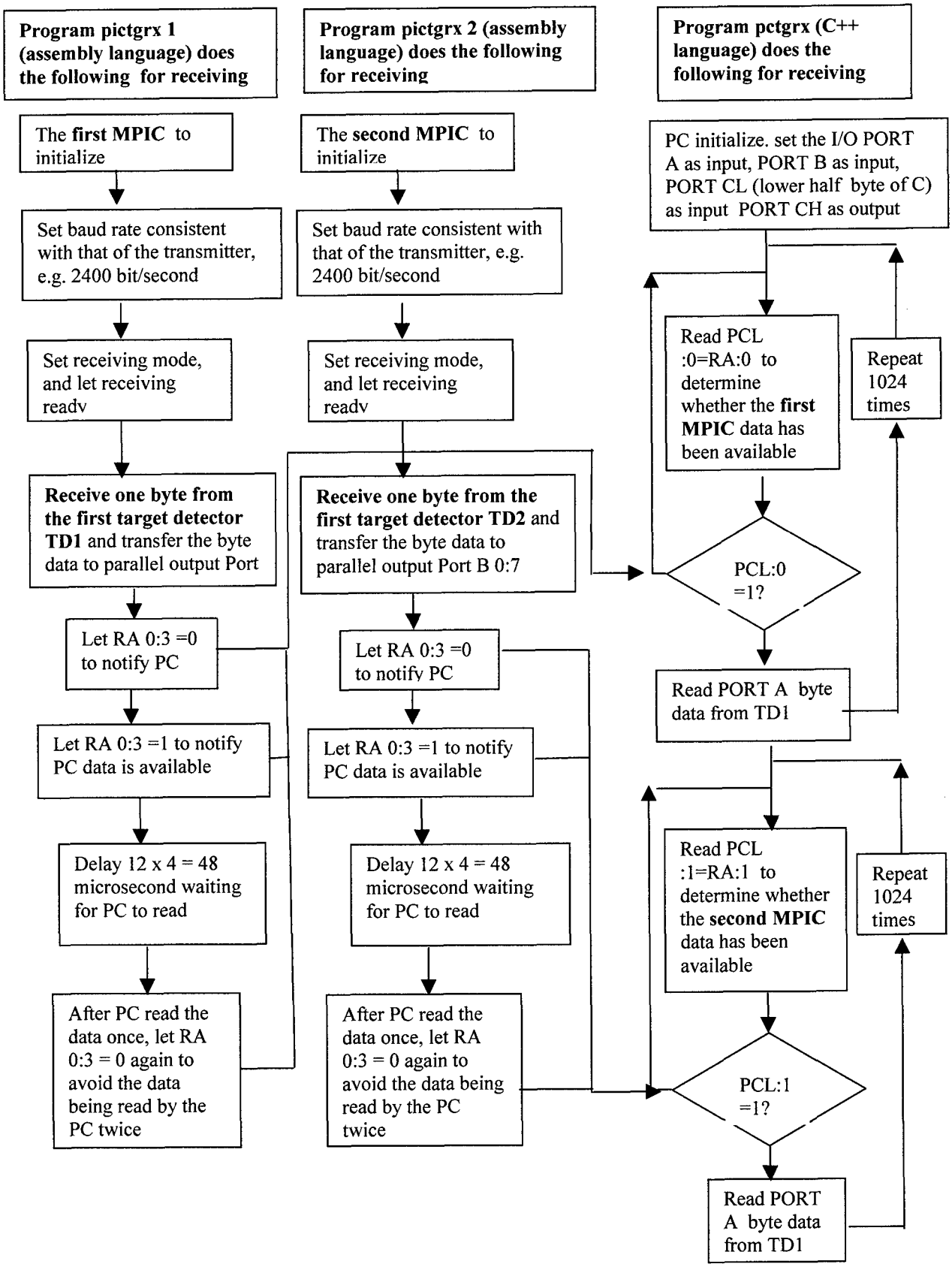

Figure 49 A schematic circuit diagram for PC detector

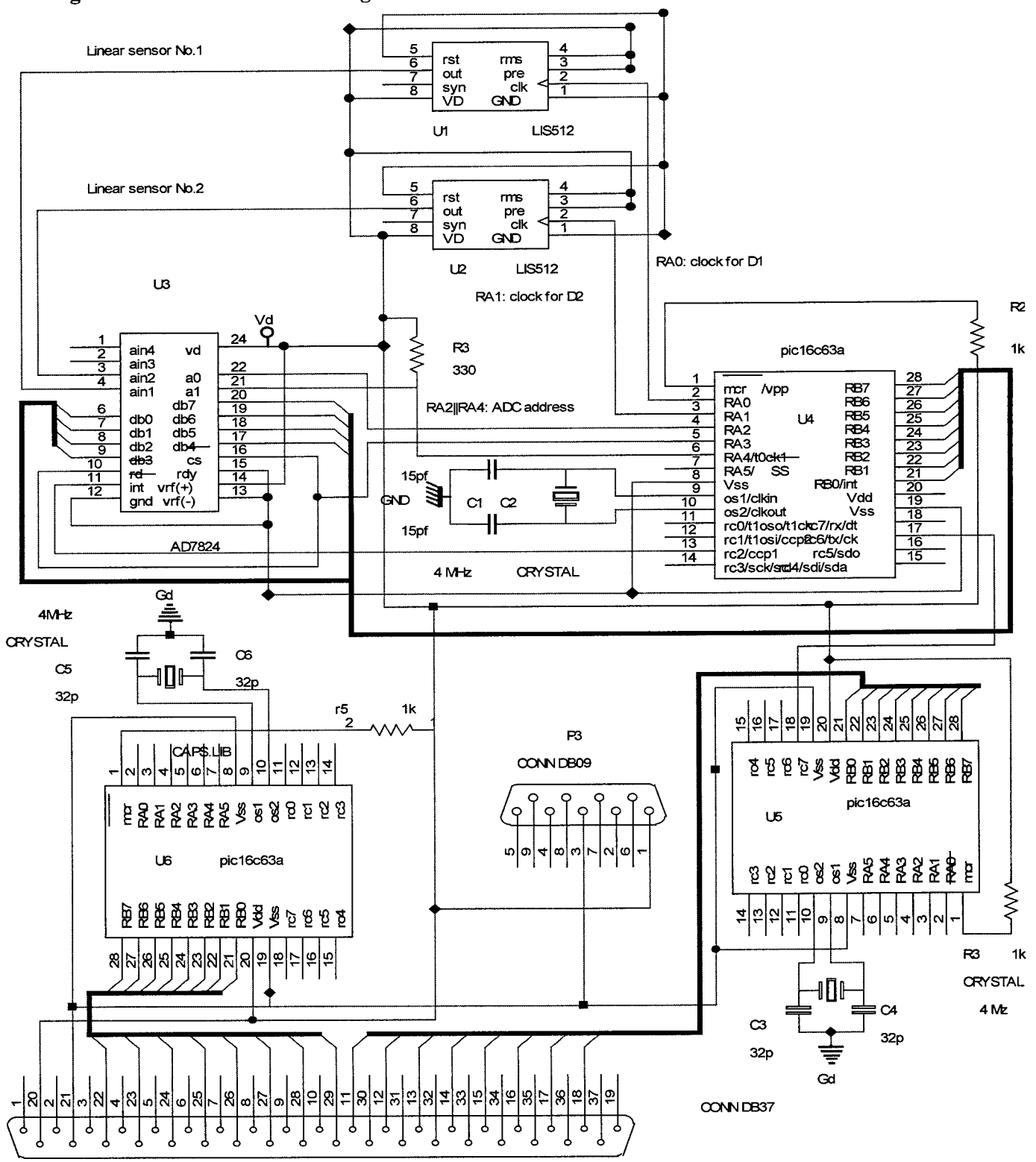

Sheet File Name:	**Advanecd Optical Technologies, Inc.**
xy0011a.sch	111 Founders Plaza, Suite 603
Modification date:	***East Hartford, CT 06108***
11/20/00	Sheet Title: X-Y detector with embedded electronics

Figure 50 Experimentally received signals

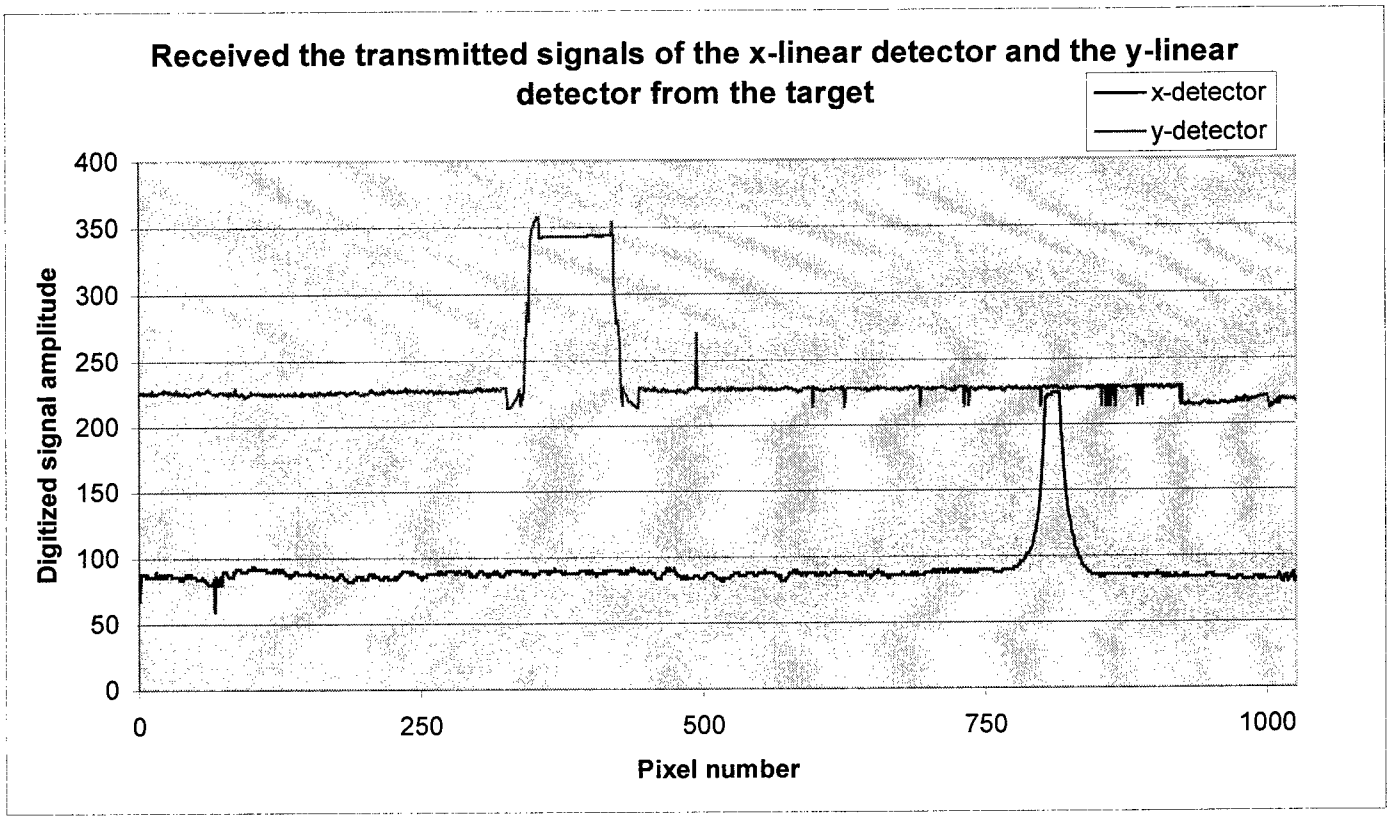

6. Development of a systematic mathematical method for calculation of 6D measurement results

We developed a systematic mathematical theory for 6D calculations. In this part we will present the following sections:

(6-a) Why is it necessary to develop a mathematical theory for 6D calculation?
(6-b) An outline description of 6D mathematical and computational features.
(6-c) The essential difficulties in solving the 6D equation systems.
(6-d) Our approach for solving the 6D mathematical calculation problem.
(6-e) An outline description of the process of calculation of the reference data base.
(6-f) An illustrative example for deriving nonlinear equation systems for 6D calculations.
(6-g) A second illustrative example for deriving nonlinear equation systems for 6D calculations.
(6-h) An outline review of the numeric method for finding solutions to a simultaneous nonlinear equation system.
(6-i) Illustrative computer tests results.
(6-g) An outline of mathematical software packages.

(6-a) Why is it necessary to develop a mathematical theory for 6D calculation?

The question is how to evaluate the 6D final results from experimental measurement data. Before and during the present contract, we were led by a common understanding that 6D calculations were merely certain numerical calculations based on directly using a number of triangle formulas. We thought that even though the formulas could be rather complicated, the final results could always be expected to be obtainable. This impression came from currently available commercial instruments, such as certain 3D laser range-finder instruments, etc, because these instruments invariably use triangle formulas to calculate the final results. This common understanding was generally taken for granted by every one, including us. According to this understanding, there should be no essential difficulty in developing mathematical calculations for the 6D case. Because of this, 6D mathematical computations were taken only as a conventional numerical calculation work, and simply not listed in the Work Statement.

However, with the development of the contract work, this understanding turned out to be totally wrong. Through the work of the present contract, we found that in contrast to any currently available commercial **3D** measurement instruments, **the six-dimensional (6D) calculation is an unsolved scientific problem.** That is, to our best knowledge, before the present contract work, no one has ever been able to provide a method that can be used for calculation of 6D results based on experimentally measured optical data. We also found that a number of important mathematical difficulties exist in the calculation of final results. The most important problem is that 6D calculations require solving a nonlinear equation system, and the state-of-the-art computational mathematics have been unable to provide a solution to the nonlinear problem. We extensively surveyed publications and consulted mathematics experts, but the conclusion

was the same. How to calculate 6D final results is an unsolved scientific problem.

The work for the mathematical theory and numerical implementation of the computer programs shows that the amount of mathematical work was enormous. According to our written records in the present Phase II Contract, performing analytical derivations required more than 300 pages of handwritten formulas. Recorded in legally qualified laboratory notebooks, the new mathematical theory occupies close to 100 pages. Each analytical and numerical step underwent countless checks and double checks, and was tested and retested. Because such mathematical expressions are very long and complex, without such excessively careful work, the final results could be totally meaningless, because even the smallest error in the middle could ruin all the subsequent calculations.

It might seem at first glance that such a huge amount of mathematical work may not be absolutely necessary. However, we found that, in fact, this is an issue at the foundation of 6D technology. It is a critical component regarding whether the present approach is feasible or not, and whether *any* 6D technology is feasible. If no one can actually give the final results, any 6D program would be meaningless. So, in the present Phase II Contract, we directed our efforts to solving the problem. We conducted systematic research work and solved a number of important and difficult mathematical problems. As a result, **through the intensive effort of the present contract, we have developed a systematic method for providing a reliable solution to this important scientific problem.**

Note that the 6D mathematical theory is essential not only for the present contract, but also for any other 6D measurement approaches. In our opinion, the mathematical theory for 6D measurements accomplished in the present Phase II Contract is a piece of creative and valuable work both in optical engineering and in mathematics. It has laid a firm foundation for future 6D technology development and is the first of its kind. To our best knowledge, no one has provided similar results. The basic approach for developing the 6D mathematical theory and measurement technique has been filed as a U.S. patent [8]. The patent text is attached in the final report as a reference.

(6-b) An outline description of 6D mathematical and computational features

In this section, we will first give a broad picture of the 6D mathematical calculations. In the subsequent sections we will describe the mathematics in more detail. The following is a brief list of the basic features for 6D geometry calculations.

It is assumed, the target (the test asset), such as an antenna dish, has three position parameters (x,y,z) in the fixed laboratory coordinate system and three rotation parameters (α,β,γ) around a fixed coordinate system moving with the subject at (x,y,z). If we conduct an optical measurement and obtain 6 independent measured data, then, in principle, the 6 unknown parameters can be calculated. However, when we actually write down the mathematical relationships between the 6 measured parameters and the 6 unknown parameters, we found the following features:

(6-b-1) The relationships are a group of simultaneous equations. This indicates that the unknown parameters and the known parameters are mixed in an implicit form, and unknown parameters cannot be written as an explicit expression of the known parameters. The form of the relationships is:

$$f_1(x_1, x_2, x_3)=0 \qquad (6\text{-}1)$$
$$f_2(x_1, x_2, x_3)=0$$
$$f_3(x_1, x_2, x_3)=0$$
$$\ldots\ldots\ldots\ldots\ldots$$

If the relationships were simple explicit expressions, then the 6 unknown parameters could be calculated forward. That would be very simple. One has to solve the equation system first, then the results for each of the 6 unknown parameters can be obtained. Note that this is essentially different from the case of 3D calculations. In 3D calculations, the unknown variable can always be written in the form of explicit expressions. The reason for the difference comes from the fact that 3D calculations are always forward calculations, and the 6D calculations are always backward calculations. Forward calculations start from the given known parameters (the measured data) and write out an explicit expression for the unknown. Backward calculations produce equations, where the known parameters (the measured data) and the unknown parameters exist in a form of equations.

(6-b-2) The simultaneous equations in the equation system are nonlinear and cannot be reduced to be linear. It is generally known that in a linear equation system, there should be no problem finding the solution to give all the unknown parameters. But since it is nonlinear, for modern analytical and computational mathematics, there is no general way to follow to obtain a solution [10].

(6-b-3) Some additional features make the problem even more challenging: when writing the equation systems, the minimum equation number should be 6. However, in the process of establishing the relationship, some additional unknown quantities always are involved. For example, some quantities of vector length enter the equation system. Thus the total equation number is more than 6, usually as large as 9. Thus, in practice, the equation system can have 9 nonlinear equations, with 9 unknown variables; 3 of them can be expressed through the 6 basic unknown variables.

Thus, the equation system is a rather complicated nonlinear system, with no available method for finding the solutions.

(6-c) The essential difficulties in solving 6D equation systems

The first essential difficulty is that most or all equations in the system are nonlinear equations. It is generally impossible to make these equations linear through any mathematical or physical methods. When nonlinear equations are encounterered, the best effort is generally to use so-called linearization approximation to make the equation

systems linear, because solving nonlinear equation systems is a formidable mathematical task. However, it must be noted that in the present case (6D measurements) it is impossible to make the equations linearized. This impossibility comes from the simple fact that all the interested geometry quantities are related through a complicated combination of triangle functions such as sinα, cosα, sin2α, cos2α, sinβ, cosβ, sin2β, cos2β, sinγ, cosγ, sin2γ, cos2γ, and so forth. The rotation angles simply can not be approximated as small angles close to zero. Thus, the essence of the 6D measurement parameters are not linear and can never be approximated by using linear approximations. Because of this, it can be concluded that the equations used for 6D parameters from experimentally measured data are always nonlinear.

For a nonlinear equation system, the most important question is whether the equation system is solvable or not. Fig. 51 is a brief list of the answer to this question.

Figure 51 A brief list regarding what kind of equation systems are solvable or not solvable

Equation /variable number / Linear /Nonlinear	1	2-3	>3
Linear Equations	Solvable using matrix methods	Solvable using matrix methods	Solvable using matrix methods
Nonlinear Equations	Basically solvable	No general methods. It is not known whether solvable or not	No general methods, generally not solvable

In 6D measurement, the relationships that connect the measurement results and the 6D unknown parameters (3 translational position parameters and 3 rotation angles) are nonlinear equation systems. The number of equations in the system is generally 6, so there has been no mathematical method to provide a solution. We surveyed the mathematical literature and measurement publications, but could not find any method available for solving the problem. The 6D calculation method turns out to be a severe technical obstacle.

The following is a more specific explanation regarding the essential difficulty of solving nonlinear equation systems. Currently, solving a single nonlinear equation is based on least-square methods. In recent years, very sophisticated least-square methods have been developed for solving problems [10]. Notably, Levenberg-Marquardt provides a good example for using an error function χ^2 for giving a maximum likehood estimate (minimum error estimate) as the solution. When there are multiple unknown parameters and multiple nonlinear equations, the most important difficulty is the so-called "local minimum trap." Because of the local minimum trap, superficial minimum values can be obtained; however, these local minimum values do not reprsent the true solution, but only give false solutions to the problem. The situation is illustrated in Fig. 52 using a single parameter as an example. Suppose the linear function is $y = f(x)$, where $f(x)$ is a nonlinear

function. The task is to find x_0 so that $f(x_0) = 0$, and x_0 is the true solution of the equation.

Figure 52 The problem of local minimum traps in solving nonlinear equations

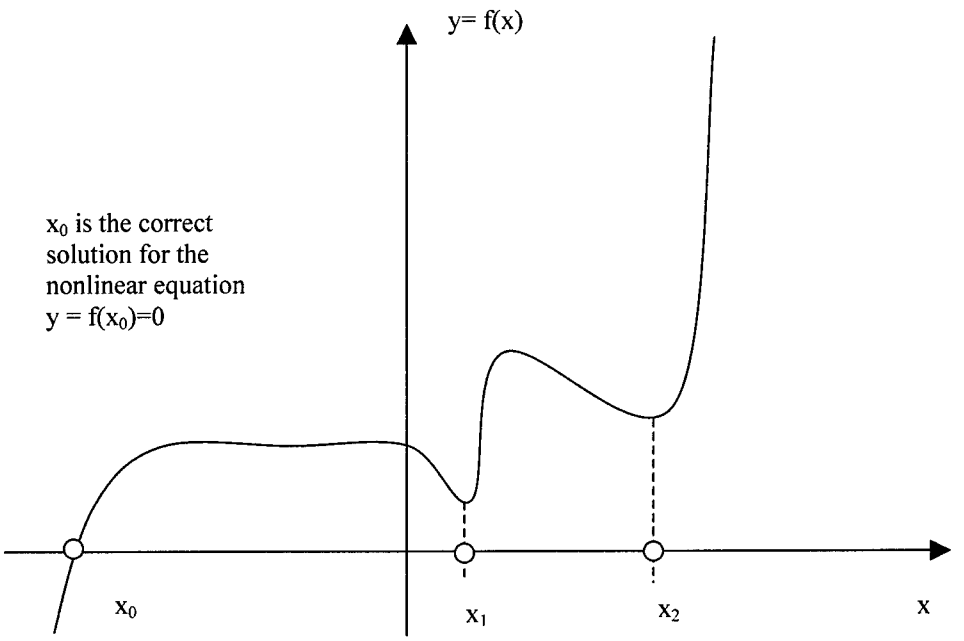

Illustration of the local minimum trap problem in solving nonlinear equations
Because the equation is nonlinear, there are numerous $x_1, x_2, \ldots x_i, \ldots$values that give the funtion a local minimum value within a small region. These $x_1, x_2, \ldots x_i, \ldots$are local traps, and are not the true solution of the equation. These false solutions lead to complete failure in the computation process in using least-square methods for finding the solutions to the equation.

When the equation number is only one, or close to one, there are certain specific methods for avoiding the local traps. However, whether the true solution can really be approached is still not known. The problem becomes extremely severe when the number of the equations are much more than one. The problem becomes practically not solvable when the number of equations is larger than 3 or even more. Even according to the state-of-the-art computation mathematics, the number of false solutions becomes inifinitely large. An authorative computation mathematics textbook, written by a group of today's leading mathematicians [10], states:

"We make an extreme, but wholly defensible, statement: There are ***no*** good, general methods for solving (equation) systems of more than one nonlinear equation. Furthermore, it is not hard to see why (very likely) there ***never will be*** any good, general methods" (Emphasis is from the original text. See p. 379 of reference [10]) .

During the process of executing the present Phase II program, it has become

very clear that a common intuitive understanding regarding 6D measurement techniques is totally wrong. Based on conventional wisdom, it is generally conjectured that in the development of a 6D measurement system, the mathematical calculation of the 6D parameters should present no problem. Actually we were led by such misunderstanding before. Before the program started, we thought that the mathematical calculation might be extremely complicated, because there are so many parameters, and that the structure of the formulas could be very complex. However, we believed that as long as we were patient and weren't put off by the complexity of the mathematical formulas, we could eventually obtain the results. Actually the situation turns out to be far more grave than we expected. It is impossible to get any meaningful results even using the most sophisticated present-day mathematical computation methods.

(6-d) Our approach for solving the 6D mathematical calculation problem

We developed a systematic mathematical theory for solving the above described problems. As a result, the nonlinear equation systems in connection with the 6D calculations become solvable through the efforts of the present Phase II Contract. The main points of our methods are outlined as follows.

(6-d-1) First, using extensive analytical tools, we successfully reduced the 9 equations into 6 equations in the equation systems, a one-step advance in removing excessive complications.

(6-d-2) Second, we introduced a powerful intermediate coordinate system, which can further reduce the complications. After all quantities are transformed into the intermediate coordinate system, only the three rotation angles are present explicitly in the equations as unknown variables. The 3 rotation angle parameters are related with the measurement results. The 3 position variables do not explicitly present in the new equation system. Thus, through the intermediate coordinate system, the number of the nonlinear equations in the equation system can be further reduced to be 3. After the 3 rotation angles are calculated, the remaining 3 unknown position parameters can be further calculated.

(6-d-3) Now the task is reduced to solving a nonlinear equation system having only 3 equations with only 3 unknown variables. However, solving a simultaneous nonlinear equation system with 3 equations still presents a formidable challenge. We further developed an effective method for solving such nonlinear equation systems.

We identified that the essential difficulty in solving the nonlinear equation system is due to numerous local minimum traps, which tend to give wrong numeric values as false solutions. The problem with the local minimum trap was briefly illustrated in the above sections. We have developed an effective approach that can eliminate this problem.

Our method for eliminating the local minimum trap problem takes advantage of the immense power of modern computers. Modern computers have enormous memory

capacity and exceedingly high speed compared with their earlier counterparts. Today, even a common high-end PC workstation can have a greater memory capacity and speed than did a supercomputer that could only be nationally owned ten years ago. By utilizing this technology, the local minimum trap can be solved. The method is briefly outlined as follows:

Before starting to solve the nonlinear equation system, we first established an extremely large data base and stored it in the computer RAM for reference.

First, we reversed the nature of the problem: we assumed that the unknown 6D parameters (3 positions and 3 rotation angles) are given, and the task is to find the measurement results through calculations. Note that this changes the task into a forward calculation. There is no difficulty in doing so and a data base thus can be calculated in advance and stored in the computer for reference.

The data base is a numeric reference table that relates the 6D parameters and measurement data. The value of each unknown 6D parameters has a well-defined, limited range. Because of the enormous capacity of modern computers, the reference table can be compiled so comprehensively that the numeric relationship can be presented with a reasonable accuracy (for example, 3-5%). This comprehensive data base determines the gross behavior of the 6D parameters. If we use Fig. 52 as an illustration, the data base is a discrete numeric table of the curve $x^i = g(y^i)$ with an understanding that each y^i or x^i represents a point in 6D space. In the process of using the least-square data fitting method for solving the nonlinear equation system for finding x_0, we use this huge data base as a reference grid to exclude the false solutions caused by the local minimums. For example, in Fig. 52, the local minimum x_1 and x_2 can be determined as a local minimum trap, because they are located far from the true solution, so they can be identified through consulting the reference table and discarded (automatically) by the computer. Only x_0 is identified as the true solution, because the exact value of the solution x_0 can be predicted with an accuracy of 3-5% . A more detailed description is given below.

(6-e) An outline description of the process of calculation of the reference data base

A basic geometry fact is when the 6D parameters of an antenna, including 3 position parameters (X_o, Y_o, Z_o) , and 3 rotation parameters (α,β,γ)) are given, for a well-defined experimental condition, the calculations for the 6 measured promoters is a forward calculation. By forward calculation we mean deriving triangle formulas and computing the numeric values. So there is no important difficulty in the forward calculations. The 6 measured parameters (p_1, p_2, q_1, q_2, s_1, s_2) can be forward-calculated through writing out the geometry relationships. The 6 measured parameters are actually the bright spots recorded in the image sensors. By analyzing the geometry, six explicit expressions can be written for the coordinate positions in the fixed laboratory system for the recorded bright spots.

$$
\begin{aligned}
p_1 &= p_1 (X_o, Y_o, Z_o, \alpha, \beta, \gamma), \\
p_2 &= p_1 (X_o, Y_o, Z_o, \alpha, \beta, \gamma), \\
q_1 &= p_1 (X_o, Y_o, Z_o, \alpha, \beta, \gamma), \\
q_2 &= p_1 (X_o, Y_o, Z_o, \alpha, \beta, \gamma), \\
s_1 &= p_1 (X_o, Y_o, Z_o, \alpha, \beta, \gamma), \\
s_2 &= p_1 (X_o, Y_o, Z_o, \alpha, \beta, \gamma)
\end{aligned} \qquad (6\text{-}2)
$$

To establish a reference data base, first we specify the maximum value range for each of the 6D parameters (X_o, Y_o, Z_o, α, β, γ). The maximum variation range of the 6D parameters (X_o, Y_o, Z_o, α, β, γ) can be well estimated according to the actual experimental conditions in the anechoic chamber, for example, for the position coordinate range of the test assets, -10 feet < (X_o, Y_o, Z_o) < 10 feet , and the rotation angles, $\alpha_{min} < \alpha < \alpha_{max}$, with $\alpha_{min} = -\pi/2$, and $\alpha_{max.} = \pi/2$. The same is true for β and γ. Then we divide the entire range of the angle α into 20 intervals with the average interval $\delta\alpha = (\alpha_{max} - \alpha_{min}) / 20$. Take the α value to be each of the grid point, so $\alpha_i = i \cdot (\alpha_{max} - \alpha_{min}) / 20$, for i = 1, 2, 3, ... 20. Do the same for all the 6D parameters (α,β,γ) and (X_o, Y_o, Z_o). Then take a combination of each data set of the 6 parameters as initial values to calculate the corresponding imaging measurement results and compile a reference table.

The data volume for the reference table should be $(20)^6 = 64 \times 10^6$. If each data value takes 4 bytes for storage in computer memory, the total memory size for the data base would be $4 \times 64 \times 10^6 = 256$ Mbytes, a rather large memory, but still within a reasonable range of memory capacity for a professional PC computer.

Next, we store the data base in computer RAM for quick access. In the process of doing the data fitting for solving the nonlinear equation systems, we used the data base as a reference grid for keeping the solution close to the data given by the data base. Note that each new set of the input data for trial must be obtained within the reference table. This will eliminate the problem of false solutions.

(6-f) An illustrative example for deriving nonlinear equation systems for 6D calculations

In this section we will give an example of how to analytically derive the 6D equation system. The procedure for deriving the 6D equation systems has the following major steps:

(6-f-1) Clearly define the experimental conditions. This includes clearly defining all physical measurement conditions and geometry conditions of the experimental setting.

(6-f-2) Write down equations. Generally there must be 9 equations, because there must be some indirect geometry quantities, such as line length values, involved in the expressions.

(6-f-3) Using analytical tools to reduce the number of the equations to 6. This means that in the equations, only the 6D parameters (number : 6) to be determined, and the 6 measurement parameters are included in the equations, any other indirect quantities must be removed.

(6-f-4) Draw a special intermediate coordinate frame system and transform all quantities into the special intermediate coordinate system. Using the intermediate coordinate system can reduce the number of equations to 3. This is to be explained in Fig. 55 and Fig. 57.

(6-f-5) Simplify the equations as much as possible and give a final analytical form of the equations suitable for use in computation for solving the equation system.

In the next section, we will define a measurement system that uses 3 retroreflectors fixed on the target. Each 2D image sensor records 3 bright spots. Since each bright spot in the imaging plane gives 2 independent coordinate parameters, the total number of the measurement result data is 6. Use the 6 measured parameters to evaluate the 6D parameters.

This example can be directly applied when using a laser range-finder instrument to do the measurement. The 6D parameters can be evaluated through the equations derived in this section.

The basic geometry setting is shown in Fig. 53, where only one retroreflector (at the position denoted P) is explicitly drawn for representation. The second retroreflector is Q and the third is S. Q and S are omitted in the drawing without affecting writing the equations.

The coordinate system XYZ is the world coordinate system. The coordinate system UVW is the camera coordinate system fixed at point O, which is the center of the imaging lens. The UVW system relative to the XYZ system has 6 independent parameters: 3 translational (for point O), and 3 rotational parameters (around point O).

Figure 53 One of the most basic 6D measurement geometry conditions

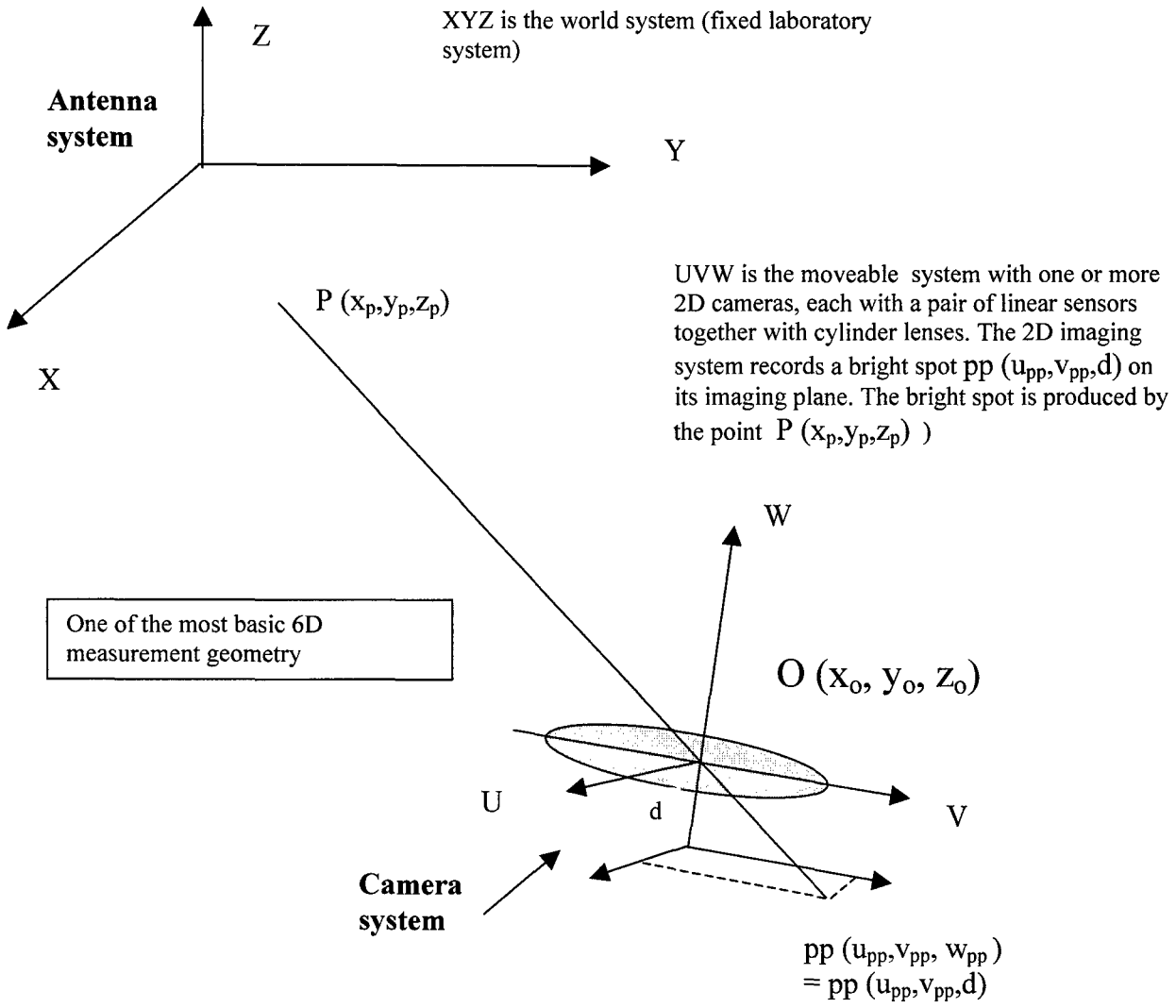

The task is :

$P(x_p, y_p, z_p) \Leftrightarrow (\alpha,\beta,\gamma)$ & $O(X_o, Y_o, Z_o)$ with 6 unknown parameters (α,β,γ) and (X_o, Y_o, Z_o)

$\Leftrightarrow$ PP (x_p, y_p, z_p) as expressed in XYZ

$\Leftrightarrow$ PP (u_{pp}, v_{pp}, w_{pp}) as expressed in UVW

The point P (x_p, y_p, z_p) with 3 coordinate parameters (x_p, y_p, z_p) are known in the fixed laboratory system. The point PP (u_{pp}, v_{pp}, w_{pp}) with 3 coordinate parameters (u_{pp}, v_{pp}, w_{pp}) are known in the 2D imaging system UVW. Note that each set of the recorded data from the 2D imaging sensor can only provide 2 independent parameters, because $w_{pp} = d$, where d is the distance from the lens center to the imaging plane.

Because each 2d image detection system can only provide 2 independent coordinate parameters (u_{pp}, v_{pp}, d) where d is a constant, 3 light-emitting points are required for uniquely determining a set of 6D parameters (α,β,γ) and (X_o, Y_o, Z_o). Thus, one way for 6D measurement is to give 3 independent points $P(x_p, y_p, z_p)$, $Q(x_q, y_q, z_q)$, and $S(x_s, y_s, z_s)$ in the fixed world coordinate system, and records 3 sets of 2D imaging data. The following is a list of the data.

$P(x_p, y_p, z_p) \Leftrightarrow (\alpha,\beta,\gamma)$ & $O(X_o, Y_o, Z_o)$ with 6 unknown parameters (α,β,γ) and (X_o, Y_o, Z_o)

$\Leftrightarrow$ PP (x_p, y_p, z_p) as expressed in XYZ

$\Leftrightarrow$ PP (u_{pp}, v_{pp}, d) as expressed in UVW

$Q(x_q, y_q, z_q) \Leftrightarrow (\alpha,\beta,\gamma)$ & $O(X_o, Y_o, Z_o)$ with 6 unknown parameters (α,β,γ) and $(X_o, Y_o, Z_o) \Leftrightarrow$ QQ (x_q, y_q, z_q) as expressed in XYZ

$\Leftrightarrow$ QQ (u_{qq}, v_{qq}, d) as expressed in UVW

$S(x_s, y_s, z_s) \Leftrightarrow (\alpha,\beta,\gamma)$ & $O(o_x, o_y, o_z)$ with 6 unknown parameters (α,β,γ) and (X_o, Y_o, Z_o)

$\Leftrightarrow$ SS (x_s, y_s, z_s) as expressed in XYZ

$\Leftrightarrow$ SS (u_{ss}, v_{ss}, d) as expressed in UVW

For certainty, we selected $z_p = z_q = z_s = 0$. That is, the 3 points P, Q, and S are selected to be on the XY plane.

The directly written equation system is a 9 x 9 equation system that contains 9 unknown parameters, related by 9 simultaneous nonlinear equations. Using standard mathematical manipulation, the 9 x 9 equation system can be reduced to a 6 x 6 equation system. The reason is: the three scalar parameters t_p , t_q , and t_s characterizing the distances can be removed from the equation system through normalizations. The essence is to consider only the relationship between the unit direction vectors.

$$OPP\ (u_{pp}, v_{pp}, d) = R\ (\alpha, \beta, \gamma) \cdot PO\ (x_o-x_p, y_o-y_p, z_o-z_p) \cdot t_p \qquad (6\text{-}3)$$

$$OQQ\ (u_{qq}, v_{qq}, d) = R\ (\alpha, \beta, \gamma) \cdot QO\ (x_o-x_q, y_o-y_q, z_o-z_q) \cdot t_q$$

$$OSS\ (u_{ss}, v_{ss}, d) = R\ (\alpha, \beta, \gamma) \cdot SO\ (x_o\text{-}x_s, y_o\text{-}y_s, z_o\text{-}z_s) \cdot t_s$$

$$R = R_\alpha \cdot R_\beta \cdot R_\gamma \tag{6-4}$$

with $$R_\alpha = \begin{vmatrix} 1 & 0 & 0 \\ 0 & \cos\alpha & -\sin\alpha \\ 0 & \sin\alpha & \cos\alpha \end{vmatrix}, \tag{6-5}$$

with $$R_\beta = \begin{vmatrix} \cos\beta & 0 & \sin\beta \\ 0 & 1 & 0 \\ -\sin\beta & 0 & \cos\beta \end{vmatrix}, \tag{6-6}$$

with $$R_\gamma = \begin{vmatrix} \cos\gamma & -\sin\gamma & 0 \\ \sin\gamma & \cos\gamma & 0 \\ 0 & 0 & 1 \end{vmatrix}, \tag{6-7}$$

The 6 x 6 equation system can be written as follows.

$$OPP\ (u_{pp}, v_{pp}, d) / \|OPP\| = R\ (\alpha, \beta, \gamma) \cdot PO\ (x_o\text{-}x_p, y_o\text{-}y_p, z_o\text{-}z_p) / \|OP\| \tag{6-8}$$

$$OQQ\ (u_{qq}, v_{qq}, d) / \|OQQ\| = R\ (\alpha, \beta, \gamma) \cdot QO\ (x_o\text{-}x_q, y_o\text{-}y_q, z_o\text{-}z_q) / \|OQ\|$$

$$OSS\ (u_{ss}, v_{ss}, d) / \|OSS\| = R\ (\alpha, \beta, \gamma) \cdot SO\ (x_o\text{-}x_s, y_o\text{-}y_s, z_o\text{-}z_s) / \|OS\|$$

A critically important step is to introduce a special coordinate system, through which the 6 nonlinear simultaneous equation systems can be reduced to have only 3 equations. In the 3 equations only 3 rotation angles are explicitly present in the equations. The intermediate coordinate system is shown in Fig. 54. The intermediate coordinate system is the coordinate system ${}^1U^1V^1W$. The system is fixed in the target system together with the system UVW. However, the system ${}^1U^1V^1W$ is parallel to the laboratory system XYZ.

To make a transformation from UVW to ${}^1U^1V^1W$, write down all quantities originally expressed in UVW through rotation transformation into the expressions in the system ${}^1U^1V^1W$. Note that for this rotation transformation, the tranformation matrix is $R^{-1}(\alpha, \beta, \gamma)$, which is the inverse transformation of $R\ (\alpha, \beta, \gamma)$.

Figure 54 The special intermediate coordinate system as discovered in the present Phase II Contract

Illustration of the intermediate coordinate system.

We discovered a powerful intermediate coordinate system that can reduce the nonlinear equation number from 6 to 3 in the equation system for solving the 6D measurement problem.
The intermediate coordinate system is ${}^{1}U{}^{1}V{}^{1}W$. This is critical progress made in the present Phase II Contract to make the 6D equation systems solvable.

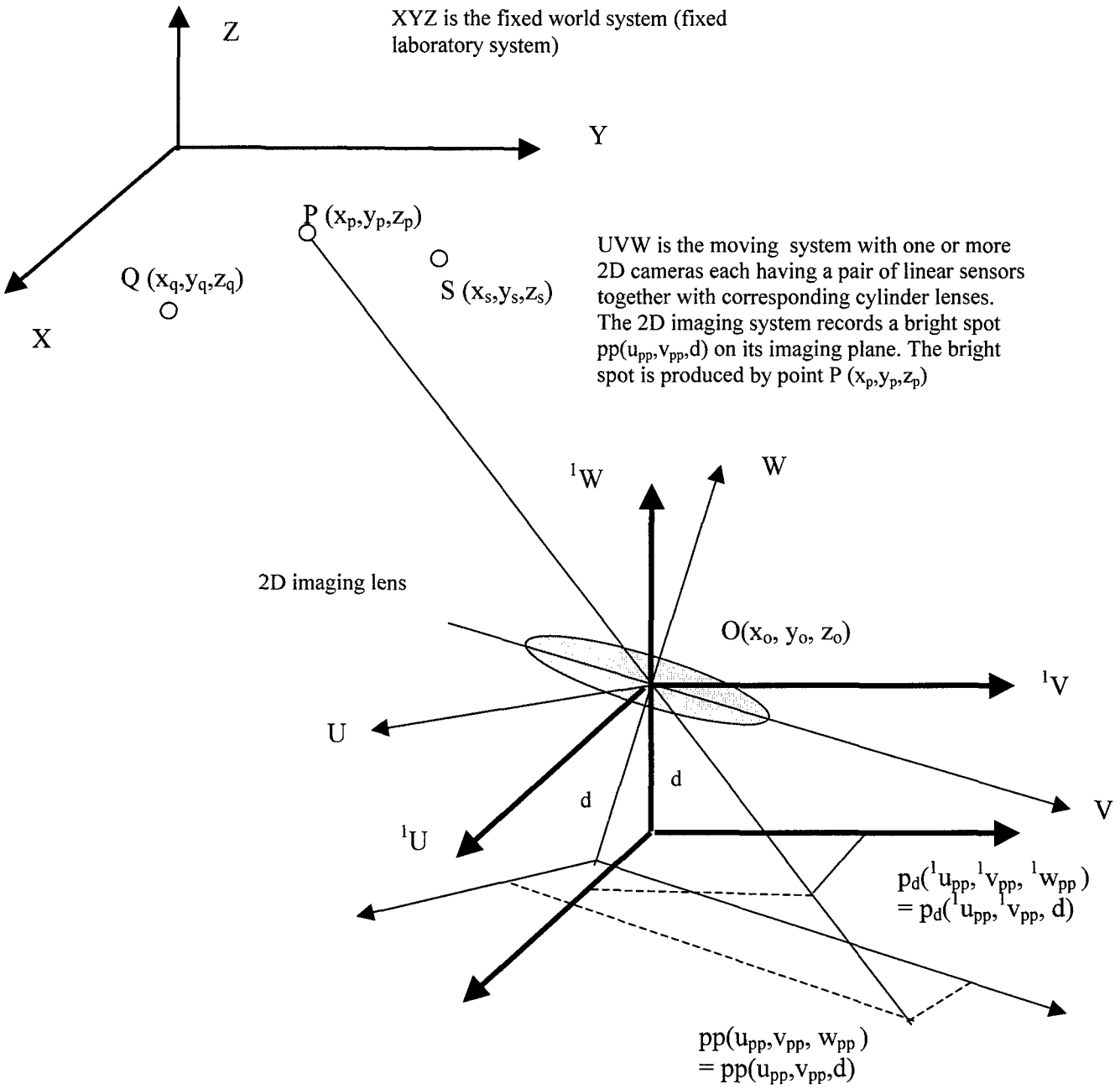

The coordinate system ${}^1U{}^1V{}^1W$ is an intermediate system fictitiously constructed. The axes of the coordinate system ${}^1u{}^1v{}^1w$ are parallel to those of the coordinate system XYZ. That is, in relation to the system XYZ, ${}^1u{}^1v{}^1w$ has only translational movement, and does not have rotational movement. In relation to the system uvw, ${}^1u{}^1v{}^1w$ has only rotaional movement, and does not have translational movement.

A subject point P (x_p, y_p, z_p) in the fixed world coordinate system XYZ is recorded by the imaging camera on the imaging plane as a point PP (u_{pp}, v_{pp}, d), where d is the distance from the the center of the lens to the focal plane (the imaging plane).

The intermediate rotation from the uvw system to the fictitious coordinate system ${}^1u{}^1v{}^1w$ is critically important for making the nonlinear simultaneous equation system solvable. Without using the coordinate system there are 6 unknown parameters, and 6 simultaneous equations. This makes the solution extremely complicated and practically unsolvable. With the intermediate coordinate system, the 6 unknown parameters are divided into two groups, each having only 3 unknown parameters and 3 independent equations.

The straight line P-O-PP crosses the system ${}^1u{}^1v{}^1w$ at the corresponding imaging plane at point P_d (${}^1u_{pp}$, ${}^1v_{pp}$, d). The quantities u_{pp}, v_{pp} are the image data that can be read from the image sensor . So are the image data u_{qq}, v_{qq} , u_{ss}, v_{ss} . Next calculate the coordinate OPP in the system ${}^1u{}^1v{}^1w$ and in the system uvw.

OPP in the system ${}^1u{}^1v{}^1w$ is expressed as OPP(u_{pp}, v_{pp}, w_{pp}) = OPP(u_{pp}, v_{pp}, d), because w_{pp} = d. On the other hand, OPP in the system ${}^1u{}^1v{}^1w$ is expressed as OPP(${}^1u_{pp}$, ${}^1v_{pp}$ ${}^1w_{pp}$,) = OPP (${}^1u_{pp}$, ${}^1v_{pp}$, d), because ${}^1w_{pp}$ = d.

$$\mathbf{OPP} = \mathbf{u}_{pp} + \mathbf{v}_{pp} + \mathbf{w}_{PP} \qquad (6\text{-}9)$$

$$\mathbf{OPP} = {}^1\mathbf{u}_{PP} + {}^1\mathbf{v}_{PP} + {}^1\mathbf{w}_{PP} \qquad (6\text{-}10)$$

$${}^1u_{PP} = R_{11}\, u_{PP} + R_{12} v_{PP} + R_{13}\, w_{PP} \qquad (6\text{-}11)$$

$${}^1v_{PP} = R_{21}\, u_{PP} + R_{22} v_{PP} + R_{23}\, w_{PP} \qquad (6\text{-}12)$$

$${}^1w_{PP} = R_{31}\, u_{PP} + R_{32} v_{PP} + R_{33}\, w_{PP} \qquad (6\text{-}13)$$

At what point does **OPP crosses the plane** ${}^1w_{PP}$ in the System ${}^1u{}^1v{}^1w$?

Write the equations (46-1) (46-2) (46-3) into a equation system, which contains a common parameter ξ, then find out ξ,

$${}^1u_{PP} \equiv {}^1u_{PP\xi} = \xi\,(R_{11}\, u_{PP} + R_{12} v_{PP} + R_{13}\, w_{PP}\,) \qquad (6\text{-}14)$$

$${}^1v_{PP} \equiv {}^1v_{PP\xi} = \xi\,(R_{21}\, u_{PP} + R_{22} v_{PP} + R_{23}\, w_{PP}\,) \qquad (6\text{-}15)$$

$${}^1w_{PP} \equiv {}^1w_{PP\xi} = \xi\,(R_{31}\, u_{PP} + R_{32} v_{PP} + R_{33}\, w_{PP}\,) \qquad (6\text{-}16)$$

The crossing point in ${}^1w_{PP\xi} = d$

Then,

$$\xi_p = \frac{d}{R_{31}\, u_{PP} + R_{32} v_{PP} + R_{33}\, w_{PP}} \qquad (6\text{-}17)$$

So, $$ {}^{l}u_{Pd} = d\,\frac{(R_{11}\, u_{PP} + R_{12} v_{PP} + R_{13} d)}{(R_{31}\, u_{PP} + R_{32} v_{PP} + R_{33} d)} \qquad (6\text{-}18)$$

for point p,

$$ {}^{l}v_{Pd} = d\,\frac{(R_{21}\, u_{PP} + R_{22} v_{PP} + R_{23}\, d)}{(R_{31}\, u_{PP} + R_{32} v_{PP} + R_{33}\, d)} \qquad (6\text{-}19)$$

for point q

$$ {}^{l}u_{qd} = d\,\frac{R_{11}\, u_{qp} + R_{12} v_{qp} + R_{13}\, w_{qp}}{R_{31}\, u_{qp} + R_{32} v_{qp} + R_{33}\, w_{qp}} \qquad (6\text{-}20)$$

$$ {}^{l}v_{qd} = d\,\frac{R_{21}\, u_{qp} + R_{22} v_{gp} + R_{23}\, w_{qp}}{R_{31}\, u_{qp} + R_{32} v_{qp} + R_{33}\, w_{qp}} \qquad (6\text{-}21)$$

For point s

$$ {}^{l}u_{sd} = d\,\frac{R_{11}\, u_{sp} + R_{12} v_{sp} + R_{13}\, w_{sp}}{R_{31}\, u_{sp} + R_{32} v_{sp} + R_{33}\, w_{sp}} \qquad (6\text{-}22)$$

$$ {}^{l}v_{sd} = d\,\frac{R_{21}\, u_{sp} + R_{22} v_{sp} + R_{23}\, w_{sp}}{R_{31}\, u_{sp} + R_{32} v_{sp} + R_{33}\, w_{sp}} \qquad (6\text{-}23)$$

For the 3 point p, q ,s, $p(x_p, y_p, z_p)$, $q(x_q, y_q, z_q)$, $s(x_s, y_s, z_s)$

$$\frac{x_p - x_o}{z_p - z_o} = \frac{{}^{l}u_{Pd}}{d}, \quad \frac{y_p - y_o}{z_p - z_o} = \frac{{}^{l}v_{Pd}}{d} \qquad (6\text{-}24)$$

$$\frac{x_q - x_o}{z_q - z_o} = \frac{{}^{l}u_{qd}}{d}, \quad \frac{y_q - y_o}{z_q - z_o} = \frac{{}^{l}v_{qd}}{d}$$

$$\frac{x_s - x_o}{z_s - z_o} = \frac{{}^{l}u_{sd}}{d}, \quad \frac{y_s - y_o}{z_s - z_o} = \frac{{}^{l}v_{sd}}{d}$$

$$x_p - x_o = (z_p - z_o)\frac{{}^1u_{Pd}}{d}$$

$$x_q - x_o = (z_q - z_o)\frac{{}^1u_{qd}}{d}$$

$$x_p - x_q = z_p\frac{{}^1u_{Pd}}{d} - z_q\frac{{}^1u_{qd}}{d} + (-z_o)\frac{{}^1u_{Pd}}{d} + z_o\frac{{}^1u_{qd}}{d}$$

$$x_p - x_q - (z_p\,{}^1u_{Pd}/d - z_g\,{}^1u_{sd}/d) = z_o(-{}^1u_{Pd}/d + {}^1u_{qd}/d) \qquad (6\text{-}25)$$

Similarly $\quad y_p - y_o = (z_p - z_o)\,{}^1v_{Pd}/d$

$$y_q - y_o = (z_p - z_o)\,{}^1v_{qd}/d$$

$$y_p - y_q = z_p\,{}^1v_{Pd}/d - z_q\,{}^1v_{qd}/d + (-z_o)\,{}^1v_{Pd}/d + z_o\,{}^1v_{qd}/d$$

or $\quad y_p - y_q - (z_p\,{}^1v_{Pd}/d - z_q\,{}^1v_{qd}/d) = z_o(-{}^1v_{Pd}/d + z_o\,{}^1v_{qd})$

$$\frac{d(x_p - x_q) - (z_p{}^1u_{Pd} - z_q{}^1u_{qd})}{d(y_p - y_q) - (z_p{}^1v_{Pd} - z_q{}^1v_{qd})} = \frac{-{}^1u_{Pd} + {}^1u_{qd}}{-{}^1v_{Pd} + {}^1v_{qd}}$$

$$\frac{d(x_p - x_q) - (z_p\,{}^1u_{Pd} - z_q{}^1u_{qd})}{-{}^1u_{Pd} + {}^1u_{qd}} = \frac{d(y_p - y_q) - (z_p{}^1v_{Pd} - z_q{}^1v_{qd})}{-{}^1v_{Pd} + {}^1v_{qd}} \qquad (6\text{-}26)$$

$$\frac{d(x_p - x_q) - (z_p\,{}^1u_{Pd} - z_q{}^1u_{qd})}{-{}^1u_{Pd} + {}^1u_{qd}} = \frac{d(y_p - y_s) - (z_p{}^1v_{Pd} - z_s{}^1v_{sd})}{-{}^1v_{Pd} + {}^1v_{sd}}$$

$$\frac{d(x_p - x_q) - (z_p\,{}^1u_{Pd} - z_q{}^1u_{qd})}{-{}^1u_{Pd} + {}^1u_{qd}} = \frac{d(x_p - x_s) - (z_p{}^1u_{Pd} - z_s{}^1u_{sd})}{-{}^1u_{Pd} + {}^1u_{sd}}$$

When $z_p = 0, z_q = 0, z_s = 0$, similarly the rule holds

$$\frac{x_p - x_q}{{}^1u_{Pd} - {}^1u_{qd}} = \frac{y_p - y_q}{{}^1v_{Pd} - {}^1v_{qd}} \qquad (6\text{-}27)$$

${}^1u_{Pd}, {}^1u_{qd} \ldots {}^1v_{Pd}, {}^1v_{qd}, \ldots$ are calculated according to (6-18) through (6-23)

$$\frac{x_p - x_q}{{}^1u_{Pd} - {}^1u_{qd}} = \frac{y_p - y_s}{{}^1v_{Pd} - {}^1v_{sd}} \qquad (6\text{-}28)$$

$$\frac{x_p - x_q}{{}^1u_{Pd} - {}^1u_{qd}} = \frac{x_p - x_s}{{}^1u_{Pd} - {}^1u_{sd}} \qquad (6\text{-}29)$$

all terms $= \frac{z_o}{d}$

(6-27), (6-28), and (6-29) establish 3 nonlinear equations for α,β,γ. Solve 3 nonlinear, simultaneous equations for α,β,γ. Then, using α,β,γ, calculate x_o, y_o, z_o to obtain a complete set of 6D parameters.

(6-g) A second illustrative example for deriving nonlinear equation systems for 6D calculations

The experimental conditions for 6D measurements are more than one. A brief list and a brief analysis of all major experimental conditions are presented in [8]. In the following we will briefly mention another geometry condition that is important for the actual experimental conditions of the present system design.

In this 6D measurement design, as shown in Fig. 1, two tags are mounted on the test asset (antenna) each with a 2D photo-detector. Another 2D photo-detection system is placed near the measurement station (the PC). Total measurement parameters are 8. Among the 8 measured parameters, only 6 are independent. The other 2 parameters can be used for a consistency check.

The experimental condition is shown in Fig. 55. The mathematical method is basically the same as described above. One critical step is the use of an intermediate coordinate system. When certain quantities are calculated in the intermediate system, the total number of equations can be reduced to 3. Thus, a 3 simultaneous nonlinear equation system is a reasonable number to solve.

This mathematical derivation is also very long and cannot be quoted here. A detailed mathematical derivation can be found in the Laboratory Note Book No. 2 (pp. 74-100) . In the following, only final equations and relevant expressions are listed.

Figure 55 A second basic geometry condition for 6D measurements

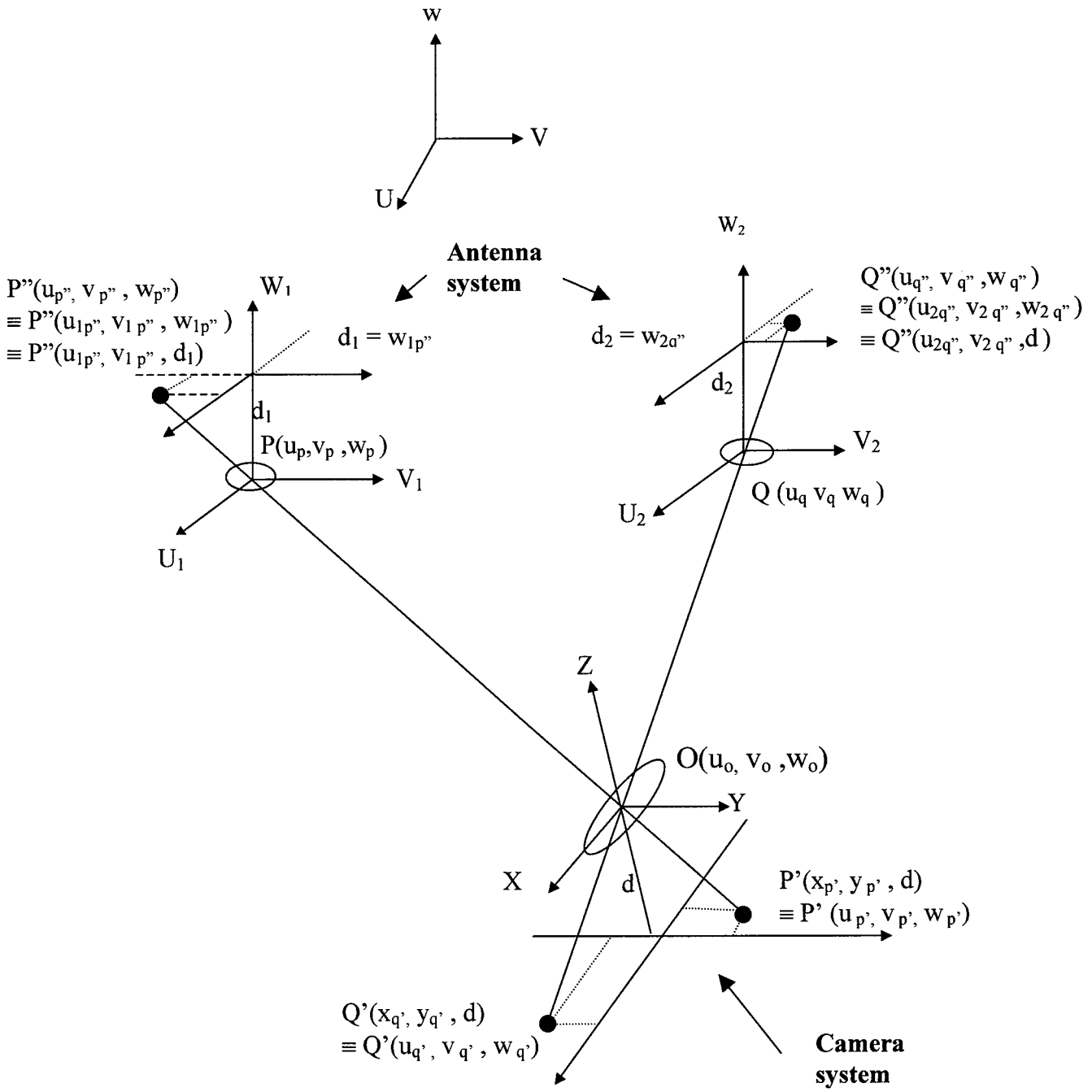

uvw, $u_1v_1w_1$, $u_2v_2w_2$ having axes parallel to each other. Common reference: uvw. uvw system is fixed with the antenna; xyz is the optical

Figure 56 The special intermediate coordinate system that makes the 6D calculation problem solvable for the second basic geometry condition

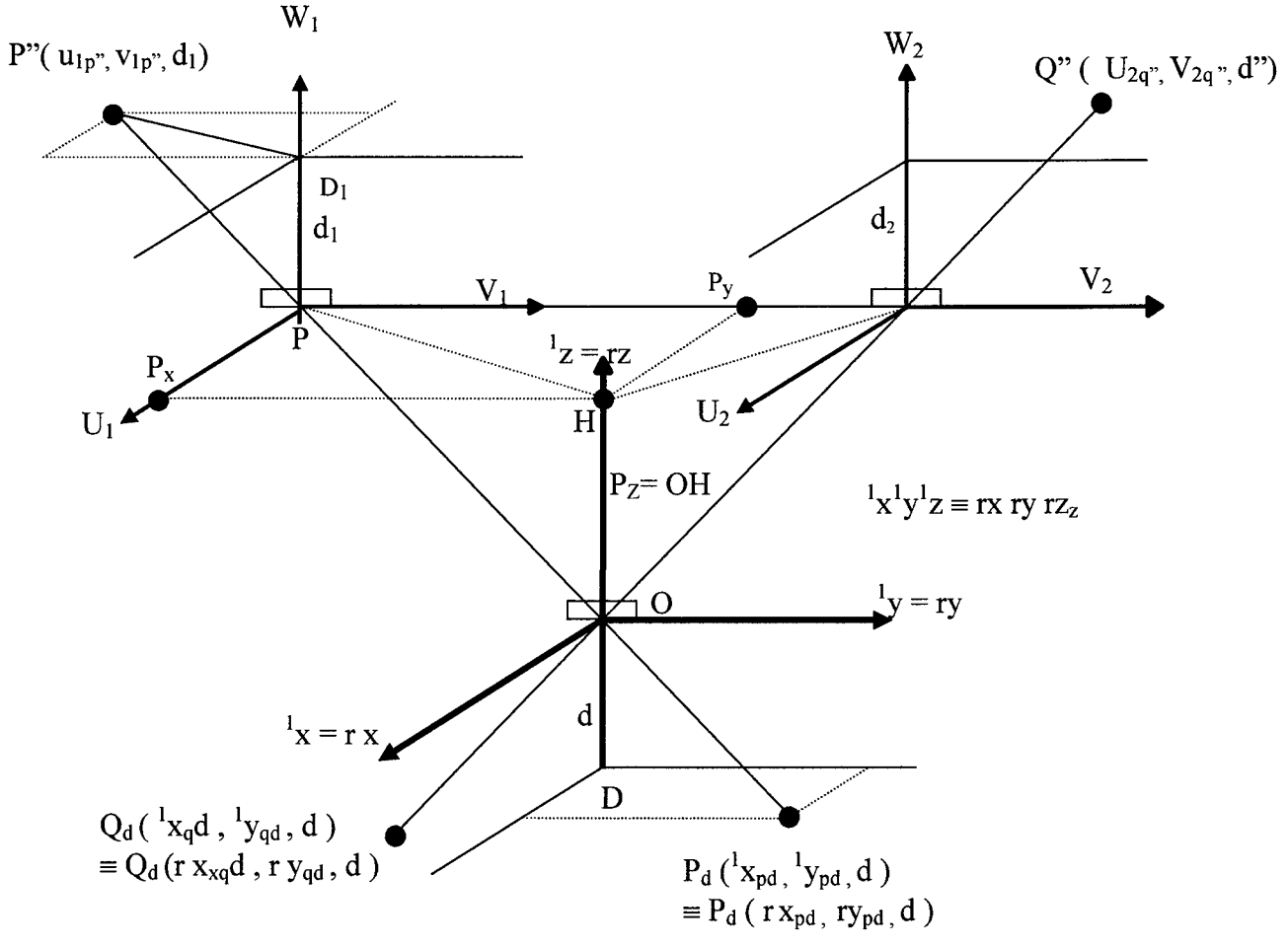

$^{1}u_{pp} \longrightarrow x_{pp}$, $^{1}u_{Pd} \longrightarrow x_{pd}$ original formula, $^{1}u_{Pd} = d \dfrac{R_{11}\,u_{PP} + R_{12}v_{PP} + R_{13}d}{R_{31}\,u_{PP} + R_{32}v_{PP} + R_{33}d}$

$^{1}u_{Pd} \longrightarrow {}^{1}x_{pd}$, $u_{pp} \longrightarrow x_{pp}$

$$^{1}x_{Pd} = d\,\frac{R_{11}x_{PP} + R_{12}y_{PP} + R_{13}d}{R_{31}\,x_{PP} + R_{32}y_{PP} + R_{33}d} \qquad (6\text{-}30)$$

$$^{1}y_{Pd} = d\,\frac{R_{21}x_{PP} + R_{22}y_{PP} + R_{23}d}{R_{31}\,x_{PP} + R_{32}y_{PP} + R_{33}d} \qquad (6\text{-}31)$$

Similarly for the line Q- O - QQ (x_{qq} ,y_{qq} ,d)

$$^{1}x_{qd} = d\,\frac{R_{11}x_{qq} + R_{12}y_{qq} + R_{13}d}{R_{31}\,x_{qq} + R_{32}y_{qq} + R_{33}d} \qquad (6\text{-}31)$$

$$^{1}y_{qd} = d\,\frac{R_{21}x_{qq} + R_{22}y_{qq} + R_{23}d}{R_{31}\,x_{qq} + R_{32}y_{qq} + R_{33}d} \qquad (6\text{-}32)$$

Next, link $^{1}x_{Pd}$, $^{1}y_{Pd}$, $^{1}x_{qd}$, $^{1}y_{qd}$ with the recorded data by the u_1 v_1 w_1 and u_2 v_2 w_2

$$\frac{^{1}x_{Pd}}{d} = \frac{u_{1pp}}{d_1}\,,\ \frac{^{1}x_{Pd}}{d} = \frac{u_{1pp}}{d_1}\,,$$

$$\frac{^{1}x_{qd}}{d} = \frac{u_{2qq}}{d_2}\ \text{, and}\quad \frac{^{1}y_{qd}}{d} = \frac{v_{2qq}}{d_2} \qquad (6\text{-}33)$$

Any 3 of the 4 equations in (6-33) can be used to detemine R (α,β,γ) for α,β,γ.

Calculation of displacement vector OP, PQ is given as the experimental conditions using a similar relationship.

(6-h) An outline review of the numeric method for finding solutions to simultaneous nonlinear equation systems

The computational method and the software subroutine is basically an improved least-square method. The method is selected from numerous software packages that were popularly used in supercomputers in the 1970s and 1980s. The core is taken from a very popular computational mathematics book, *Numeric Recipes* [10].

Assume we have a nonlinear equation system:

$$\begin{aligned} F_1(x_1, x_2, x_3)&=0 \\ F_2(x_1, x_2, x_3)&=0 \\ F_3(x_1, x_2, x_3)&=0 \end{aligned} \qquad (6\text{-}34)$$

Expressed in a vector form

$$\mathbf{F}(x_1, x_2, x_3)=0$$

or

$$\mathbf{F}(\mathbf{x})=0$$

When each new set of argument is tried, $\mathbf{x}_{new} = \mathbf{x}_{old} + \delta\mathbf{x}$

$$F_i(\mathbf{x} + \delta\mathbf{x}) = F_i(\mathbf{x}) + \sum_{j=1,2,3} (\partial F_i(\mathbf{x}) / \partial x_j)\delta x_j + O(\delta\mathbf{x}^2)$$

The matrix of partial derivatives appearing in the equation is the Jacobian matrix $\underline{\mathbf{J}}$

$$J_{ij} \equiv \partial F_i(\mathbf{x}) / \partial x_j$$

In matrix notation, equation () is:

$$\mathbf{F}(\mathbf{x} + \delta\mathbf{x}) = \mathbf{F}(\mathbf{x}) + \underline{\mathbf{J}} \cdot \delta\mathbf{x} + O(\delta\mathbf{x}^2)$$

By neglecting terms of order $\delta\mathbf{x}^2$ and higher, and by setting $\mathbf{F}(\mathbf{x} + \delta\mathbf{x}) = 0$, we obtain a set of linear equations for corrections $\delta\mathbf{x}$ that moves each function closer to zero simultaneously, namely

$$\underline{\mathbf{J}} \cdot \delta\mathbf{x} = -\underline{\mathbf{F}} \qquad (35)$$

Matrix equation (35) can be solved by using a standard method for solving a linear

equation system. The corrections are then added to the solution vector

$$x_{new} = x_{old} + \delta x$$

$$\delta x = - J^{-1} \cdot F$$

How do we decide whether the δx is or is not a local minimum? A reasonable strategy is to require that the step δx decreases $| F |^2 = F \cdot F$.
Instead of requiring $F \cdot F$. decreases, we require the direction (decent direction) where $F \cdot F$ decreases. This criterion is used to select the new δx.

By using the available basic subroutines with certain adaptations, we developed a complete software package for 6D applications.

(6-i) Illustrative computer tests results

The mathematical methods, including all expressions, were derived, checked, and double-checked with extreme care, and tested individually before any one of them were used in the computation programs. The excessive care to ensure the accuracy of each formula is absolutely necessary. This is because the mathematical expressions are usually very long and complex; any slight omission could ruin every subsequent step.

Because these programs are very long, it is not appropriate to list the text of these programs here. Listed in Fig. 57 is an illustrative example of the computer printout for running the software for solving the nonlinear equation system for 6D calculations.

Figure 57 A computer printout to show the results of solving 6D nonlinear equation systems

The following is the measured data as recorded by detectors (assumed)
xppexp= -11.333000 yppexp= -10.333000 xqqexp= -11.097168
The data group should be recorded at the 3 rotation angles (expressed in radians):
α = **xa = 0.11780** ; β = **xb = 0.157080**; γ = **xc = 0.196350.**
The above data are forwardly calculated results that were already known before solving the equations.

The Computer program starts solving the equation system (having 3 nonlinear equations) through data fitting. In the data fitting the 3 measured quantities (xppexp, yppexp, and xqqexp) are given input, the task is to find out 3 unknown rotation angle values. The following is taken from a computer printout during the program execution.

The first iteration: its: 1 xits: 0.039270 0.353429 0.392699
Fits: 2.388324e+000 6.378206e+000 2.119399e+000
xch: 0.039370 0.353429 0.392699 fd1: 2.38603 fd2: 6.37441 fd3: 2.11712
f0: 2.543873e+001

alam: 1 alamin 6.901e-007
xln: 0.122806 0.209670 0.247793**(These are the trial 3 rotation angle values)**

Fln: 0.28172 0.909155 0.218836 **(These are the deviations from zero for each function)**

FF: 4.769093e-001**(This is the average deviation of the 3 function values from zero)**

test: 9.091552e-001
test2: 1.449065e-001 **(The test criteria have not been met, the program continues)**

The second iteration: its: 2 xits: 0.122806 0.209670 0.247793
Fits: 2.817205e-001 9.091552e-001 2.188356e-001
xch: 0.122906 0.209670 0.247793 fd1: 0.280415 fd2: 0.906892 fd3: 0.217504
f0: 4.769093e-001
alam: 1 alamin 1.93475e-006
xln: 0.119300 0.157984 0.198755
Fln: -0.0329113 -0.00315196 -0.0355641
FF: 1.178947e-003
test: 3.556413e-002
test2: 5.168624e-002

The third iteration: its: 3 xits: 0.119300 0.157984 0.198755
Fits: -3.291129e-002 -3.151956e-003 -3.556413e-002
xch: 0.119400 0.157984 0.198755 fd1: -0.0340784 fd2: -0.00521884 fd3: -0.0367662
f0: 1.178947e-003
alam: 1 alamin 3.83392e-005
xln: 0.117596 0.156807 0.196147
Fln: -5.76579e-005 -0.000102145 -4.74009e-005
FF: 8.002420e-009
test: 1.021448e-004
test2: 2.608299e-003

The fourth iteration: its: 4 xits: 0.117596 0.156807 0.196147
Fits: -5.765789e-005 -1.021448e-004 -4.740088e-005
xch: 0.117696 0.156807 0.196147 fd1: -0.00122852 fd2: -0.00216965 fd3: -0.00125399
f0: 8.002420e-009
alam: 1 alamin 0.0108692
xln: 0.117599 0.156816 0.196154
Fln: -1.21777e-007 -2.06488e-007 -1.15749e-007
FF: 3.543240e-014
test: 2.064880e-007
test2: 9.194016e-006

The fifth iteration: its: 5 xits: 0.117599 0.156816 0.196154
Fits: -1.217769e-007 -2.064880e-007 -1.157492e-007
xch: 0.117699 0.156816 0.196154 fd1: -0.001171 fd2: -0.00206774 fd3: -0.00120673
f0: 3.543240e-014
alam: 1 alamin 13.3747
xln: 0.117599 0.156816 0.196154 (These are the trial values for the 3 rotation angles)
Fln: 1.98204e-007 -1.33811e-008 1.95457e-007 **(These are the deviations from zero for each function)**
FF: 3.883366e-014 **(This is the average deviation of the 3 function values from zero)**
test: 1.982041e-007
test1: 0.000005

Tests passed, data fitting completed. The last group of data is the solution. So the final solution for the 3 rotation angles are:

xln: α **= xln1 = 0.117599;** β **= xln2 = 0.156816;** γ **= xln3 = 0.196154**

Before the program started, as listed at the beginning, the exact 3 rotation angle values should be:

α **= xa = 0.11780 ;** β **= xb = 0.157080;** γ **= xc = 0.196350.**

These results show that the program works reliably.

(6-j) An outline of mathematical software packages

We developed a software package for 6D measurements, which is enclosed on disk with the final report. An outline of program types is listed below.

1. A program that can solve the nonlinear equation systems with a simple structure.

2. Software to perform rotation transformations.

3. Software to perform calculations of the data base.

4. Software to correct real geometry conditions.

5. A complete package for performing front-to-end calculations of the 6D measurement results.

Each of the above programs were carefully double-checked and tested with numeric values.

7. Enhanced photo-detector for 6D measurements

During the execution of Contract No. F 04611-98-C-0020, a new photo-detection technology emerged. This is the two-dimensional (2D) CMOS image sensor. Because the 2D CMOS image sensor has a random-access feature, this device is especially good for building a 2D direction-resolvable photo-detector for 6D measurements.

No change is made to the above mentioned contract. However, we present this report for further reference, as a supplement to the final report of the above contract. This report is to fulfill the commitment made in February 2000 for extension of the contract completion schedule.

This report consists of the following sections:
(7-a) A description of the enhanced intelligent 2D sensor
(7-b) Preliminary experimental work for the new 2D photo-detector

(7-a) A description of the enhanced intelligent 2D sensor

A schematic presentation of the intelligent 2D sensor is shown in Fig. 1. The sensor is composed of 6 parts:
(a) a specialty sphere lens,
(b) a specialty fiberoptic plate,
(c) a liquid crystal modulator with a semi-transparent mirror,
(d) an active pixel two-dimensional CMOS sensor,
(e) a microcontroller,
(f) a micro-cell battery.

Figure 58 An enhanced 6D tag based on use of CMOS 2D active pixel sensors

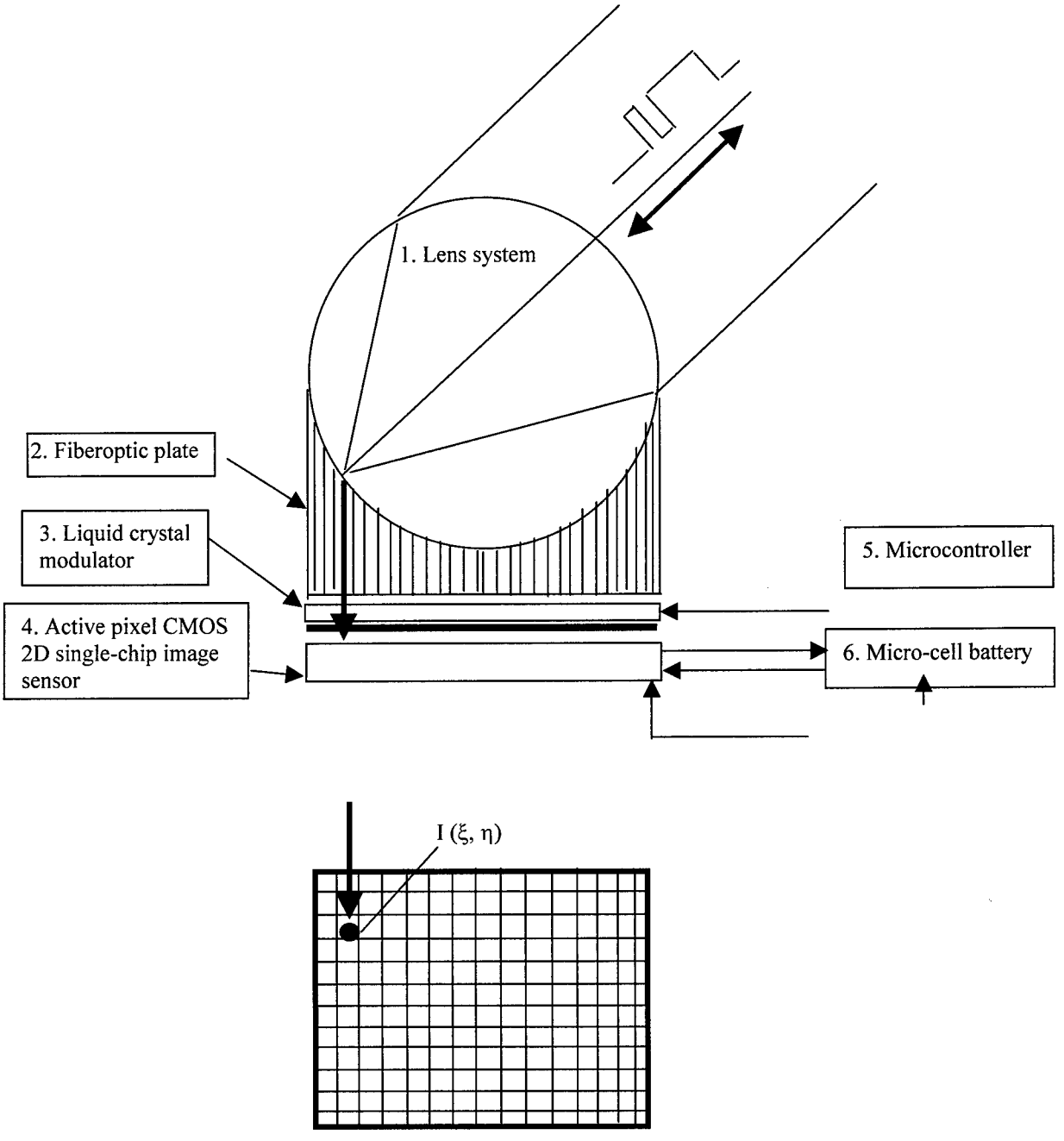

A bright spot is detected by the active pixel 2D image sensor and the microcontroller at the position (ξ, η). The microcontroller converts I (ξ,η) into a modulation code. The liquid crystal modulator transmits the code back to the laser source site. The photo-detection system at the laser source site decodes the data into two orientation angles of the tag in relation to the incident laser beam direction. The coordinate data (ξ, η) has a one-to-one correspondence with two orientation angles (the zenith angle θ and the azimuth angle φ) : $\xi = R \cdot \cos\theta \cdot \cos\varphi$; $\eta = R \cdot \cos\theta \cdot \sin\varphi$, where R is the radius of the sphere lens.

The basic structures remain the same as that described in the final report of the above mentioned contract. The key enhancement is to use the latest achievements of microelectronics and imaging devices to further conduct accurate on-site measurement of the orientation of the target, and to transmit the orientation data of the target to the control station. In the enhanced device, a novel active pixel CMOS two-dimensional image sensor, together with an embedded microprocessor is used for an intelligent photo-detector. The active pixel CMOS image sensor directly conducts the measurements, while the embedded microprocessor is programmed to control the entire data acquisition, data transfer, data processing, and data communication process. The device is intelligent it is controlled by the embedded microprocessor, which is essentially a single-chip microcomputer.

The following is a brief description of the recently developed active pixel 2D image sensor and the microcontroller, and how the two integrated chips execute the measurement functions.

The active pixel CMOS image sensor is a novel imaging device invented in 1995 by the Jet Propulsion Laboratory of NASA. Recently, high performance, commercial products have become available. Compared with the well-known CCD image sensors, the active pixel CMOS image sensor provides many unique features. Active pixel CMOS image sensors are especially important for the present program for position and orientation measurements. The most important features of the novel image sensors are:

1) In contrast to CCD sensors, which use a special fabrication method and special equipment for making photo-sensitive sensors, the CMOS image sensor uses the same equipment and fabrication method as other conventional CMOS integrated circuit chips. Because of this, many electronic circuits can be built into a single chip in the same process for fabrication of the image sensor. Usually, to use a standard CCD sensor, complicated accessory driving circuits are needed near the image sensor to provide various clock signals and control signals. Furthermore, a complex computer board (called a frame grabber) is needed for digitizing and processing the image data. In contrast, even for the first CMOS image sensors, everything is integrated inside the IC chip. So, the CMOS image sensor can provide a highly integrated single-chip image sensor. This is especially favorable for using the device in a highly compact device such as a 6D sensor.

2) The CCD sensor is intrinsically a frame-based device. For obtaining the signal intensity data from any single pixel, the entire frame of the image data must first be transferred and then selected for the interested pixel address from the entire frame data set through computer programming. In contrast, the active pixel CMOS image sensor is a random-access device, much like a random access memory IC chip. Any pixel data can be direct accessed without the need to transfer the entire frame of data. This feature creates a significant difference between the CCD sensor and the active pixel CMOS sensor when the pixel number is very large. For example, for the position and orientation measurements, essentially only one single pixel data with the peak signal intensity (the "brightest spot") is important. When the image sensor has a

pixel number as large as 1,000 x 1,000, to obtain the data for the brightest pixel, using a CCD sensor, 1,000 x 1,000 = 10^6 pixel data must all be first transferred and digitized. By utilizing the novel active pixel CMOS sensors, in principle, only a few pixel data need to be transferred and processed. This unique feature will make the speed and other performance parameters exceedingly high, and in the meantime, make the system structure exceedingly simple.

3) Other unique features of the CMOS image sensors include lower power consumption and lower costs. The electric power required by a CMOS image sensor is usually 3 to 5 times less than that of a comparable CCD sensor. The cost difference in many cases can be very large.

A brief review of the microcontroller.

Microcontrollers can be used as an embedded microprocessor for 6D measurements. A microcontroller is a high performance single-chip microcomputer of 5 to 10 years ago. A microcontroller has everything needed for a complete programmed computer control for the specific applications, in the present case, for 6D measurements. However, instead of being a large computer, a microcontroller is a single IC chip with an extremely small footprint. Unlike microprocessors, a microcontroller has built-in erasable ROM for user programming, built-in RAM for storing data, built-in input/output (I/O) ports for interaction with external world, a built-in Analog-to-Digital Converter (ADC) for handling analog quantities, and built-in communication hardware. Other notable features of today's microcontrollers include very low power consumption and very reasonable costs. For example, the microcontrollers from Microchip Corporation PIC16xxx series have 2K programmable ROM, 128 bytes of RAM, internal clock and timers, 13 I/O lines, and 4 channel ADC. The IC chip has a RISC processor structure, working at 4 MHz to 36 MHz clock rate. The IC chip has a function to automatically switch from work mode to sleep mode and drains only 2 mA at work mode, 10 μA at sleep mode. The cost is less than $10. The typical size of the microcontroller IC chip is only 1 cm x 1 cm x 5 mm. The microcontroller provides an ideal device for complete electronic control and intelligent operation of the above described retroreflecting modulator.

The following is a list of the favorable features of the microcontrollers for 6D measurements:

(a) The I/O pins can be used to provide any desired digital code signals to the liquid crystal modulator. A single chip provides any variation of desired code through programming in advance.

(b) The I/O pins can be used to provide any desired complex digital signals for timed control of the operation of the active pixel 2D sensor. These signals include start signals, clock signals, address signals, etc.

(c) The analog input pins can be used for input of the analog signals from the image sensor, and further to digitize the analog signals and store the digitized results in the microcontroller's data registers.

(d) The internal RAM can use the microcontroller to store a number of sequential analog signal intensity values and then make comparisons between theses values, finally selecting the pixel address with the largest signal intensity. All other data are discarded.

Therefore the combination of an active pixel CMOS sensor with a microcontroller can provide a novel type of position-sensitive photo-detector. So far, the novel device, the active pixel CMOS image sensor has been designed only for imaging applications. Because of the above mentioned salient features, the active pixel CMOS image sensor will eventually be designed with a structure specifically for position sensitive photo-detection. If this is true, the position data (the brightest pixel address) should be able to be obtained instantaneously, after the laser light hits the device. That is to say, from the instant the laser beam hits the device, within a few microseconds, the data for the brightest pixel can be obtained through the microcontroller.

(e) Most advanced microcontrollers have communication ports for data communication with other devices.

Currently available commercial active pixel CMOS image sensors do not give special consideration to the applications for position sensitive photo-detection. However, by using the intelligent capability of the microcontroller, the signal intensity and the address of the brightest pixel can still be obtained within a short time. For example, we can expect that data processing time can be microseconds.

Fig. 59 is an illustration of how to process a one-dimensional image sensor data. Because the image sensor has a random-access feature, and because the light intensity distribution has a finite width, a possible search method is to transfer the data at a step with an appropriate number of pixels. When the first pixel with a signal intensity different from zero is identified, then around the pixel to transfer a small number of data, the peak position can be reached. If the pixel number for a 2D sensor is 1,000 x 1,000, for a standard CCD sensor, 10^6 pixel data must be processed to obtain the peak value data. For the first CMOS 2D sensors with the same pixel number, about 1,000 pixel data transfer should be sufficient. So the preliminarily estimated data processing time is less than 1 mS.

Figure 59 Method for identifying the brightest spot in the CMOS 2D active pixel sensor

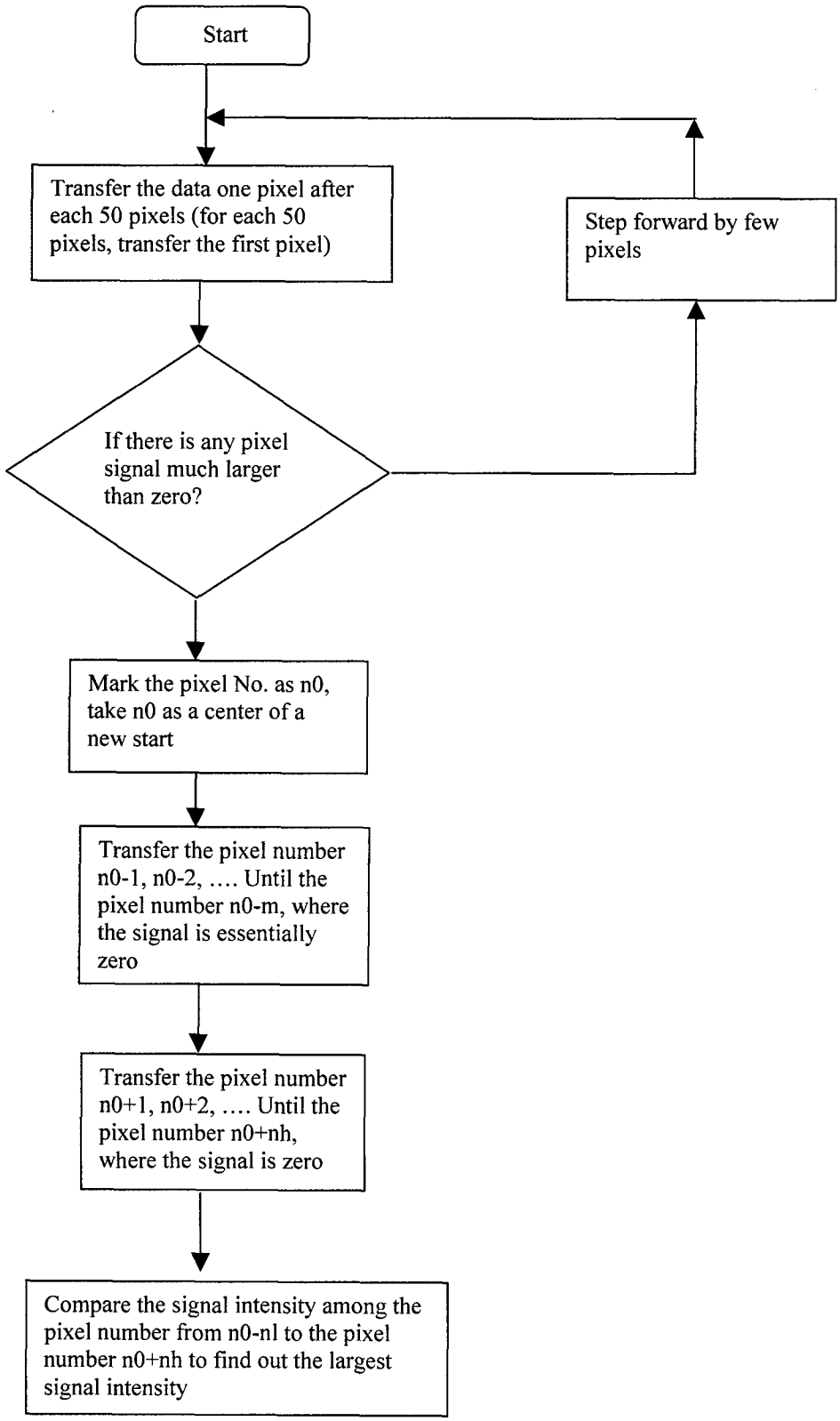

(7-b) Preliminary experimental work for the new 2D photo-detector

(7-b-1) A brief list of the specification data of the 2D sensor PB1024.

Recently, a 2D CMOS image sensor PB1024 became commercially available (by Photobit, CA). The PB1024 has the following two features especially favorable for use for 6D measurements:

1. The 2D image sensor has an appropriate spatial resolution with a pixel number of 1,024 x 1,024, and an exceedingly high frame transfer rate of 500 frames per second. That is, it takes 2 ms to transfer an entire frame of pixel data (1,024 x 1,024).
2. The image sensor has a "open structure, " allowing direct transfer of any desired pixel in a random-access way.

(7-b-2) A brief description of the 2D sensor PB1024 structure.

A schematic of the sensor structure is shown in Fig. 59. The following is a description of the sensor structure. The image sensor has 1,024 x 1,024 pixels, each pixel is 10 μ x 10 μ. Each column has an ADC for multi-channel digitizing. Total: 1,024 ADC working in parallel. The sensor provides multi-channel output to maximize the data transfer speed.

There are 8 channels for parallel outputs; each has an 8 bit resolution, so the sensor has a total of 8 x 8 = 64 pins for output.

Each output pin works at 66 MHz. After each row data is digitized, the data is transferred to output sequentially for the first 8 pixels in the same row, to the last 8 pixels in the same row by 1024/8 = 126 operations of data transfer.

The 2D sensor has an open structure for users to use random-access to directly transfer data from any pixel. A 10-bit address line allows any pixel to be directly transferred to the output.

Figure 60 Structure of CMOS APS PB1024

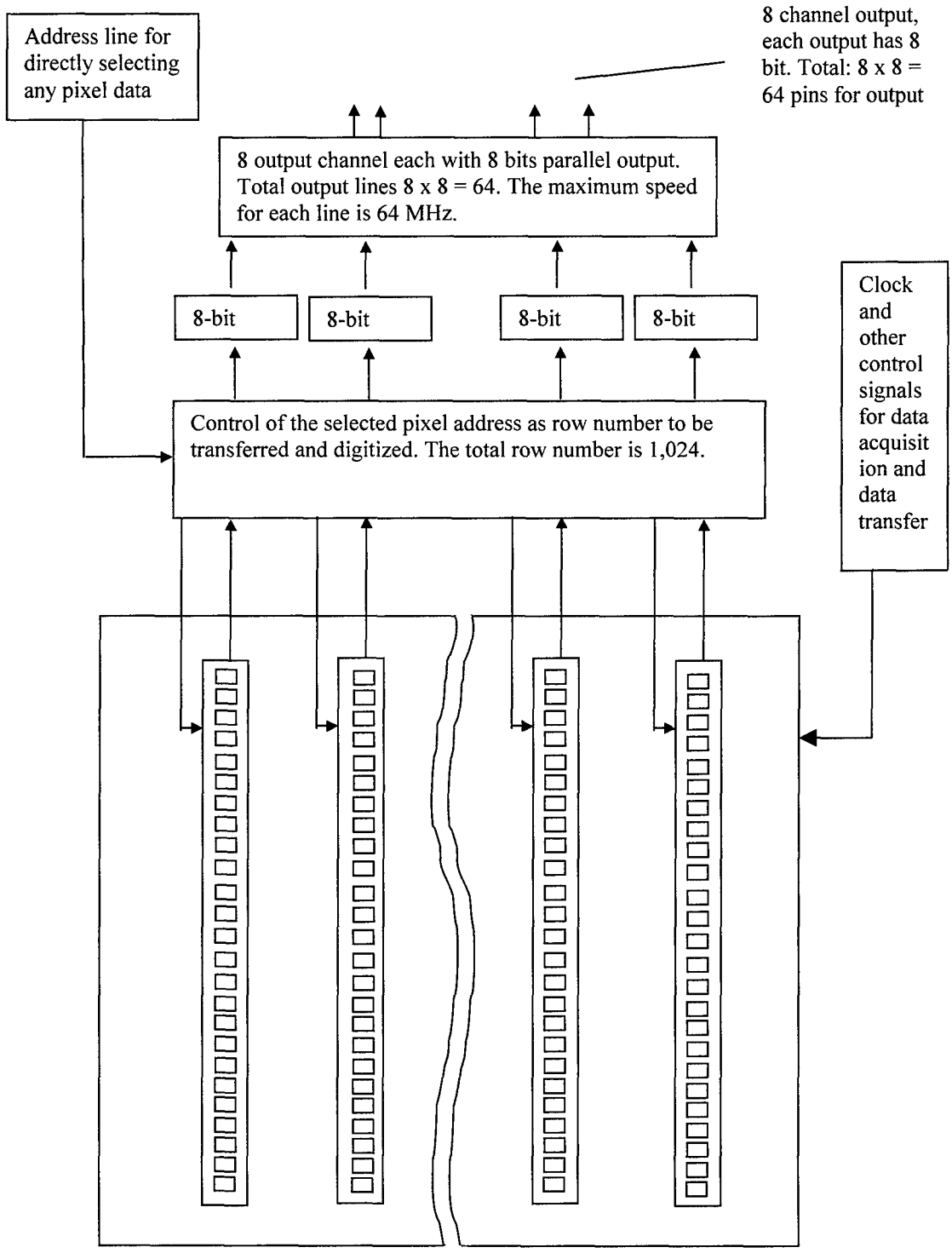

The most important technical advantage of using a single 2D detector instead of using a pair of linear detectors is the highest photo-detection efficiency, because the light energy collected by a conventional 2D lens is completely focused to single pixels without wasting light energy. But using 2D detectors requires a much higher speed of data acquisition hardware. So far, except for the CMOS APS PB1024, no 2D image sensor can provide an adequate data transfer speed as required for real time 3D surface imaging. The exceedingly high speed of the APS PB1024 can meet the speed requirement for the present project. However, the novel 2D sensor PB1024 provides a technical challenge to the embedded microprocessor. The following is a description for how to select an appropriate embedded microprocessor.

We designed and constructed a preliminary 2D intelligent photo-detector based on use of the active pixel CMOS 2D photo-detector controlled by an embedded microprocessor. The data acquisition and data preprocessing is conducted by the embedded microprocessor. The intelligent detector assembly as a whole is controlled in turn by a personal computer. The purpose of the experimental work is for a preliminary test of the concept of the 2D intelligent embedded detector based on use of a 2D CMOS active pixel image sensor for 6D measurements.

Fig. 61 is a schematic circuit diagram. According to the circuit design, a printed circuit board was custom made. Fig. 62 is a picture of the whole photo-detector board. The work was preliminary. Further work is needed for further tests.

Fig. 61 Schematic circuit diagram of intelligent 2D CMOS APS with embedded microprocessor control

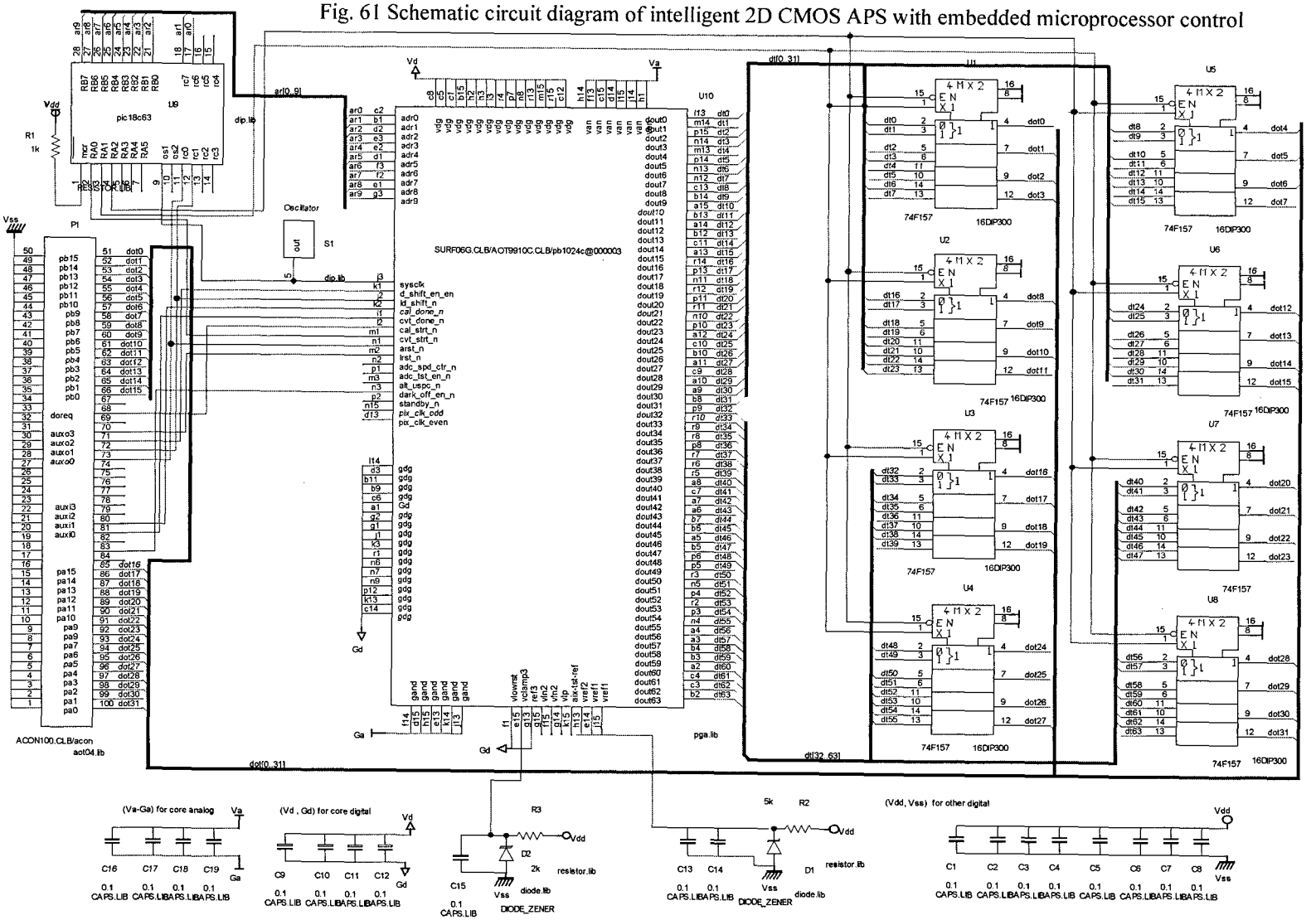

Figure 62 A picture of the CMOS 2D APS photo-detector with an embedded microprocessor

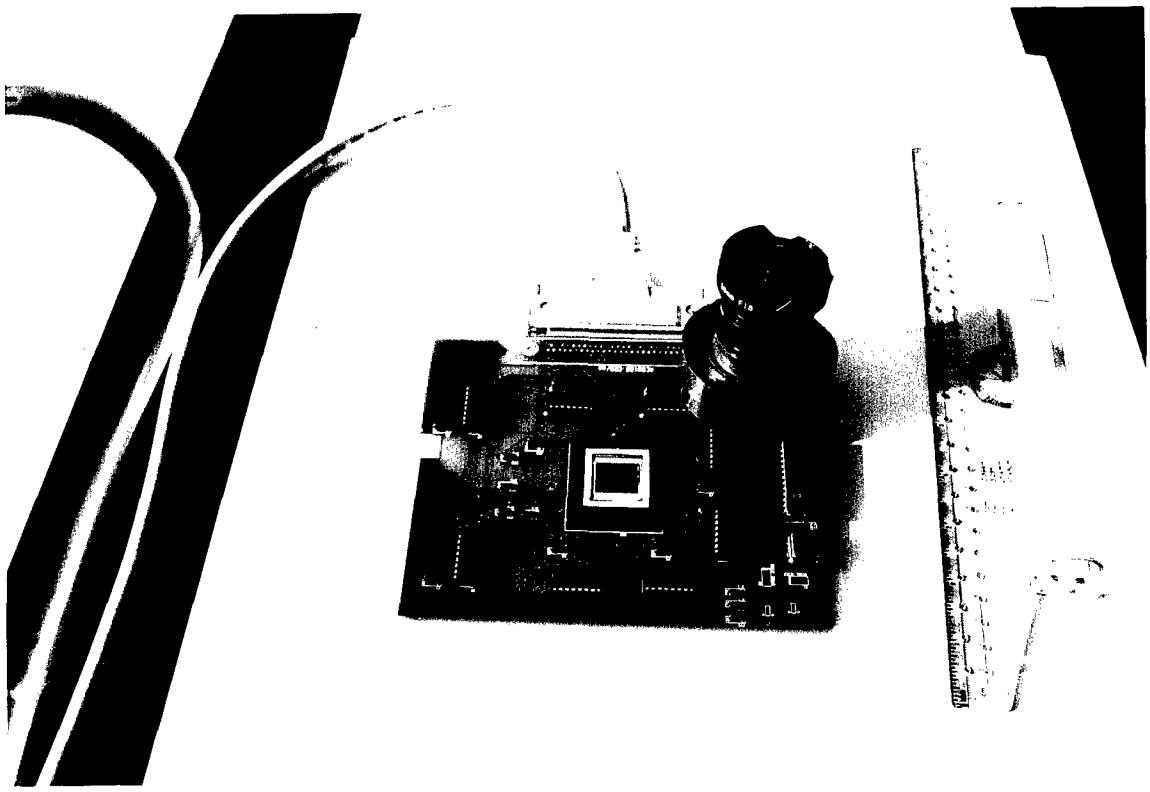

8. Conclusions

(A) In the present Phase II Contract for development of a 6D measurement system, we successfully identified, developed, and tested the following critically important component technologies for construction of 6D systems: (1) a systematic mathematical theory for 6D calculations; (2) a laser beam delivering system with full electronic control of light direction in a broad field of view; (3) a retroreflective modulator; (4) an intelligent 2D direction-resolvable photo-detection system; and (5) a data communication system between the test asset and the measurement station.

(B) These critical components represent a number of new technology areas. They are the technical foundation for any 6D measurement approach, including the present approach, as well as any other optical approaches. It is necessary to focus special and substantial efforts on the development of these critically important components.

(C) Based on successful development of the above described critical components, the proposed automated 6D measurement system is feasible.

9. Further work for the construction of a 6D system

Based on successful development of the above mentioned critical components, the construction of a fully operational 6D measurement system can be immediately implemented. There should be no technical difficulty, only (a significant amount of) implementation work. The following is a list of the work to be done, a quantitative estimate of the amount of work, major milestones, and the cost.

Broadly, the construction of the 6D system can be divided into two stages: the first stage is the construction of a fully operational prototype; the second stage is construction of a standard product. Note that after the completion of the first stage, the instrument will be ready for certain uses and for participating in certain airplane tests. After completion of the second stage, the instrument can be sold as a standard product.

(9-a) Stage 1: Construction of a fully operational prototype.

This includes the following 4 subtasks and milestones:

(9-a-1) Combined operation of the laser search and the tag response.

The basic operation is that the laser shall deliver the light beam to any arbitrarily selected desired target (test assets). When the target is selected, the laser beam stays there for a short while for 6D measurements. More detailed steps are shown in Fig. 63:

Figure 63 Task 1-1 for system construction

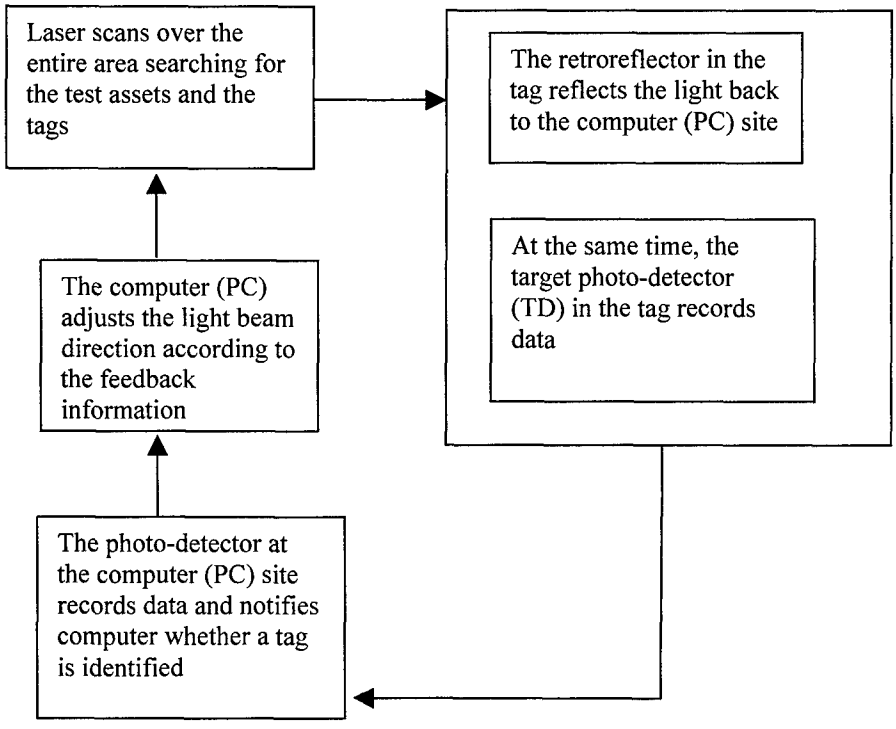

(9-a-2) Combined operation of the hardware and mathematics.

Based on the completion of step (9-a-1), the computer controls a whole set of 6D data acquisition, and data processing. Then the computer uses the mathematical methods developed in Phase II to calculate the final 6D results. The calculated results shall be compared with the real data. The real data can be directly read from the test bench. Complete agreement between the calculated results and the real results shall be achieved before going further. More detailed steps are shown in Fig. 64.

Figure 64 Task 1-2 for system construction

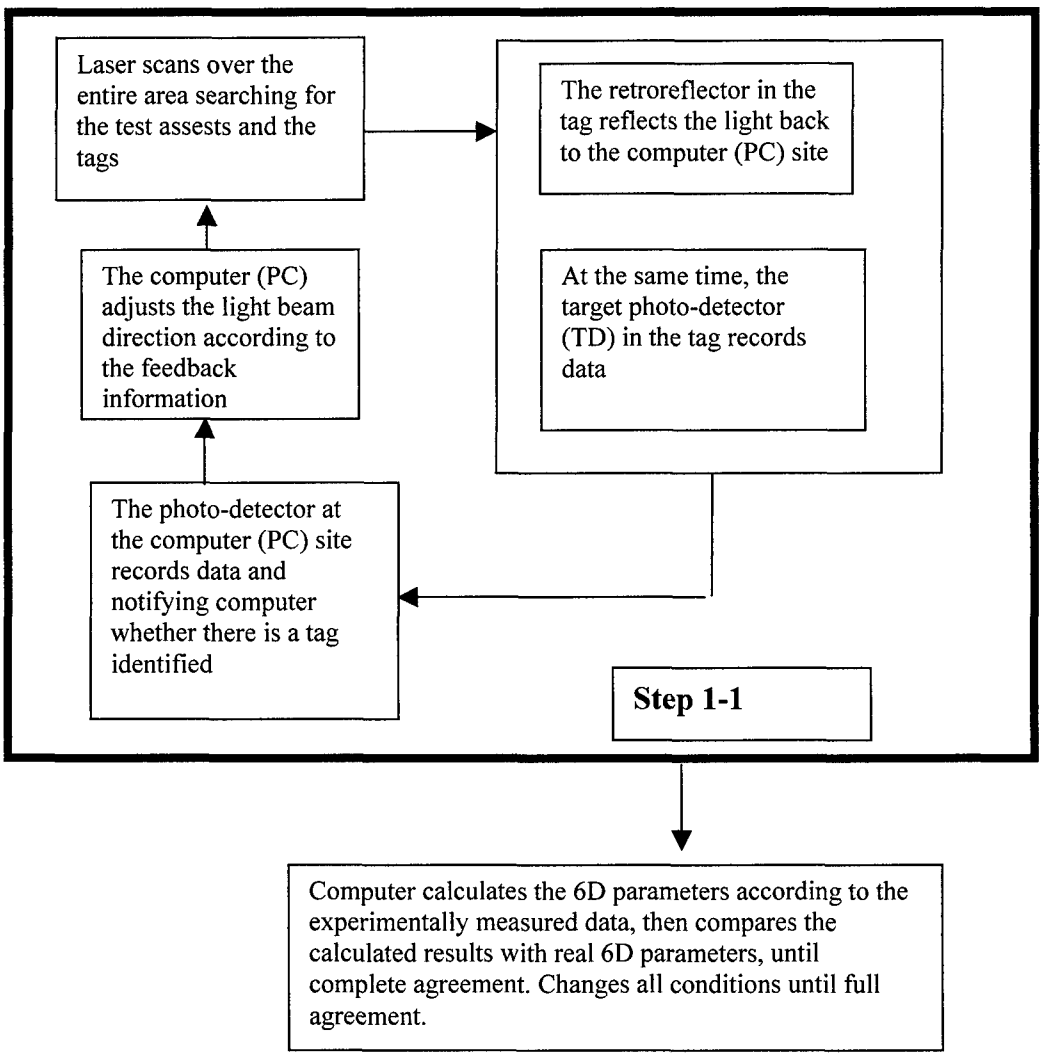

(9-a-3) Data exchange between the target and the PC site through optical communication in free-space.

In 1-1 and 1-2 above, the data exchange between the target and the PC site is through a wired communication link. This is necessary for testing 6D measurement principles. The optical communication link is temporarily omitted in the above steps. After the system has shown to be operational in all other parts, the optical communication component is added.

(9-a-4) Construction of the hardware and software for a fully operational prototype 6D system.

Such a system will be tested under real experimental conditions in the anechoic chamber for airplane tests.

Roughly, each of the above steps will take about 1/3 the amount of work as the present Phase II Contract. Thus, the total work for completion of the construction of a fully operational prototype (total of stage 1) will be approximately 4/3 the work amount of the present Phase II. The dollar amount should be approximately $1M. The total time schedule required depends on the needs for the system. All the above 4 steps can be completed within one year if needed. Otherwise, it can also take two years.

(9b) Stage 2: Construction of a standard product.

This stage includes two steps:

(9-b-1) Engineering development of a standard products.
This will include hardware and software.

(9-b-2) Performance enhancement.
The measurement accuracy and speed shall meet the requirements for actual airplane tests in the anechoic chamber.

A rough estimate is that the cost will be $1M. The time schedule will be 1 or 2 years.

After completion of the first level (prototype construction), the instrument will be ready for a number of actual uses. It is not necessary to wait for completion of a standard product before begin using the instruments.

10. References

1. The Optical Society of America (OSA) ed. *Handbook of Optics*, Vol. II, Chapter 19 (1995).
2. Scan Dynamics Corporation, Product Catalog (1999).
3. Aerotech corporation, Product Catalog (1999).
4. Brimrose Corporation, Product Catalog (1999).
5. The Optical Society of America (OSA) ed. *Handbook of Optics*, Vol. II, Chapter 11 (1995).
6. W.B. Wetherell, "Afocal Lenses," in R.R. Shannon et al., eds. *Applied Optics and Optical Engineering*," Vol. X, Academic Press (1987), pp.109-192.
7. W. Smith, *Modern Optical Engineering*, Second Edition, Chapter 9, 13 (1992).
8. Y.S.Chao, "Apparatus for Dynamic Control of Light Direction in a Broad Field of View," U.S. Patent No. 6,204,955 B1 (March, 2001).
9. Y.S. Chao, A number of U.S. Patents Pending (2000).
10. W.H. Press et al., "Numeric recipes in C," in *The Art of Scientific Computing,* second edition, Cambridge University Press (1992).